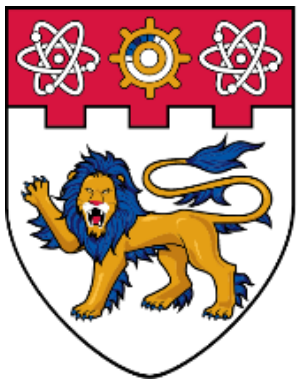

NANYANG TECHNOLOGICAL UNIVERSITY
SINGAPORE

TECHNO-ECONOMIC-ENVIRONMENTAL ASSESSMENT AND MODELLING GUIDED STRATEGIES FOR SHIP PROPULSION

NIRMAL VINEETH MENON

SCHOOL OF MECHANICAL AND AEROSPACE ENGINEERING

2025

TECHNO-ECONOMIC-ENVIRONMENTAL ASSESSMENT AND MODELLING GUIDED STRATEGIES FOR SHIP PROPULSION

NIRMAL VINEETH MENON

SCHOOL OF MECHANICAL AND AEROSPACE ENGINEERING

A thesis submitted to the Nanyang Technological University
in partial fulfilment of the requirements for the degree of
Doctor of Philosophy

2025

Statement of Originality

I hereby certify that the work embodied in this thesis is the result of original research, is free of plagiarised materials, and has not been submitted for a higher degree to any other University or Institution.

21st April 2025
. . . . . .
Date

Vineeth Menon
. . . . . .
[Nirmal Vineeth Menon]

Supervisor Declaration Statement

I have reviewed the content and presentation style of this thesis and declare it is free of plagiarism and of sufficient grammatical clarity to be examined. To the best of my knowledge, the research and writing are those of the candidate except as acknowledged in the Author Attribution Statement. I confirm that the investigations were conducted in accord with the ethics policies and integrity standards of Nanyang Technological University and that the research data are presented honestly and without prejudice.

. . 23 April 2025. . .
Date

[Professor Chan Siew Hwa]

Authorship Attribution Statement

This thesis contains material from **six** (6) paper(s) published in the following peer-reviewed journal(s) / from papers accepted at conferences in which I am listed as an author.

Chapter 3 is published as **Menon, N.V**. and Chan, S.H., 2022, March. Hydrogen as a Source of Green Energy for Marine Applications. In *2022 6th International Conference on Green Energy and Applications (ICGEA)* (pp. 22-26). IEEE.

The contributions of the co-authors are as follows:

- I prepared the manuscript drafts. Prof Chan edited the manuscript.
- I designed the study and performed all the data collection and analysis.
- I interpreted the results and presented my findings.
- I presented the paper at the 6th International Conference of Green Energy and Applications, Singapore.

Chapter 4 is published as **Menon, N.V**. and Chan, S.H., 2022. Technoeconomic and environmental assessment of HyForce, a hydrogen-fuelled harbour tug. *International Journal of Hydrogen Energy*, *47*(10), pp.6924-6935.

The contributions of the co-authors are as follows:

- I prepared the manuscript drafts. Prof Chan edited the manuscript.
- I designed the study and performed all the data collection and analysis.
- I interpreted the results and presented the findings.

Chapter 5 is published as **Menon, N.V**., Nguyen, V.B., Quek, R., Kang, C.W., Zhang, B. and Chan, S.H., 2024. Modelling guided energy management system for a hydrogen–fuelled harbour tug. *Energy Conversion and Management: X*, p.100642

The contributions of the co-authors are as follows:

- I wrote the drafts of the manuscript with inputs from Dr. Nguyen.
- I formed the methodology and investigation directions.
- I consolidated the data together with Dr Nguyen and Dr Quek.
- Prof Chan and Dr Kang edited the manuscript.

Chapter 6 is published as **Menon, N.V**. and Chan, S.H., 2023, April. Optimized Power Sharing Models for HyForce: A Hydrogen-Powered Harbor Craft. In *International Conference on Clean Energy and Electrical Systems* (pp. 137-151). Singapore: Springer Nature Singapore.

The contributions of the co-authors are as follows:

- I prepared the manuscript drafts. Prof Chan edited the manuscript.
- I designed the study and performed all the data collection and analysis.
- I interpreted the results and presented my findings.
- I presented the paper at the 5th International Conference of Clean Energy and Electrical Systems, Tokyo, Japan.

Chapter 6 is published as Roslan, S.B., Tay, Z.Y., Konovessis, D., Ang, J.H. and **Menon, N.V**., 2023. Rule-based control studies of LNG–battery hybrid tugboat. *Journal of Marine Science and Engineering*, *11*(7), p.1307.

The contributions of the co-authors are as follows:

- I provided the domain expertise
- I facilitated the data collection and interpretation
- Mr Roslan wrote the manuscript, and I reviewed and suggested changes

Chapter 7 is published as **Menon, N.V**. and Chan, S.H., 2024, June. Model Predictive Control Framework for an All-Electric Hydrogen Powered Harbour Craft. In *International Conference on Electrical Engineering and Green Energy*.

The contributions of the co-authors are as follows:

- I prepared the manuscript drafts. Prof Chan edited the manuscript.
- I designed the study and performed all the data collection and analysis.
- I interpreted the results and presented my findings.
- I presented the paper at the 7th International Conference of Electrical Engineering and Green Energy, Los Angeles, USA.
- I was awarded the best presentation award.

21st April 2025
Date

Vineeth Menon
[Nirmal Vineeth Menon]

Acknowledgements

To my dear supervisor, Professor Chan Siew Hwa, for whom nothing I have accomplished in this study would have been possible. Thank you for recognising my unique position as an industrial student. Your trust in my ability to deliver to the standard you have come to expect has always been encouraging. Our thought-provoking conversations have always guided me to push my boundaries and were instrumental in the accomplishments of this thesis.

To my colleagues and friends, Dr Van Bo, Dr Raymond Quek, and Dr Kang Chang Wei from the Institute of High-Performance Computing at A*STAR, a BIG thank you for the relentless support and collaboration over the past years. Your patience and curious minds will forever serve as an inspiration.

I sincerely appreciate the program sponsor, the Economic Development Board of Singapore and colleagues at Seatrium for providing this platform, the Industrial Postgraduate Programme (IPP) and continued support.

Most importantly, this journey would not have been possible without the support of my family. I want to thank my loving wife, Rachel, for standing by my side throughout and blessing me with my two loving children, Aryan and Anya, who were both born during my course of study. Their smiles and warm hugs have been a solid motivation to keep moving forward. Seeing them grow reminds me of the baby steps we take to handle life's challenges.

My parents, Amma and Papa. Thank you for constantly checking in on me and encouraging me never to give up. You are my symbol of strength and an unwavering pillar of support.

Lastly, to my late mother-in-law, Lena. Words cannot describe how much I miss you. I know you have been rooting for me from above. This one is for you.

Abstract

As concerns over the shipping industry's environmental impact grow, the International Maritime Organisation (IMO) has implemented strict regulations to monitor ships' energy efficiency and emissions during operation. Ships with highly dynamic loads often struggle to maintain energy-efficient operations with conventional mechanical propulsion systems. Tugboat, for instance, rely heavily on specific design factors, including the installed capacity of generators and batteries. This thesis uses the tugboat as a case study to explore hydrogen as a fuel source, aiming not only to meet environmental regulatory requirements but also to develop an optimal powertrain configuration required to achieve the best trade-off between design, environmental benefit, and operating costs.

In this thesis, the conceptualisation and development of HyForce, a hydrogen-powered tugboat, begin with an in-depth techno-economic and environmental assessment. This study's signpost for commercial competitiveness is influenced primarily by the projected liquified hydrogen cost of 5.1 USD per kg in 2040 with a 2,000 USD/kW capital cost for fuel cells. Emissions analysis from a well-to-wake perspective shows reductions of 26.9% and 75.6% for fossil-based hydrogen and renewable hydrogen, respectively, compared to traditional diesel fuel.

To enhance viability, an energy management study guided by modelling was conducted, optimising power allocation to improve fuel efficiency and reduce emissions. A digital twin of HyForce was developed in a virtual domain to simulate the performance characteristics in a 'real-world' scenario, which includes environmental conditions such as wind, waves, sea, currents, and friction. A power requirement of 93 kW to 1892 kW is needed to achieve 5 to 12 knots with friction peaking at 97.3 kN. Additionally, wind speeds of 10 m/s increased resistance by 3 kN.

However, HyForce's resistance is mitigated by the design of the propulsion system, which can deliver a thrust power of 2 MW.

The design optimisation process begins by modelling HyForce's power distribution system in MATLAB/Simulink, simulating its response to operational demands. This research identified the number of towing jobs a harbour craft could perform between bunkering intervals as the cost function for optimisation. A theoretical framework was developed to govern the power-sharing strategies, enhanced by statistical data that accurately represent the powertrain's performance. This approach has shown a 15% increase in on-hire availability for the tugboat.

A notable contribution of this research is the introduction of a novel optimisation approach for shipboard power management, incorporating fuel consumption, power device lifecycle costs, and emissions penalties. Additionally, the study explores an advanced model predictive control (MPC) strategy a hierarchical architecture that optimally allocates power among different energy sources on a vessel, ensuring cost-effective, multi-objective control. The system effectively handles load fluctuations and disturbances, improving overall system stability.

Table of Contents

List of Figures

List of Tables

List of Abbreviations

3D	Three- Dimensional
AC	Alternating Current
ATR	Auto - Thermal Reforming
BMS	Battery Management System
BoP	Balance of Plant
bp	Bollard Pull
CAPEX	Capital Expenditure
CCUS	Carbon Capture, Utilisation, Storage
CFD	Computational Fluid Dynamics
CH_4	Methane
CII	Carbon Intensity Index
CO_2	Carbon Dioxide
CRL	Commercial Readiness Level
DC	Direct Current
ECA	Emission Control Areas
ECMS	Equivalent Consumption Minimisation Strategy
ECR	Exhaust Gas Recirculation
EEDI	Energy Efficiency Design Index
ESS	Energy Storage System
FID	Final Investment Decision
GDP	Gross Domestic Product
GHG	Greenhouse Gases
GWP	Global Warming Potential

H_2O	Water
HAZID	Hazard Identification
HAZOP	Hazard and Operability Analysis
ICE	Internal Combustion Engine
IMO	International Maritime Organisation
IPCC	Intergovernmental Panel on Climate Change
kN	Kilo Newton
kW	Kilowatt
LCA	Lifecycle Assessment
LOA	Length Overall
MCR	Maximum Continuous Rating
MEGC	Multiple Element Gas Containers
MEPC	Marine Environment Protection Committee
MPC	Model Predictive Control
MW	Megawatt
N_2O	Nitrous Oxide
OPEX	Operational Expenditure
PEM	Proton Exchange Membrane
PM	Particulate Matter
PMS	Power Management System
PTI	Power Take In
PTO	Power Take Off
QUICK	Quadratic Upstream Interpolation for Convective Kinematics
RANS	Reynolds-averaged Navier Stokes
RPM	Revolutions Per Minute

SCR	Selective Catalytic Reduction
SMR	Steam Methane Reforming
SOC	State of Charge
SOFC	Solid Oxide Fuel Cell
TRL	Technology Readiness Level
USD	United States Dollar
WTW	Well-to-Wake

List of Symbols

Θ_c	Vessel Direction (°)
ω	Wake Fraction
μ_{sw}	Dynamic Viscosity of Seawater (kg/ms)
μ_{fw}	Dynamic Viscosity of Freshwater (kg/ms)
η_P	Propellor Efficiency
ρ	Density (kg/m^3)
A_F	Frontal Projected Area (m^2)
A_L	Lateral Projected Area (m^2)
B	Breadth of HyForce (m)
C_F	Friction Coefficient
C_{F0}	Reference Friction Coefficient
C_{SR}	Coefficient of Surface Roughness
C_m	Midship Section Coefficient
$Cost_{Fuel}$	Fuel Cost (USD)
$Consumption_{Fuel}$	Fuel Consumption Rate (kg/s)

$Capex_{Propulsion}$	Capital Cost for Propulsion Equipment (USD)
$Capex_{Storage}$	Capital Cost for Fuel Storage Equipment (USD)
$CO_2\ cost$	Carbon Dioxide Tax in Dollars (USD)
D	Diameter (m)
F_x	Force in the x Direction (N)
$F_{Operational}$	Propulsive Forces to Meet Operational Requirements (N)
g	Gravitational Acceleration (m/s^2)
H	Water Depth (m)
H_w	Wave Height (m)
J_p	Advance Coefficient of the Propellor
J_h	Advance Coefficient of the Hull
K_T	Thrust Coefficient
K_{Qo}	Torque Coefficient – Open Water
K_{Qs}	Torque Coefficient – Turbulent Flow
L_{BWL}	Length of the Bow on Water Line (m)
L_W	Length of HyForce (m)
$\dot{m}_{batt}$	Energy Consumption from Batteries (kWh)
$\dot{m}_f$	Fuel Consumption from Fuel Cells (g/s)
M_x	Moment in the x Direction (Nm)
n	Revolutions Per Minute (RPM)
N_p	Number of Propellers
$OPEX$	Operational Cost (USD)
P_{batt}	Battery Power (kW)
Q	Torque Produced by the Shaft (N)

R_{AWL}	Resistance Attributed to waves (N)
Re	Reynolds Number
R_{Total}	Total Resistance (N)
s	Equivalence Factor
S	Wetted Area of HyForce (m^2)
S_{APP}	Wetted Area of HyForce – Appendages (m^2)
S_A	Salinity of the Water (g/kg seawater)
SOC	State of Charge (%)
t	Thrust Deduction Fraction
T	Temperature (°C)
Th	Thrust (N)
T_{CO}	Total Cost of Ownership (USD)
U_{ref}	Wind Reference Velocity (m/s)
V_{actual}	Vessel Speed – Observed (knots)
V_c	Water Current Velocity (m/s)
V_{set}	Vessel Speed – Setpoint (knots)
ΔV_{depth}	Change in Vessel Speed Due to Water Depth (knots)
V_s	Relative Velocity of the Vessel and Water (m/s)
$\Delta V_{current}$	Change in Vessel Speed Due to Water Current (knots)

Chapter 1

Introduction

This chapter aims to provide a broad context for the impetus for maritime decarbonisation and the challenges the industry faces in institutionalising the necessary changes to meet the emission reduction goals set by the International Maritime Organisation. It introduces alternate powertrains capable of reducing emissions and discusses the benefits of setting the stage for this work's main objectives.

1.1 Background and Motivation

Climate change is an existential crisis of this century. The repercussions of a changing climate can be observed today. In 2024, the world recorded the highest temperature of 17.16°C, which superseded a previous high observed one year ago [1]. This trajectory is alarming, considering that minute shifts in global temperature can potentially result in disastrous consequences. Rising sea levels, sudden and erratic changes in weather, heat waves resulting in forest fires, and drought are some consequences experienced today. This situation is exacerbated by the unjust nature in which it affects global citizens. Countries with a lower gross domestic product might not have the necessary resources to invest in the required infrastructure to combat this evolving situation [2]. This could inevitably result in a mass exodus of people seeking refuge in neighbouring countries, causing other political and societal issues.

The Intergovernmental Panel on Climate Change (IPCC) highlighted the role of carbon dioxide (CO_2) emissions from fossil fuel combustion as a primary driver of global warming. International agreements such as the Kyoto Protocol (1997) and later the Paris Agreement (2015) focused on reducing CO_2 emissions to mitigate climate change.

The main driver for these emissions originates from human activity to fulfil energy needs. The energy trilemma (i) energy security, (ii) environmental sustainability, and (iii) energy equity (affordability) remain to this day a challenging and delicate balance [3]. This is further resonated by the United Nations Sustainable Development Goals (UNSDG), which recognises clean and affordable energy as one of the 17 goals necessary for prosperity now and in the future.

Examples of GHGs include Carbon Dioxide (CO_2), Methane (CH_4), Nitrous Oxide (N_2O) and fluorinated gases. These gases have varying degrees, which they negatively attribute to the 'greenhouse effect' primarily driven by the time they remain in the atmosphere. A widely accepted practice to quantify and express these emissions is to use CO_2 as the baseline, resulting in the global warming potential (GWP) for the above gases being 1, 28, and 265, respectively, with fluorinated gases having a wide range depending on their composition. The source of GHG emissions is documented extensively and monitored regularly [4, 5] , and the GHG emissions are segregated by sectors to provide a more representative illustration of the main sources of such emissions [6].

The Intergovernmental Panel on Climate Change (IPCC) 6th report published in 2024 provides further granularity on the various sectorial contributions to the overall global emissions [6, 7]. This report has identified that the shipping sector, a significant contributor in transporting goods and freight, is responsible for about 3% of global CO_2 emissions.

Shipping and the maritime industry predominantly rely on marine diesel engines as the primary prime mover to provide vessels' propulsive power and onboard electricity. This inevitably translates to the combustion of fossil-based fuels emitting several of the GHGs listed above and more, including particulate matter (PM), sulphur oxides (SO_x) and water vapour (H_2O) [8]. Growing concerns about the harmful effects of SO_x emissions from shipping on human health have led to restrictions on the use of heavy fuel oil within 200 nautical miles from shore. These

restrictions are due to the high sulphur content in this fuel, which exceeds the permissible levels for the transportation sector.

The appeal to use diesel engines derives from the simplicity of the design for marine vessels as they have a fixed design basis, driving down costs and complexity. Marine diesel engines are mechanically connected to the propellors via a shaft, while generators produce the electricity required for onboard loads such as ventilation and lighting. The size of the engines is designed to ensure that the maximum needed propulsive power can be met. Ocean-going vessels such as container vessels and bulk carriers typically have a relatively constant load demand, allowing for engines to be right-sized to operate at their most optimal setpoint.

From a regulatory perspective, the International Maritime Organisation (IMO) has mandated the reporting of shipping emissions to their Data Collection System (DCS) to track, report, and enforce the Carbon Intensity Index (CII) requirements by 2026. The CII rates ship alphabetically from A to E, with A being the most efficient. Penalties such as trading restrictions and suspension from trading apply to vessels that repeatedly receive a D rating. Furthermore, new-build vessels must declare their Energy Efficiency Design Index (EEDI), an index expressing the CO_2 emission at 75% of the rated installed shaft power as a function of the cargo carrying capacity and distance travelled. It can be described as:

$$EEDI = \frac{m_{CO2} \text{ @ } P_i=75\%}{(m_{cargo})(distance)} \quad (1\text{-}1)$$

Where m_{CO2} is the mass of carbon dioxide produced in grams, m_{cargo}. The cargo-carrying capacity is in tonnes, and the distance is given in nautical miles. While EEDI is a one-off certification, CII will be assessed annually in 2023, with stricter emissions limits imposed yearly.

To address this requirement for compliance to IMO CII requirements, there are several low-carbon fuels are emerging as critical enablers in the transition to a decarbonised energy system,

particularly in sectors where direct electrification is infeasible due to technical or operational constraints. These include long-haul aviation, maritime shipping, heavy-duty transport, and certain industrial processes. Among the range of alternative energy carriers being explored, electricity, green hydrogen, green methanol, and green ammonia represent some of the most prominent options, each with distinct characteristics in terms of technological maturity, well-to-wake (WTW) emissions, and energy density.

Electricity, when generated from renewable sources such as wind, solar, or hydro, has near-zero WTW emissions and is already well-established in light-duty transportation and stationary applications. However, its storage in batteries presents limitations for high-energy-demand sectors, owing to the relatively low gravimetric energy density of current lithium-ion technology (~0.25 MJ/kg) and the associated weight and charging constraints.

Green hydrogen, produced via electrolysis powered by renewable electricity, offers a high gravimetric energy density (~120 MJ/kg), making it attractive for energy-dense applications. Nevertheless, its low volumetric energy density, even in compressed or liquefied form, presents significant storage and transport challenges. Moreover, the infrastructure for large-scale hydrogen production, distribution, and utilisation—such as pipelines, refuelling stations, and compatible engines or fuel cells—is still in its early stages of development.

Green methanol, synthesised from green hydrogen and captured carbon dioxide, offers a more energy-dense and logistically manageable alternative (~20 MJ/kg; ~15.6 MJ/L). As a liquid at ambient conditions, it is compatible with existing fuel infrastructure with relatively minor modifications, and several methanol-capable marine engines are already commercially available. However, its climate benefit depends heavily on the source of carbon used in synthesis and the upstream energy mix.

Green ammonia, produced via the Haber-Bosch process using green hydrogen and nitrogen from air, has recently gained traction as a carbon-free marine fuel. While its energy density (~18.6 MJ/kg; ~11.5 MJ/L) is lower than methanol, ammonia's carbon-free combustion offers substantial emissions reductions. Yet, its toxicity, corrosiveness, and the need for specialised storage and handling present significant operational and safety concerns.

In summary, the suitability of each low-carbon fuel is context-dependent, influenced by factors such as energy requirements, infrastructure readiness, safety considerations, and full lifecycle emissions. No single fuel is universally optimal; rather, a portfolio approach tailored to specific sectors and geographies is likely to be necessary in the broader energy transition.

Tugboats, ferries, and other near-shore vessels have a wide operating window due to the nature of their missions. This adds to the complexity of maintaining the engine at the most optimum operating point. Tugboats have a very dynamic operating profile with varying load demands and duration. This can be illustrated by broadly defining three modes of operation for tugboats: (i) hotel, (ii) transit, and (iii) bollard pull. A typical load profile for tugs is shown in Figure 1-1 below [9].

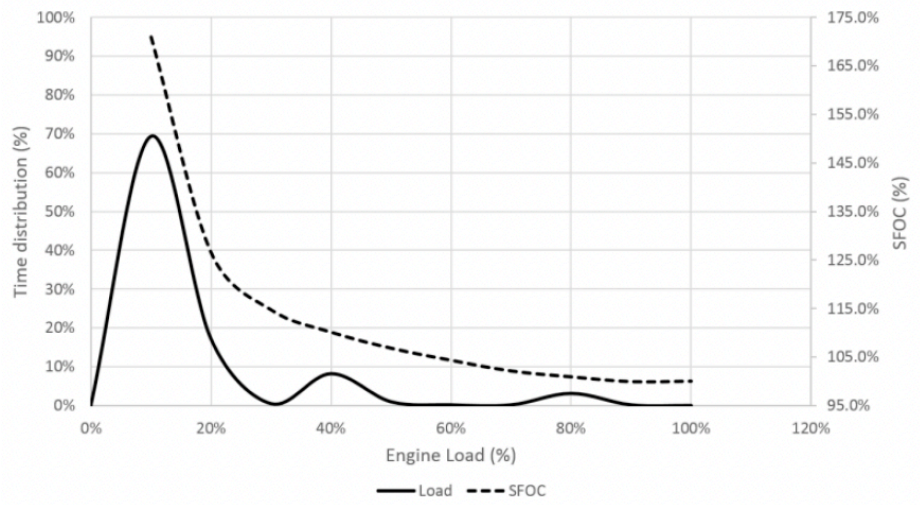

Figure 1-1: Tugboat load distribution

As illustrated in Figure 1-1 above, approximately 70% of the time, the tugboat is operating in a low load condition. Nevertheless, the powertrain must be designed to handle peak loads, which are less than 10% of the overall operational envelope. Furthermore, the Specific Fuel Oil Consumption (SFOC) for marine diesel engines are higher outside the optimum operating point of 65% to 75% of their Maximum Continuous Rating (MCR). Essentially, mechanical propulsion for tugboats is inefficient, leading to higher fuel consumption and, by extension, more GHG emissions.

This specific marine application presents an opportunity to consider alternatives such as an electric propulsion system. The solution offers benefits, including higher efficiency and operational flexibility [10-12]. Driven by advancements in microgrid technological components such as power electronics and motor drives, integration with alternate energy storage sources and electrochemical conversion devices has become seamless. Including batteries, super-capacitors, and fuel cells transforms the conventional diesel–mechanical powertrain into an all-electric marine vessel [13]. With the possibility of load allotment to the various power sources available onboard the vessel, optimisation of the electric propulsion architecture unlocks the possibility of operating with zero emissions. Alternatively, retrofitting such technology into existing vessels can reduce emissions by up to 35% [14].

Constraints on the energy density of batteries limiting the range and charging time of batteries, weight-to-power ratio, operating temperatures, and high cost are some of the limitations that restrict the applications for which they can be considered as a solution to provide zero emissions. The most promising scenario is a short sea voyage with an established infrastructure to charge the batteries. To address this constraint, fuel cells as the main power source is gaining momentum within the maritime industry [15]. Fuel cells can be scaled up to provide power in megawatts (MW) as required for marine applications such as tugboats or large ocean-going vessels. Using hydrogen as a fuel, fuel cells produce H_2O as a byproduct with zero carbon emissions. Furthermore, as an electrochemical device, the overall efficiency and power density are favourable attributes that have led to their deployment in pilot and research projects worldwide [16].

Integration of fuel cells into the main electrical distribution system requires engineering to ensure a seamless transfer of power to the eventual consumers (i.e. pumps, motors, lighting, ventilation, etc.). Unlike traditional diesel engines, which produce power in an AC-distributed system, the fuel cell with batteries inherently operates as a DC system and hence would need to be converted to AC. However, in recent years, there has been much development in transforming the overall power and propulsion system to operate with a DC-distributed system owing to the advantages they offer [17-19]. Examples of the advantages include ease of integration, higher efficiency, and elimination of synchronisation control. This is illustrated in Figure 1-2 below.

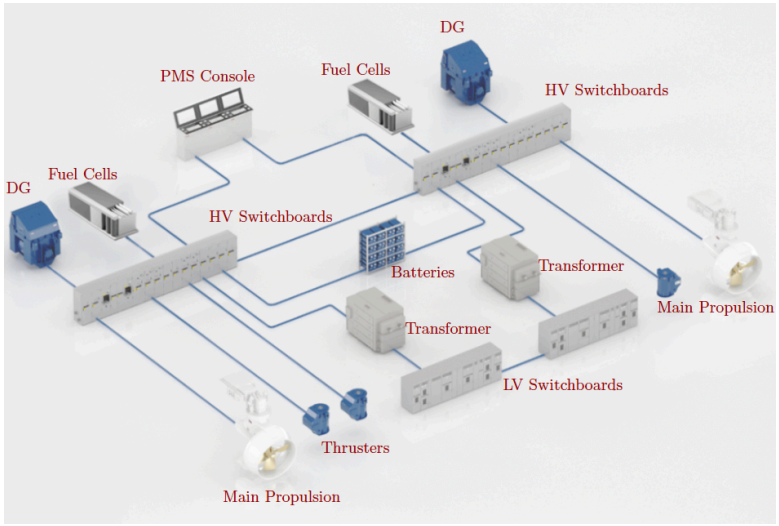

Figure 1-2: Marine powertrain architecture

1.2 Problem Statement

The impetus for revolutionary ideas and concepts to decarbonise the marine industry is clear, albeit with inherent challenges. The research gaps are evident.

- ***Techno-economic and environmental assessment for alternate fuels***

Several alternative fuel pathways capable of reducing shipping emissions are available for consideration. Unlike the traditional diesel-driven engines that dominated the industry for several decades, the future energy mix will not necessarily be a "one size fits all" solution. The specific marine application would be vital in determining the most appropriate, technically and operationally feasible solution. For large deep-sea oceangoing vessels, the challenges surrounding the endurance of the alternate fuels are a vital consideration. This refers to the distance in nautical miles the vessel can travel before the need to refuel. Correspondingly, for smaller coastal vessels, the constraint of endurance is not as influential as the space availability to integrate the larger fuel storage systems required to drive the powertrain. A holistic overview of the various contributing and mitigating factors needs to be evaluated to address the practicability of novel technologies in the marine environment. The existing body of

knowledge merely provides an elevated perspective to this research question without ringfencing onto a specific marine application [20-23].

- ***Realistic power management system control for operational marine vessels.***

Marine vessels in operation are subject to environmental factors that can contribute significantly to their overall performance. The effect of waves, wind, and water currents are typical loads that would act on the vessel during operation.

Dimensioning these loads is instrumental in ensuring that the power management strategies proposed are viable and attainable. To achieve this, a realistic virtual environment that unlocks the possibility of simulating these dynamic loads is fundamental to evaluating the vessel's operability perspectives. This requirement is traditionally achieved by doing experiments in a model test basin [24, 25]. A scaled model is built according to the design characteristics and is used as a performance validation for the vessel owner.

Introducing Energy Storage Systems (ESS) and unconventional technologies into marine vessels provides the flexibility to share the load demand across multiple power sources. Appropriately, the degree of freedom to assign load sharing increases and adds to the complexity of the Power Management System (PMS) control. The PMS must robustly address the “improved” operational flexibility and consider efficiency, emissions, and degradation on the powertrain.

Conventional methods to control the PMS, both for land-based and marine applications, are rule-based approaches. The control logic was designed to meet the requirements of pre-determined goals at the detailed engineering phase of the vessel construction or retrofit [26, 27]. Unique operational characteristics of marine vessels warrant a different technique to address (i) the propulsion architecture of the vessel’s powertrain needs to consider the mission sequences will have a direct impact on the energy required at the propellor, (ii) regulatory and safety requisites on redundancy and standby power availability, (iii) inherent differences of the

microgrid operability. For example, in a battery hybrid powertrain, the battery would power the vessel during low-load conditions, provided it is sufficiently large. When the vessel demands more power, the rule-based control logic automatically engages the engines to give the differential or potentially in excess to charge the battery. As shown, the existing body of knowledge is limited to the design of rule-based approaches that require prior knowledge and experience of operators to be fed into the design to ensure due consideration is given to all possible operating scenarios.

- ***Optimised control objectives***

Optimisation of the control schemes for marine vessels has yet to be investigated as extensively as land-based vehicles. Latest estimates show that 90% of the global vessel fleet has deployed a rule-based control for their PMS, citing the simplicity and cost of implementation [28-30]. Optimisation-based controls involve strategies to manage the PMS with pre-defined cost functions efficiently. Optimal control can be categorised as either global optimisation or real-time optimisation control. Global optimisation-based PMS, also known as offline optimisation, may not be suitable for real-time control since prior operational information may not be readily available. Consequently, global optimisation is more appropriate for validating the performance of other control strategies. The Equivalent Consumption Minimisation Strategy (ECMS) is a typical real-time optimisation method used to determine power allocation at the current step without considering future demand.

The classical Model Predictive Control (MPC) strategy is an advanced real-time optimisation approach. Still, it is susceptible to the system model and lacks robustness in optimally handling unexpected dynamic load variations. This issue is particularly relevant in marine applications, where shipboard power systems are frequently affected by external factors such as weather and ocean currents, as mentioned in the previous section. Additionally, the MPC algorithm incurs significant computational bandwidth and costs. Therefore, an improved optimisation-based

PMS strategy is needed to achieve practical multi-objective control in shipboard power management.

1.3 Objectives, Scope of Work and Approach

1.3.1 Objectives

The primary objective of this research is to conduct a detailed techno-economic and environmental assessment of a specific marine application to evaluate its compatibility with an alternate, low-emission fuel. Secondly, the concept of the world's first liquid hydrogen-fuelled tugboat, HyForce, will be developed as the baseline case study for further optimisation. HyForce will be enhanced with power management strategies aimed at optimising key metrics, such as fuel efficiency and emissions reduction. Finally, a controller will be developed to facilitate full integration of the optimised powertrain for a real-world deployment.

1.3.2 Scope of Work and Approach

Maritime decarbonisation is multifaceted and requires a holistic appreciation of the challenges it presents. This work aims to develop optimisation-based methods explicitly tailored to commercial marine vessels' PMS's power management challenges by leveraging extensive work published for land-based electric vehicles. Adopting these advanced optimisation techniques to the maritime environment aims to enhance the efficiency and effectiveness of using alternate fuels to address the industry's decarbonisation efforts while considering distinct operational demands and constraints.

Through the scope of work below, this research aims to address these challenges using a methodological and systematic approach.

1. ***Holistic evaluation of the powertrain configuration for an alternate fuel-powered marine vessel***

   This work focuses on consolidating the various alternate fuel options available for analysis. Through the screening and evaluation process, the "best-fit" marine vessel solution will consequently be selected for further development. The chosen solution will be subjected to a rigorous tech-economic and environmental assessment, considering various measurement metrics as a stress test to determine its merits and pitfalls. This includes lifecycle emissions through different molecular production pathways, total cost of ownership analysis that incorporates costs for the technology, overall engineering, construction and commissioning. Lastly, a financial analysis that considers the return on investment under different scenarios involving a carbon tax regime will be included. This aims to accurately calibrate the value proposition of the proposed solution that illustrates a representative perspective of the endeavour to decarbonise the maritime industry.

2. ***Creation of a digital twin model of the marine vessel for power management simulations***

   This work focuses on the basic design of the proposed marine vessel. Subsequently, a 3-dimensional (3D) model can be created using Navisworks to set the basis for detailed evaluation in a virtual environment. Mathematical models of the various components within the powertrain will be incorporated to establish the baseline for developing power management strategies.

3. ***Formulation of an optimised power management strategy***

   This work focuses on the critical power management challenge of determining the optimal power distribution between various sources to enhance fuel efficiency while addressing the trade-off between fuel consumption and emissions. To achieve this, the proposed power management strategy will be developed. This design allows it to effectively integrate with the system's existing power management controls, ensuring seamless operation and coordination within the power system. By optimising the power split, the strategy aims to minimise fuel usage while maintaining a balance of the desired cost functions. This approach not only enhances the overall efficiency of the power system but also effectively manages its environmental impact. The supervisory control layer will then be designed, playing a crucial role in achieving the desired integration and performance within the existing power management framework.

4. ***Development of a supervisory controller and implementation for verification and validation***

   This work addresses the formulated problem statement surrounding the limitations of a marine vessel's power and energy control strategies. Based on this analysis, an advanced supervisory power and energy management control layer would be designed. The primary objective of the proposed controller is to execute the optimised power management strategy to minimise the total cost of ownership and operation. This work proposes developing an enhanced model predictive control (MPC) strategy to achieve the desired control performance. This method will be designed to achieve the optimised allocation of power across the different sources, ultimately striving to reduce overall costs. A comprehensive analysis will be conducted to evaluate the performance of this advanced controller for implementation in real-world maritime applications.

1.4 Organisation of the Thesis

The thesis is structured and organised as a continuous flow, as shown in Figure 1-3 below. In this current chapter, an overview of maritime decarbonisation is discussed. Chapter 2 dives deeper into the various pathways available to fuel the energy transition within the industry and considers the vessel's powertrain architecture. Chapter 3 examines the overall integration of hydrogen as a source of fuel. This includes the leading technologies that convert the chemical energy of hydrogen into electrical energy for onboard power generation. Chapter 4 presents the techno-economic and environmental assessment of the identified marine application, benchmarking its performance against traditional fossil-based fuel. Chapters 5, 6 and 7 develop and validate the power-sharing strategy and optimisation-based power management to enhance the overall value proposition of implementing hydrogen as a marine fuel. Lastly, chapter 8 concludes the thesis, highlighting the contributions and significance of this research and offering recommendations for future studies.

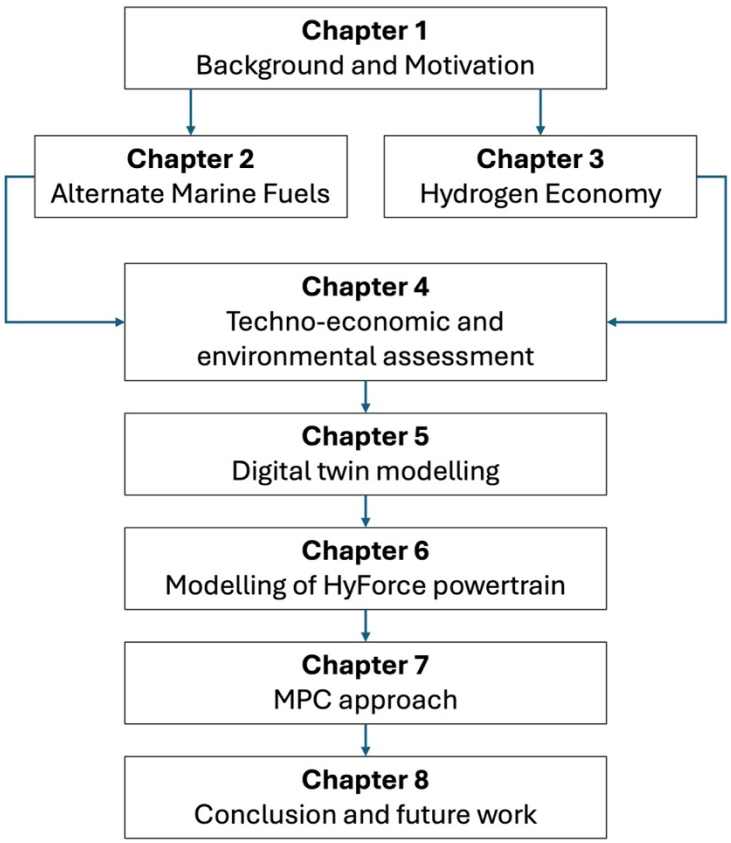

Figure 1-3: Thesis structure

Chapter 1 provides a broader context of the motivation for pursuing this research. This encompasses the current state of play within the maritime industry, problem statement formulation, scope of work, and the approach undertaken to holistically address the limitations circumventing a widespread adoption of alternate fuels in the marine industry.

Chapter 2 extensively reviews past literature surrounding alternate fuels' strengths, weaknesses, opportunities and pitfalls and their applicability in a maritime environment. The evolution of marine fuels since the inception of coal-powered steamships is briefly discussed. The proposed alternate fuels are benchmarked against metrics on a heat map to illustrate the review conducted. In addition, this chapter covers the various shipboard powertrains commonly used in marine vessels. The selected powertrain will be eventually modelled in Chapter 6 on MATLAB / Simulink.

Chapter 3 further distils the use of hydrogen as a source of marine fuel by evaluating the current state of play. This includes the production, containment, utilisation and the overall hydrogen economy. The various hydrogen production techniques are introduced together with their respective colour banding. The colour banding provides the basis for the lifecycle emissions (LCA) calculation, shown in Chapter 4. Hydrogen can be stored either in cryogenic liquefied or highly compressed form, both of which will be thoroughly evaluated. Lastly, two prominent energy conversion devices – fuel cells and internal combustion engines (ICE) are studied in detail.

Chapter 4 introduces the concept design of HyForce, a hydrogen-fuelled harbour tug. HyForce is the bedrock on which all evaluations are based. This includes an in-depth assessment of the technologies available to power this vessel, which uses fuel cells as the energy conversion device. This thorough evaluation also considers the operating economics, and the investment needed to fund this development. A comparison of the overall lifecycle emissions from well to wake emissions for different types of fuels, including liquefied and compressed hydrogen and traditional fossil-based marine diesel, was conducted. Lastly, different carbon tax regimes are implemented as part of a sensitivity analysis to determine the overall breakeven point, further highlighting the benefits of switching to zero-emission hydrogen fuel.

Chapter 5 transforms HyForce into a virtual environment for a detailed analysis of its performance. A series of simulations are enacted to replicate real-world conditions, ensuring realistic results. These include environmental factors such as wind, ocean currents, and wave height, among others. This was made possible through the detailed design and calculations of the vessel that consider the length, hull form, and appendages to determine the total resistance

of the ship as it moves through the water. The outcome of this evaluation was to ensure that sufficient power was available to perform all the identified mission scenarios.

Chapter 6 introduces a detailed and comprehensive system modelling approach. It details the development of a system-level fuel cell-powered hybrid shipboard power grid that includes both AC and DC distribution. The model incorporates the mathematical representation of key power components, as well as primary and secondary power management controls.The accuracy of this model is then fine-tuned through multiple iterations, presenting a unique power management optimisation problem aimed at minimising the total cost of vessel ownership and operation. The approach not only considers fuel costs and emission penalties but also seeks to increase the bunkering intervals for HyForce to enable a longer operational window.

Chapter 7 extensively reviews the various developments of optimisation-based control strategies for hybrid powertrains, remaining agnostic to any specific industry. This approach promotes knowledge transfer while focusing on the “best in class” solutions for adoption in the maritime sector. Specifically, three distinct strategies were evaluated, and a novel MPC is developed and implemented in HyForce.

Chapter 2

Alternate Fuels for Marine Propulsion

This chapter introduces the different pathways of future fuels used in the maritime industry and discusses the rationale for their importance. These alternate fuels are benchmarked against diverse matrices to assess their merits and pitfalls objectively. This preliminary screening offers the basis for further evaluation of hydrogen as a fuel source for marine propulsion.

2.1 Marine Decarbonisation Agenda

The maritime industry has historically been a crucial enabler for trade and commerce between countries. Shipping has maintained a solid foothold in this sector despite technological advancements, as it provides the best economies of scale. Sophisticated tools and algorithms have been developed recently to optimise freight movement and maximise efficiency for each voyage. These digital tools are predominantly tailored to facilitate last-mile deliveries as they involve processing a large amount of data in a Business-to-Consumer operating model [31]. With the shift in consumer preference to purchase goods using e-commerce platforms, these tools ensure that purchase orders are fulfilled efficiently and reliably. The critical 'handshake' between last-mile deliveries and upstream production facilities places the burden on the shipping industry to meet the high expectations expected by both the companies that produce these products and their intended customers. These expectations come in the form of lead times for delivery, due care during cargo handling and, more recently, the environmental footprint from transportation. With over 90% of the world's cargo now transported by ships, it is clear that the maritime industry is responsible for the growth of the world's economies by providing

an avenue for the cost-effective transportation of goods required to sustain the upward Gross Domestic Product (GDP) trajectory of developing countries [32].

This dominance the industry has in this sector of moving cargo can be dated back several hundreds of decades ago to the creation and use of combustion engines, which was a pivotal backbone to the societal economy in the 2nd Industrial Revolution. Even before this, albeit on a much smaller scale, ships with sails carried cargo for trade between the East and the West. Goods such as silk, tea and spices travelled to the West, and in exchange, precious metals, horses, and technology were sent to the East [33]. The maritime industry has not taken this dominance for granted. Continuous improvements and innovative solutions have always been explored and implemented to ensure the optimised use of resources [34, 35]. Close collaborations between key stakeholders, including international bodies such as the IMO, governments, ports, and industry players, have resulted in several revolutionary measures to optimise port management and ambitious targets to combat visible signs of climate change by being accountable for the emissions they produce [36-39]. In December 2015, 196 signatories to the Paris Agreement, a landmark multilateral climate change accord, pledged to communicate their plans to reduce anthropogenic GHG emissions. These plans, known as Nationally Determined Contributions (NDC), are to be submitted every five years to reflect progression to achieve a country's highest possible ambition. In partnership with this goal, the IMO has consequently adopted ambitious GHG reduction targets to be achieved incrementally by 2050. Compared to the 2008 emission baseline, these targets have consequently motivated the maritime industry to decarbonise their operations as a business-as-usual trajectory projected to be inadequate to meet the 50% reduction in absolute GHG emissions goal by 2050 [40]. The fourth IMO GHG study in 2020 employed a new method which was able to distinguish the emissions of international shipping from domestic estimated that shipping accounts for 2.89% of the total global CO_2 emissions or 1,056 million tonnes of CO_2 equivalent in 2018,

approximately 90% of 2008 emissions which based on this new method stands at 1157 million tonnes of CO_2 equivalent [40]. This method is aligned with IPCC's guidelines and recommendations [41].

As part of this incremental approach, IMO envisages a near-term goal of reducing the carbon intensity, a measurement of carbon dioxide emissions per ton of cargo transported per nautical mile, by 40% by 2030 to serve as a necessary checkpoint to validate the industry's systematic, methodical plans for 2050. To meet this target, IMO has tightened the EEDI, requiring new ships built in 2025 to be 30% more efficient than a reference level of vessels of the same type and size. As of 2024, the current carbon intensity reduction, compared to 2008 levels is at 30% [42].

Moving forward, an anticipated increase in demand for international shipping is projected by the United Nations Conference on Trade and Development (UNCTAD) [43], and prudent long-term sustainable solutions are needed to address the potential upward trajectory of absolute emissions. The use of energy-saving technologies and improvements to operational efficiency would have a tangible effect on the carbon intensity but to realise the 2050 goals, a substantial amount of effort by the IMO and the industry would be required to explore the use of low-carbon and alternative fuels along with several GHG pathway models [44, 45]. Several Life-Cycle Assessments (LCA) of potential fuels have been conducted and published [46-49] to this effect. These assessments are guided by the standardised ISO 14040:2006 metric, which encompasses raw material acquisition, production, construction, operation, demolition, and recycling. This standard streamlines the data to ensure that it is accountable and verifiable. Furthermore, these LCAs consider several unique factors such as human health, environmental impact, and social aspects from a 'cradle to grave', which provide a holistic overview of the true impact of potential candidates to replace fossil fuels. Examples of fuels identified for consideration include liquefied natural gas, liquefied petroleum gas, methanol, biofuels,

hydrogen, and ammonia. These fuels have diverse feedstocks, pre- and post-treatment requirements, energy capacity, and technological maturity. Assess these fuels comparatively, it would be beneficial to benchmark these fuels against different rubrics for a levelized analysis. These could include green credentials, price, energy density, availability, infrastructure and storage, and technology maturity, as seen in Table 2-1 with its corresponding legend [50-52].

Table 2-1: Alternative fuels benchmarking against different performance criteria[20]

Fuel	Green Credentials	Price	Energy Density	Availability	Infrastructure and Storage	Maturity of Technology
LNG						
LPG						
Methanol						
Biofuels						
Hydrogen						
Ammonia						

Strong	Neutral	Weak

All forerunning future fuels identified provide a spectrum of benefits to leverage and challenges to overcome. Besides its intrinsic properties, much of the consideration for selecting the fuel of choice would also largely depend on the type of marine vessel needed to fulfil the desired application. With many marine vessels available, understanding the features and limitations of the ship's design would clarify the ability to satisfy the operational requirements whilst powered by an alternative future fuel. Referencing Table 2-1 above, this could broadly depend on energy density and storage space. Consideration should also be given to the geopolitical preferences and availability of the desired alternative fuel [53]. Unlike traditional fuels, which

are available across the globe due to their longstanding usage and demand, future fuels will require heavy investments to develop the necessary infrastructure. Furthermore, due to their intrinsic properties, these fuels would likely result in the developed infrastructure being tailored explicitly for one future fuel, which is unlikely to be interchangeable [54]. This would undoubtedly lead to hesitation in commitment as governments would delay their final investment decision till some level of coherence within the industry is reached.

2.2 Future Fuels for Marine Propulsion

For centuries, marine vessels have used fossil-based fuels for propulsion. The industry started with solid-state fuels such as coal and transitioned to liquid-based fuels such as heavy fuel oil and diesel. Over the past decade, gaseous fuels such as natural gas have gained traction with several shipowners as the preferred fuel choice. The common denominator which is to ensure the reliable movement of ships from the point of loading to the point of unloading, however, has stayed the same. The continued reliance on fossil-based fuels has inevitably been driven by their availability, technical knowledge of use, and predictable price fluctuations.

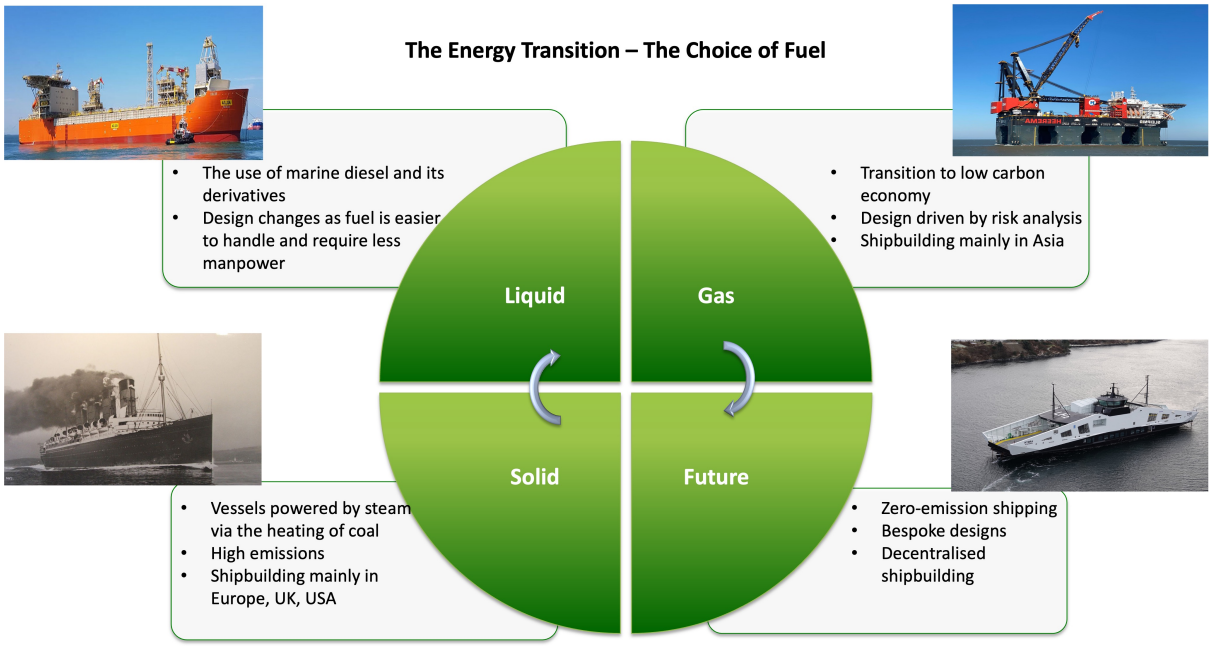

Figure 2-1: Marine fuel transition

Major disruptions to the supply chain of these fossil-based fuels would undoubtedly cause significant impairments to the world's economy, considering that over 90% of the world's cargo is moved by ships. Hence, a realistic and systemic approach must be considered for a just energy transition. The overarching future energy landscape is anticipated to be notably different driven by the shared vision of reducing or potentially eliminating the release of GHG emissions. The energy transition for the marine industry will be strongly aligned with the developments of several adjacent land-based sectors. These include the automotive, aviation, land transportation, and energy for domestic and industrial uses. The availability and preferred choices of fuel in these industries would provide a sound value proposition to the marine industry to follow suit. This is primarily guided by the dependence on land-based production of these future fuels to be used in the marine industry. It is prudent to acknowledge that regardless of the industry in question, the goal is clear: limit the rise in global temperature to below 1.5°C compared to pre-industrial levels to negate the negative impacts of climate change.

According to the IMO, the reporting of GHG emissions of any fuel will need to consider the emissions produced throughout its entire lifecycle. This aims to give a holistic representation of the emissions produced, with the goal of accountability and a concerted effort to reduce these emissions.

The well-to-wake (WtW) emissions framework represents a holistic approach to assessing the environmental impact of fuels over their entire life cycle, from initial feedstock acquisition to final energy conversion onboard a vessel. In contrast to simpler emission accounting methods, such as tank-to-wake (TtW) or well-to-tank (WtT), the WtW approach captures all upstream and downstream processes, enabling a more accurate and equitable comparison of fuels with different production and utilisation pathways.

WtW analysis is particularly critical in the maritime context due to the sector's diversity in vessel types, fuel requirements, and voyage profiles. Additionally, as the industry explores a range of zero- and low-carbon fuels—including electricity, hydrogen, ammonia, and methanol—traditional TtW assessments are no longer sufficient. For example, green hydrogen and green ammonia emit no carbon dioxide at the point of use but may have significant upstream emissions depending on the electricity source and production process. Without WtW accounting, such fuels could be incorrectly assumed to be carbon neutral.

The WtW framework is divided into two main components, as mentioned above and comprises the following:

1. **Well-to-tank (WtT):** This includes all emissions associated with fuel production, starting from resource extraction (e.g., water for electrolysis, biomass for biofuels, or air for nitrogen in ammonia) to the delivery of usable fuel to the vessel's fuel tank. WtT emissions cover:
    a. Feedstock extraction and processing
    b. Fuel synthesis and refinement

c. Fuel compression, liquefaction, or other conditioning

d. Transportation and distribution

e. Onboard storage systems and handling

2. **Tank-to-wake (TtW)**: This refers to emissions produced during fuel conversion into mechanical or electrical energy onboard the vessel. This stage includes:

    a. Combustion or oxidation of fuel in engines or fuel cells

    b. Emissions of all GHGs

    c. Conversion efficiency and losses

A central aspect of any WtW assessment is the clear and transparent definition of system boundaries. Without consistent boundaries, comparisons between fuels can be misleading. For example, if one study includes infrastructure construction (e.g., electrolyser or battery manufacturing) and another does not, the results will not be directly comparable. These boundaries are aligned with ISO 14040 and ISO 14044 standards for Life Cycle Assessment (LCA) and are appropriate for decision-making at the operational level (fuel switching, vessel retrofitting, infrastructure development).

There are several different energy transition pathways identified to achieve this goal collectively. These pathways include a mix of (i) incorporating carbon capture technologies with fossil-based fuels to prevent GHG release (ii) using zero-carbon fuels (iii) using carbon-neutral fuels. Examples of these pathways are shown below:

2.2.1 Hydrogen

Hydrogen is crucial in the global energy landscape, produced, transported, and consumed in large quantities across various sectors. As of 2020, global hydrogen demand was approximately 88.5 million tonnes annually, with the majority of this demand coming from industrial applications and oil refining, according to the International Energy Agency (IEA). Despite its widespread use, the existing hydrogen industry faces significant environmental challenges. The

current methods for hydrogen production are predominantly carbon-intensive, leading to substantial greenhouse gas emissions. Specifically, about 95% of hydrogen is produced through steam methane reforming (SMR) of natural gas, a process known as 'grey hydrogen.' This method is highly polluting, releasing between 70 and 100 million tonnes of CO_2 annually, as reported by the European Commission. The environmental impact of grey hydrogen is a primary concern, mainly as hydrogen production is often concentrated in coastal and inland ports, where the infrastructure for production and transportation is most developed.

Given the environmental challenges associated with grey hydrogen, there is a growing emphasis on developing low-carbon alternatives. One of the most promising alternatives is green hydrogen, also called e-hydrogen. Green hydrogen is produced through water electrolysis, using electricity generated from renewable sources such as wind, solar, or hydropower. This method of production results in a fuel that is free from greenhouse gas emissions, making it an attractive option for reducing the carbon footprint of hydrogen production. Green hydrogen is an absolute zero GHG fuel on a well-to-tank (WTT) lifecycle basis. Furthermore, when used with Proton Exchange Membrane Fuel Cells (PEMFCs) onboard, green hydrogen can achieve full well-to-wake (WTW) zero GHG emissions.

Two main types of electrolysers are used to produce green hydrogen: alkaline electrolysers and Proton Exchange Membrane (PEM) electrolysers. Both of these technologies are mature and have reached Commercial Readiness Level (CRL) 10, indicating their readiness for large-scale deployment. Alkaline electrolysers are a well-established technology that has been used for many years. PEM electrolysers are a more recent innovation that offers certain advantages, such as higher efficiency and the ability to operate at variable loads, making them well-suited for integration with renewable energy sources.

As of 2021, the global capacity for green hydrogen production was still relatively modest, with around 600 MW of operational electrolyser capacity worldwide. This capacity corresponds to

producing approximately 90,000 tonnes of green hydrogen per year. The distribution of this capacity was uneven, with 200 MW located in China and 170 MW in Europe. However, the industry is rapidly expanding, and significant growth is expected soon. An additional 1.6 GW of electrolyser capacity, either at the Final Investment Decision (FID) stage or under construction, will come online globally by 2023. This expansion is driven by the growing recognition of green hydrogen's potential to decarbonise various sectors, particularly heavy industries that are difficult to electrify and are currently significant sources of greenhouse gas emissions.

The transition to green hydrogen is essential for achieving global climate goals, as it offers a pathway to reducing emissions from a wide range of industries, including steelmaking, chemical production, and transportation. As the demand for green hydrogen increases, competition for this valuable resource will intensify, particularly in the coming decade. The importance of green hydrogen extends beyond its direct use as a fuel; it also serves as the foundation for the production of 'e-fuels,' such as e-ammonia and e-methanol. These e-fuels are crucial for maritime transport and aviation sectors, where electrification is challenging and must be scaled up to be widely adopted.

In the European Union, efforts to scale up green hydrogen production are already underway. The FuelEU Maritime initiative, for example, mandates that by 2034, at least 2% of maritime fuel in the EU must be sourced from green hydrogen or green hydrogen-derived e-fuels. This regulatory push is expected to drive significant investments in European green hydrogen infrastructure and production capacity. Additionally, Norway is taking proactive steps to secure its future hydrogen supply. Norwegian shipping companies are signing agreements of intent with green hydrogen producers to ensure a steady fuel supply for future zero-emission fleets. These agreements are part of a broader strategy to position Norway as a leader in transitioning to a hydrogen-based economy.

In Singapore, the national hydrogen strategy was released by the Ministry of Trade and Industry in October 2022, signalling a push in exploring hydrogen's role in their energy mix. The calibrated approach undertaken by Singapore ensured that sufficient investment was made available to experiment, develop, and support research, infrastructure and supply chains, as well as a competent workforce. However, due to the land scarcity in Singapore, the use of renewable energy for green hydrogen production is limited. Furthermore, with Singapore buying water from neighbouring countries like Malaysia for domestic consumption, it would be challenging to justify its use (i.e. water) for energy production. However, Singapore's energy infrastructure remains compatible with integrating alternate sources of energy, including electrons delivered via subsea cables.

One of the challenges facing the green hydrogen industry is the so-called chicken-and-egg problem, where the development of hydrogen infrastructure and the adoption of hydrogen as a fuel are interdependent. To overcome this challenge, some producers are taking a comprehensive approach by supplying green hydrogen and providing the necessary infrastructure to support its use. For example, companies offer quayside compressed hydrogen in standard ISO containers, making it easier for ships to refuel with hydrogen at ports. This integrated approach helps to address the infrastructure bottlenecks that have historically slowed the adoption of new fuels.

In summary, while the current hydrogen industry relies heavily on carbon-intensive production methods, the shift towards green hydrogen offers a promising solution for reducing greenhouse gas emissions and advancing global climate goals. Green hydrogen production capacity development is accelerating, driven by regulatory initiatives, technological advancements, and growing demand from industries seeking to decarbonise. As green hydrogen becomes more widely available, it will play a critical role in the energy transition, supporting the production of e-fuels and enabling the decarbonisation of otherwise difficult sectors to electrify. The next

decade will be crucial for the scale-up of green hydrogen, and the actions taken now will determine its role in the future energy landscape.

2.2.2 Ammonia

Ammonia is widely available globally as a nitrogen-based fertiliser and has been instrumental in increasing agricultural yields. The process of producing ammonia has been industrialised through the Haber-Bosch process by scientists Fritz Haber and Carl Bosch. This process synthesises ammonia from nitrogen and hydrogen under high temperatures and pressure over an iron catalyst, enabling commercially viable ammonia production in 1913. This breakthrough has since set the precedence for developing more energy-efficient modern-day ammonia production plants, which encapsulated an integrated energy balance scheme to allow for an optimised design that reduced equipment sizes for compressors and catalyst volumes in the reformers. These improvements have produced over 180 million tonnes of ammonia annually, accounting for 1.5% of global emissions [55]. The distribution network for the produced ammonia for further refinement to end products is mostly localised, with about 10% or approximately 14 to 17 million tonnes transported as marine cargo in its liquified form. Specialised liquified gas carriers allow ammonia to be stored at cryogenic temperatures at atmospheric or ambient temperatures with pressure exceeding 16 bars. This is typically influenced by the type of storage tank used, which can either be fully or semi-refrigerated. Pressurised tanks, however, would have a layer of insulation to prevent heat ingress and minimise boil-off [56]. As ammonia contains 17.6 wt.% hydrogen, it can be used as a fuel [57]. This diversification in the end use of ammonia requires a different set of considerations with consideration for safety in the event of an inadvertent release of toxic ammonia gas. Its high toxicity can harm marine life if released into the water through spills or leaks, potentially causing long-term ecological damage. Ammonia is also highly irritating and dangerous to ship crew, requiring careful handling, ventilation, and protective equipment. In confined shipboard

spaces, even small leaks can create significant health and safety risks. Additionally, ammonia's corrosive properties can affect marine infrastructure if not properly contained. These factors necessitate stringent safety protocols, specialized fuel systems, and emergency response plans to protect both crew and the surrounding marine ecosystem.

2.2.3 Methanol

Methanol is an organic chemical widely used to manufacture olefins, which are subsequently used to make end products, including plastics, paints, and detergents. The primary source of methanol production comes from synthesis gas, an off-stream from oil refineries or coal gasification [58]. Syngas as it is commonly referred to, a mixture of carbon monoxide and hydrogen undergoes further refinement to produce methanol. One such production method is via the Fischer–Tropsch synthesis, or gas-to-liquid technology [59]. This fossil-based production pathway generally contributes to the bulk of methanol production today albeit a growing percentage now comes from alternate sustainable sources. These pathways include feedstocks such as biomass and captured carbon dioxide which can be converted to methanol via pyrolysis and hydrogenation respectively [60, 61]. Considering that methanol contains carbon atoms, there are several counterarguments as to whether this is indeed a future fuel for marine propulsion. The rationale for considering this as a future fuel is driven by the motivation that methanol can be regarded as a carbon-neutral fuel. This implies that the carbon dioxide released during its use phase (i.e. when converting from chemical potential energy to valuable work as a fuel) was removed from the atmosphere during the extraction phase (i.e. as a biomass).

Furthermore, this rationale is also valid if captured carbon is used as a feedstock. The use of methanol as a fuel could potentially be carbon negative if the released carbon during utilisation is captured using carbon capture technologies and recycled to produce methanol in a closed-loop circular carbon economy [62].

2.2.4 Electrification

Marine electrification is an alternate pathway for zero-emission shipping using electrons for energy. Fuel cells, ESS or marine batteries allow vessels to eliminate emissions, add redundancy as a backup power source, increase energy conversion efficiency, and reduce maintenance by reducing rotating equipment on board the vessel. These advantages have encouraged the number of electrified ships in operation to progressively increase, as shown in Figure 2-2 below [63, 64].

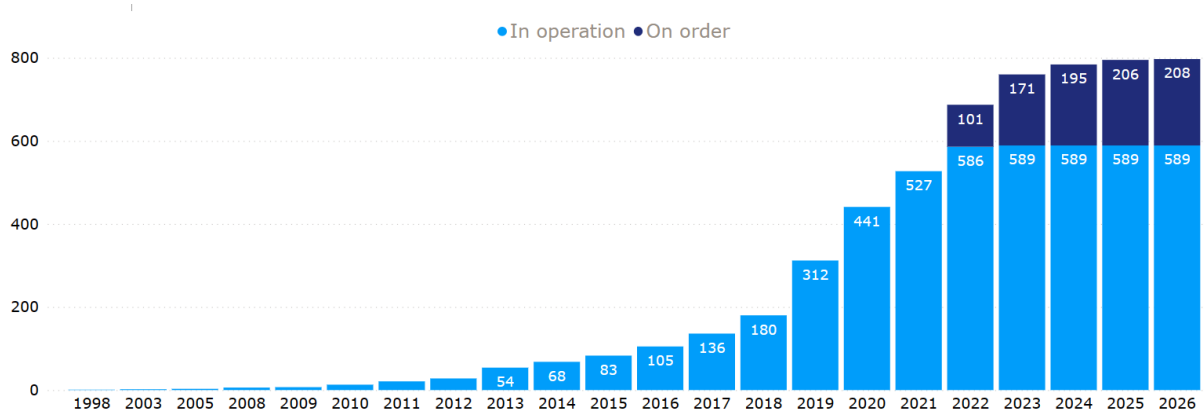

Figure 2-2: Number of electric vessels in operation and order book outlook

Marine batteries have been designed and used to address several different applications as part of the overall marine propulsion system as illustrated in Figure 2-3 below.

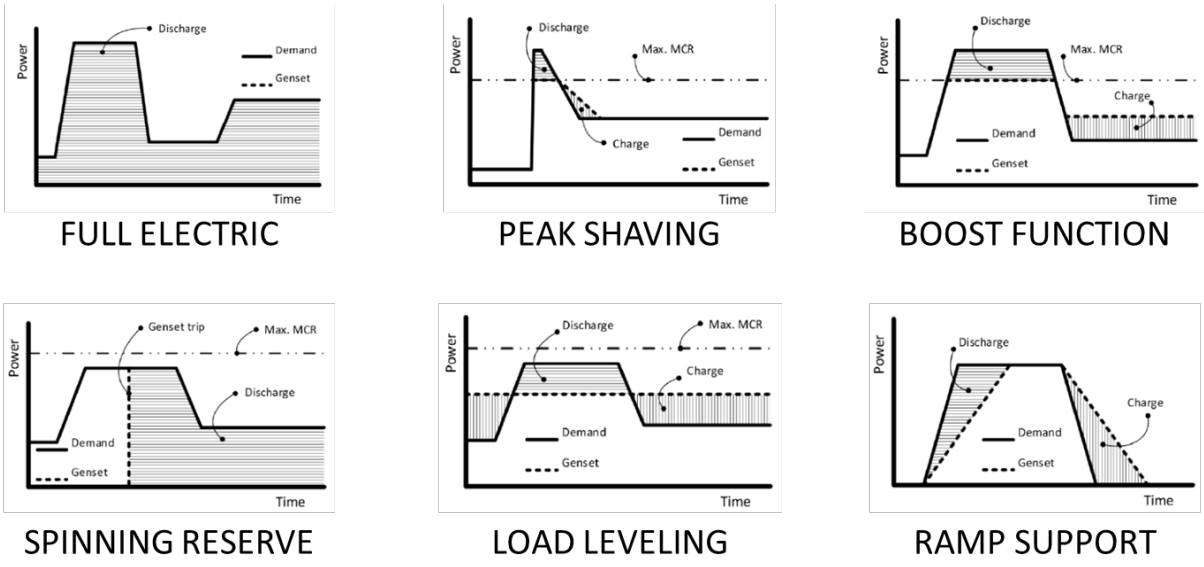

Figure 2-3: Different applications for marine batteries

These applications are described in Table 2-2 below:

Table 2-2: Description of the operational scenarios supported by marine batteries

Operational Scenarios	**Description**
Full Electric	The complete use of batteries for propulsion as an energy source
Peak Shaving	Batteries used to support the intermittent peak loads experienced by the vessel during operations
Boost Function	Batteries assist to increase the performance capability of the vessel for short periods of time as required. This provides an alternate to sizing a bigger primary energy source to reduce cost and footprint
Spinning Reserve	Batteries provide backup power source for mission critical applications
Load Leveling	Batteries allow the primary energy source to run at constant load (i.e. primary energy source fixed at most optimum operating point)
Ramp Support	Batteries are used to offset to required power and consequently reducing the ramping stress on the primary energy source

Electrified vessels can be classified into three (3) different categories. They are:

1. **Full electric vessels:** 100% powered by batteries. Shore charging infrastructure is required to provide the necessary energy to charge the batteries. These vessels are designed to operate based on a specific voyage to ensure that there is sufficient stored energy within the batteries to complete the journey safely. Hence, there are limitations on the range and downtime to charge the batteries before embarking to the next destination.

2. **Hybrid vessels:** Combination of batteries and another energy source. Batteries are charged periodically during operations. Do not require external intervention to charge the batteries.
3. **Plug-in hybrid vessels:** A combination of onboard energy sources, including batteries designed to be charged during operations and shore charging facilities.

2.2.4.1 Pure Electric Vessels

A pure electric propulsion system relies solely on batteries as the onboard energy source, making it suitable only for vessels operating on short, isolated routes. The range of these vessels is limited by their ESS capacity, with a significant safety margin factored in. This safety margin typically includes a "take me home" capability, which ensures that the vessel can return to base even if part of the system fails or in a fire or other emergency.

Pure electric propulsion is primarily supported within a specific segment of the maritime industry, particularly for small passenger vessels that operate on short routes within sight of land and support services. These vessels, however, need to be fully integrated into the broader commercial marine industry due to their inability to meet the stringent Flag and Type Approval standards required for the safe operation of marine craft.

Since the commercialisation of maritime batteries began in 2010, there has been a significant focus on deploying fully electric vessels. This effort has involved operators, Type Approval agencies, and Flag authorities. Several vessels have been designed and built for fully electric operations, adhering to strict safety criteria that address all aspects of emergency procedures. Typically, these vessels also feature a backup charging source onboard to ensure safety in an emergency.

One critical regulation supporting the deployment of fully electric vessels is the requirement for "take me home" power. This allows vessels to operate entirely on electricity, charge at shore, and demonstrate reduced emissions and maintenance costs while ensuring safe and risk-free

operations. The current ships utilising this technology are Roll-on/Roll-off Passenger (RoPax) ferries, inland waterway vessels, port service vessels, and ships operating in micro-economies, such as high-density island hubs.

As of 2023, the market for pure electric vessels is experiencing rapid growth, driven by the development of swappable energy systems. These systems enable vessels to operate with zero emissions by using the ESS as a fuel source with a defined operational window. The capability to achieve 100% zero-emission operations is crucial for the marine industry to meet the targets set by the International Maritime Organization's (IMO) Initial GHG Strategy for 2030 and 2050. This expanding market reflects the industry's commitment to reducing its environmental impact and advancing toward a more sustainable future for maritime operations. Pure electric vessels are currently at CRL 10, but adoption within the industry has been curtailed by their operability limitations to short, isolated routes, as mentioned in the previous paragraph.

2.2.4.2 Hybrid Vessels

Hybrid electric vessels were introduced to the commercial marine industry on a large scale, enabling integration into ships of various sizes. A key motivation for this adoption was to optimise vessel operations by running power source engines and generators in a “constant speed, constant power” mode, thereby improving the efficiency of fuel-burning systems. In this setup, fuel-driven systems operate at a constant speed, while the ESS provides a dynamic response to handle intermittent loads and maintain stable power quality. This allows ships to operate in hybrid, electric, or traditional fuel-driven modes.

The result has been significantly enhanced vessel performance, reduced greenhouse gas (GHG) emissions, and lower maintenance costs. Additionally, the risk of downtime has been positively impacted, with ships experiencing more reliable operations. For operators, this means reduced costs, easier compliance with regulatory targets, and the ability to convert existing vessels to

hybrid electric systems quickly and cost-effectively. Hybrid electric systems have seen the most adoption in the maritime sector and are regarded as having reached CRL 11 with the largest installed capacity of 10 MWh in cruise vessel *AIDAprima*.

2.2.4.3 Plug-in Vessels

Plug-in hybrid electric ships are increasingly adopting dedicated onshore infrastructure, which allows them to reduce their dependence on onboard power generation. Instead of relying solely on traditional fuel sources, these vessels can charge their batteries using grid power and renewable energy, significantly lowering operational costs. This shift not only makes operations more cost-effective but also enhances the overall lifespan of the vessel by reducing wear and tear on onboard systems. The integration of shore charging infrastructure has become an essential component of this approach, enabling ships to maximise the benefits of hybrid-electric technology.

Plug-in hybrid vessels have demonstrated substantial cost savings and environmental benefits, fuelling a solid demand for adoption across the maritime industry. These vessels can operate more efficiently, reducing greenhouse gas emissions and meeting increasingly stringent environmental regulations. The ability to recharge using clean energy sources further strengthens their appeal, making them a viable solution for sustainable maritime operations.

By 2022, the adoption of plug-in hybrid vessels had gained significant momentum. A notable example of this trend is the 27,000 GT cruise ship *Color Hybrid*, which has been equipped with a 5 MWh battery system since 2019. This installation highlights the industry's commitment to embracing hybrid-electric technology on a larger scale, paving the way for more widespread implementation in the future.

2.2.4.4 Fixed Charging Infrastructure

Pure electric and plug-in electric vessels discussed in the previous section require a method of charging and a source of charging energy. Should the charging grid be powered by renewable

electricity, these vessels will consequently operate on absolute zero emissions. Vessels can charge either at shore, offshore or in swappable batteries.

Integrating fixed charging facilities presents a valuable opportunity for optimising space and resources in the maritime industry. These stations, essential for the effective operation of electric vessels, must be equipped with a substation that converts alternating current (AC) power into direct current (DC) power, which the batteries require. This conversion is straightforward but highly beneficial, allowing faster and more efficient battery charging. DC power minimises efficiency losses during the charging process, ensuring the batteries reach full charge more quickly and with minimal energy waste.

Fixed charging stations are commercially available in various power outputs, catering to the diverse needs of electric vessels. For instance, the power requirements for pure electric vessels can range from 1 MW for smaller ships to as much as 10.5 MW for larger ones. These vessels typically use automatic connections to facilitate charging, making it quick and efficient. For example, it takes just 5 to 9 minutes to charge the 1.2 MWh of energy needed for a single 4-kilometre crossing [65]. More powerful charging systems, capable of delivering up to 23 MW, are also available on the market. However, the expansion and efficiency of these systems are often limited by the infrastructure in place.

Infrastructure development poses a significant challenge when adopting fixed charging stations. Bringing sufficient power to a location, especially one that previously had little to no demand for such high energy, can be extremely costly. This is particularly true when power needs to be transmitted over long distances, resulting in high initial costs and long payback periods. Furthermore, the ability to expand existing power networks to enhance efficiency is often limited, making it difficult to justify the investment.

One solution to this challenge is to build fixed land-based battery ESS at the point of vessel use, especially where existing power generation infrastructure is available. These land-based

ESS can continuously absorb and store energy from existing power sources, which can then be rapidly transferred to vessels when they dock. This approach mitigates the high costs associated with constructing permanent infrastructure. It allows operators to rely on the existing power grid or develop local renewable energy sources to charge the land-based ESS. This strategy reduces costs and enables a quicker return on investment.

Sometimes, vessel operators are legally mandated to use renewable energy for charging. This requirement has driven the deployment of local renewable energy sources, such as solar or wind power, and the development of microgrids. Operators are also increasingly negotiating with existing energy infrastructure providers to purchase renewable energy through arbitrage, ensuring their vessels are charged sustainably.

Offshore charging technology is also advancing, with prototypes having completed harbour trials and expected to be deployed soon at offshore wind farms. This innovative method offers range extension and standby power for electrified offshore vessels, such as Crew Transfer Vessels (CTVs) and Service Operation Vessels (SOVs). By allowing these vessels to charge directly at an offshore wind turbine, the system ensures that the electricity is fully renewable, further reducing the environmental impact of maritime operations.

The rise of pure electric and plug-in electric vessels has necessitated the commercialisation of high-power charging infrastructure that can deliver rapid charging—sometimes in as little as 5 minutes—while meeting the marine industry's complex safety and operational requirements. The fixed battery market, crucial for supporting this infrastructure, is primarily dominated by systems like crane-operated or cable reel charging connections, strongly emphasising autonomous connections. These automated systems are designed to enhance safety and reliability, which are critical factors in the demanding maritime environment.

However, there are trade-offs to this approach. The need for fast charging, while essential for maintaining vessel schedules and meeting revenue targets, can reduce the lifespan of batteries.

This accelerated wear increases the cost per kilowatt-hour (kWh), as the batteries need to be replaced more frequently. Despite this, the benefits of fast charging—ensuring vessels can meet strict schedules and operational commitments—often outweigh the downsides, especially in a commercial context where time is a critical resource.

Figure 2-4: Fixed charging infrastructure

To summarise, integrating fixed charging facilities into the maritime industry offers significant advantages, from optimising space and resources to enabling faster, more efficient charging. While infrastructure development remains a substantial barrier, innovative solutions like land-based ESS and offshore charging are helping to overcome these challenges. The demand for renewable energy in vessel operations drives the deployment of local renewables and microgrids, ensuring that maritime activities become increasingly sustainable. As the market for pure electric and plug-in hybrid vessels continues to grow, so will the need for advanced charging infrastructure that balances speed, efficiency, and safety in a rapidly evolving industry.

2.2.4.5 Swappable Battery Charging

Swappable battery systems offer a streamlined approach to maritime energy management by allowing batteries to be charged offsite and physically replaced on the vessel. This method significantly reduces the time required to recharge a ship, as the vessel can quickly transition to a fully charged battery without waiting for onboard recharging. By charging the batteries separately, operators can optimise the process to lower the cost per kilowatt-hour (kWh), making energy consumption more efficient and cost-effective. The swappable battery packs are strategically designed in fixed ISO sizes, such as 20-foot or 40-foot containers to ensure compatibility to a larger range of marine vessels.

One of the critical advantages of swappable batteries is their potential to transform the financial model for shipowners. Instead of bearing the high capital expenditure (CAPEX) of purchasing batteries outright, shipowners can shift to an operational expenditure (OPEX) model through energy-as-a-service contracts. This approach reduces the upfront financial burden and offers ongoing cost savings. Several manufacturers, including EST-Floattech, Fleetzero, Furukawa & Eco Marine Power, SEAM, Shift Clean Energy, Wärtsilä, and Zero Emission Services, supply commercially swappable batteries. These companies often offer energy-as-a-service options, providing pay-per-use contracts that cover maintenance and operation, potentially reducing OPEX by up to 77%.

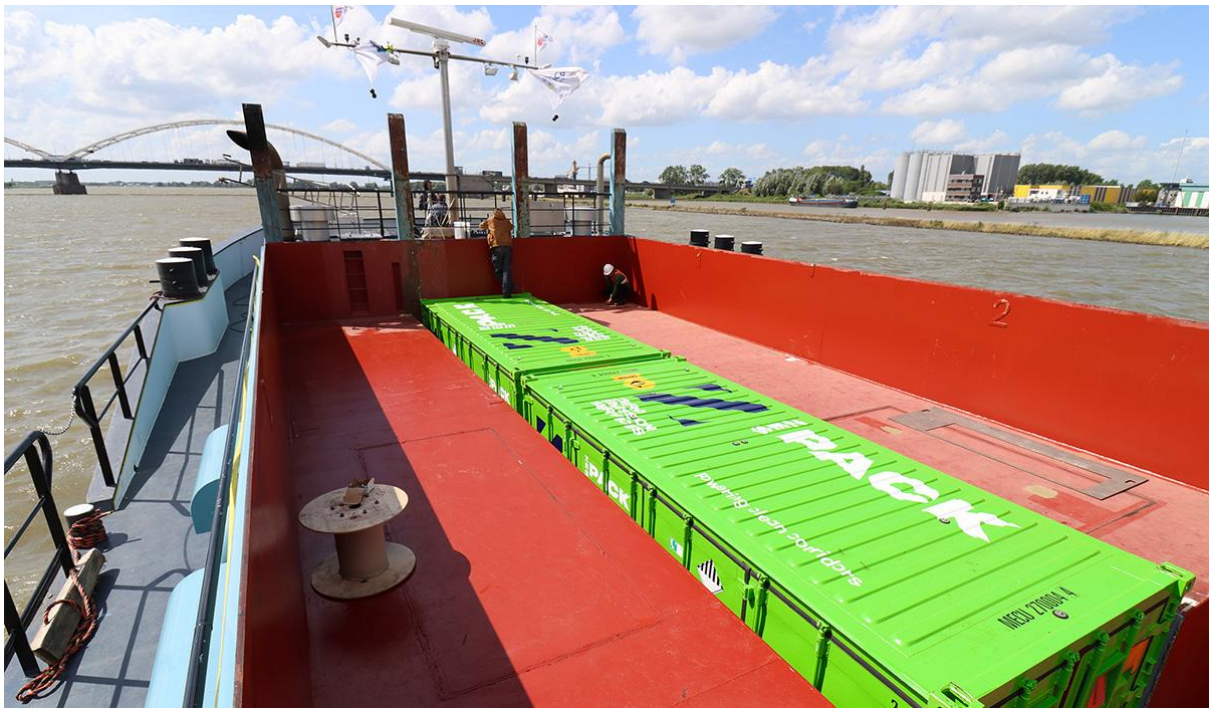

Figure 2-5: Swappable marine batteries in 20-foot ISO containers

Some suppliers have developed swappable ESS with capacities of up to 2.1 MWh, housed within standard ISO containers, to facilitate easy integration and handling. This design simplifies retrofitting existing vessels and allows for efficient quayside battery exchanges.

While the adoption of swappable battery technology in the maritime industry has been limited so far, it is gaining traction. Currently at Commercial Readiness Level 9 (CRL9), swappable batteries are expected to reach CRL10 by 2023. One supplier, Aggreko, has reported significant interest in swappable battery services, with at least 120 vessels registered for these services across 12 locations slated to open by mid-2023. This growing interest suggests that swappable battery technology could soon become a mainstream solution for reducing emissions and improving efficiency in maritime operations.

2.3 Summary of Alternate Fuels for Marine Propulsion

As the maritime industry faces increasing pressure to reduce greenhouse gas emissions and align with global decarbonisation goals, alternative fuels are becoming central to the future of

sustainable shipping. Traditional marine fuels like heavy fuel oil are being phased out in favor of cleaner energy sources, with hydrogen, ammonia, methanol, and electrification emerging as the leading contenders. Each of these alternatives presents a unique set of characteristics that influence their suitability for different vessel types and voyage profiles. Key factors such as energy density, fuel availability, greenhouse gas emissions, ease of bunkering, safety, and compatibility with existing propulsion systems all play a critical role in determining the practicality of adopting these fuels. Hydrogen and ammonia offer zero carbon emissions and are promising for long-term sustainability, but they require new infrastructure and engine designs, as well as robust safety protocols due to their storage challenges and toxicity, respectively. Methanol serves as a more transitional option, with existing compatibility and simpler handling, although it still produces CO_2 unless sourced renewably. Electrification, on the other hand, provides the highest operational efficiency and zero-emission potential, but its limitations in energy storage and range restrict its use to short-sea shipping and port operations. The following table provides a detailed comparison of these fuel options across key operational and environmental parameters to support informed decision-making in the transition to cleaner marine propulsion.

Table 2-3: Summary of alternate fuels for marine propulsion

Parameter	**Hydrogen (H_2)**	**Ammonia (NH_3)**	**Methanol (CH_3OH)**	**Electrification (Batteries)**
Energy Density (by volume)	Very low (8–10 MJ/L @ 700 bar)	Moderate (~12.7 MJ/L)	Higher (~16 MJ/L)	Low (~0.25–1 MJ/L)
Energy Density (by mass)	High (~120 MJ/kg)	Moderate (~18.6 MJ/kg)	Lower (~20 MJ/kg)	Very low (~0.1–0.3 MJ/kg)
State at Ambient Conditions	Gas (requires compression or liquefaction)	Liquid (under mild pressure)	Liquid	Solid-state or liquid-electrolyte cells
GHG Emissions (at point of use)	Zero (only water vapor)	Zero (if fully combusted or in fuel cells)	Low (CO_2, but can be renewable)	Zero (during operation)
Toxicity / Safety	Flammable, high leak risk	Toxic, corrosive, requires strict handling	Flammable, less toxic than ammonia	Safe, but thermal runaway risk
Infrastructure Maturity	Emerging	Emerging	Well-established	Limited to small vessels / short distances
Ease of Storage / Bunkering	Difficult (cryogenic or high-pressure tanks)	Easier than H_2 but still complex	Easy (liquid at ambient conditions)	Charging stations required, slow turnaround
Compatibility with Current Engines	Requires fuel cells or modified engines	Requires new engines or fuel cells	Can be used with modified ICEs or reformers	Requires electric propulsion systems
Energy Efficiency (well-to-wake)	Moderate to low (depends on production & liquefaction)	Low–moderate	Moderate (especially with onboard reforming)	High (especially with green electricity)
Best Use Cases	Fuel cell-based propulsion for clean shipping	Long-haul with zero carbon emissions	Short to medium range, easier transition fuel	Ferries, harbour craft, short-range vessels

Chapter 3

Shipboard Power System and Hydrogen Economy

This chapter introduces the different powertrain configurations for marine vessels. These time-tested propulsion systems are examined to leverage advantages and address their drawbacks. This endeavour aims to ensure the proposed novel next-generation power and propulsion system encompasses the best-in-class configuration. An in-depth, extensive review of hydrogen and its applicability in the marine environment is discussed in detail.

3.1 Augmenting Energy Efficiency for Marine Vessels

Three key factors primarily propel the motivation to enhance marine vessels' energy efficiency. They are (i) cost savings, (ii) emission reduction, and (iii) regulatory compliance. Shipowners can achieve this by considering either design or operational changes to their existing fleet to realise the benefits of improved energy efficiency. Figure 3-1 below attempts to illustrate the myriads of energy efficiency improvement measures that are currently available for consideration by shipowners. Examples of design measures include (i) hull and superstructure, (ii) alternate fuels, (iii) power systems and energy management, whereas operational measures include (i) voyage optimisation, (ii) fleet management, (iii) speed optimisation.

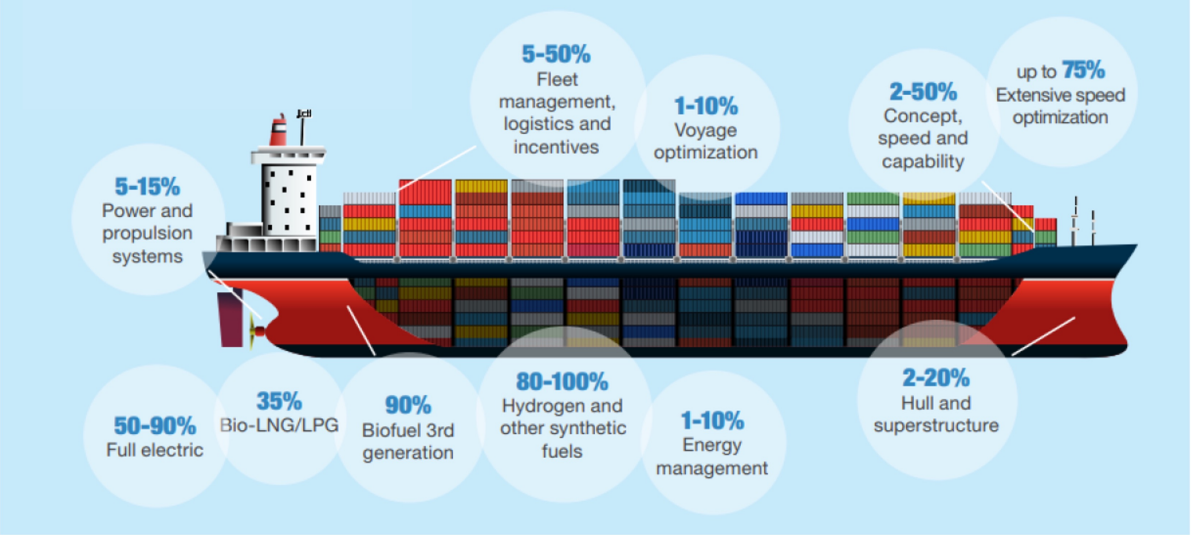

Figure 3-1: Measures to improve the energy efficiency of vessels

There have been several studies on marine vessel design where the emphasis has been on the vessel's physical properties, including optimising the cargo carrying capacity and hull form [66-70]. An [71, 72] improvement to the propellor design was explored to investigate the contribution to overall propulsion efficiency. Besides exploring ways to enhance the efficiency of ships through hull form design, researchers in an attempt to reduce fuel consumption have also investigated the use of lightweight materials for the hull specifically for high-speed crafts with civil and military applications [73]. A summary of the various technical measures to improve vessel efficiency is given in Table 3-1 below:

Table 3-1: Technical measures to improve vessel efficiency

Design Features	**Description**	**Potential Impact (%)**
Hull form optimisation	Through 3D computational fluid dynamic simulation, the vessel designer would be able to determine the most appropriate hull shape that is streamlined to reduce drag as it moves through the water	2 – 20
Propulsion optimisation	The use of pre and/or post-swirl devices to ensure the maximum efficiency of the propellor. Engine power limitation ensures that the main and auxiliary engines operate at an optimum point	15 – 25
Air lubrication technology	To reduce the friction coefficient between the keel of the vessel and water, a layer of bubbles generated by compressed air creates a new boundary layer.	5 – 10
Energy-saving devices	The use of energy-efficient lighting and the use of lightweight construction materials allows for maximum fuel efficiency	3 – 5

Compared to the more traditional naval architecture approach to optimisation, shipboard powertrain optimisation has been relatively nascent. Motivation to explore alternate fuels and powertrain configurations has only developed in recent years following changes to regulatory requirements requiring vessels to meet more stringent environmental emission standards. Some notable work in this area includes alternate zero-emission technologies, fuel cells, batteries, and windsails [74-79]. These studies include the proposed sizing methodology to ensure the most appropriate fuel cell power is considered with a motivation to limit the cost and weight increase compared to traditional fossil-based powertrains. In [77], the well-to-wake emissions of different alternate fuels were considered as part of the analysis to ascertain their

contributions to GHG emissions holistically. This study supported the technical and operational solutions for emission reduction shared in Figure 3-1 with the addition of (i) carbon capture & storage, (ii) air lubrication systems, and (iii) waste heat recovery. Furthermore, this study compared alternate fuels such as ammonia, methanol, hydrogen, and bio-LNG with marine gas oil, and tangible differences in emissions were identified.

Leveraging operational parameters to enhance energy efficiency has also been investigated to improve and address issues such as "just-in-time arrival", voyage optimisation and speed management using digitalisation [80-83]. In [82], weather forecast maps were utilised as the basis for a dynamic programming approach that included ship motion and resistance. This comprehensive review sets precedence to the involvement of digital tools to optimise vessel management for a robust approach to improving energy efficiency. The ability of a vessel to berth just as she arrives in port is the most efficient. This eliminates the requirement for the vessel to wait at anchorage pending berth availability. The time spent at anchorage is idle, and the emissions produced during this period are wasted as no meaningful work is done. In [83], the realities of port congestion were discussed and can be attributed to the uncertainty in the schedules of feeder vessels. These vessels typically have sporadic service plans, resulting in challenges when planning for berths due to uncertain arrival times. A simulation tool to minimise delays was developed based on the optimisation model with a probability distribution.

The reliance on shipping to manage the movement of cargo sustainably necessitates the development of a system-level architecture that encompasses the generation, distribution, power management, and energy storage to limit the emissions of GHG collectively. To this extent, previous studies have included power management strategies that include hybrid and fully electric powertrains [84-86]. These studies discuss heuristic control techniques, including static and dynamic optimisation with fuzzy logic for estimation. Much of these strategies

leverage previous learnings and previous work on land-based hybrid electric vehicles, which have been investigated for decades [87-90]. Broadly, while similarities exist for both hybrid cars and vessels, there are some distinct differences. Vessels typically have several independently controlled power-producing equipment, which eventually is connected to a main switchboard, which provides flexibility and an opportunity for optimisation. Controlling the engines effectively will be the research question, especially for vessels that require a dynamic response.

3.2 Shipboard Powertrain Configuration

A shipboard powertrain configuration encompasses components that generate, distribute, and transmit power to propel a vessel and operate the onboard system. The traditional powertrain typically includes diesel engines or gas turbines connected to generators that produce electrical energy, which is subsequently distributed to various ship systems. In mechanical propulsion, the engine's power is transferred through gearboxes and shafts to the propellers, providing the necessary thrust for navigation.

In modern vessels, hybrid and electric propulsion systems have become increasingly common. Hybrid powertrains often combine traditional engines with electrical systems, where the engines drive generators to produce electricity that powers electric motors connected to the propellers. Fully electric configurations rely entirely on electric power generated by fuel cells, batteries, or renewable sources, eliminating the need for direct mechanical propulsion.

The choice of powertrain configuration depends on the ship's size, purpose, operational requirements, and efficiency goals. Advanced configuration optimises fuel efficiency, reduces emissions, and enhances overall reliability. These systems must also ensure redundancy, safety, and flexibility to adapt to varying sea conditions and power demands. Examples of such systems are given in the following sections below.

3.2.1 Diesel – Mechanical Propulsion System

A typical diesel–mechanical propulsion is shown in Figure 3-2. This propulsion architecture has been the preferred choice for most vessel applications due to its cost-effective design, ease of manufacture and overall operability [91]. The main engines are the sole power source to the propellors that are directly coupled via a drive shaft. As the sole power source for propulsion, the engines are sized to ensure that their Maximum Continuous Rating (MCR) is sufficiently large enough to provide the required power at the most demanding conditions. In this configuration, all other power requirements such as the auxiliaries (i.e. hotel and electrical loads) are supported by diesel generators with adequate redundancy to ensure safe navigation and crew safety. As there is no interface between both powertrains, the decoupled standalone power management system manages load fluctuations independently leading to lower efficiency, especially in dynamic load conditions. These powertrains dominate in applications where the propulsion loads are relatively constant for much of the voyage observed in merchant shipping, including containerships, bulk carriers, and chemical tankers.

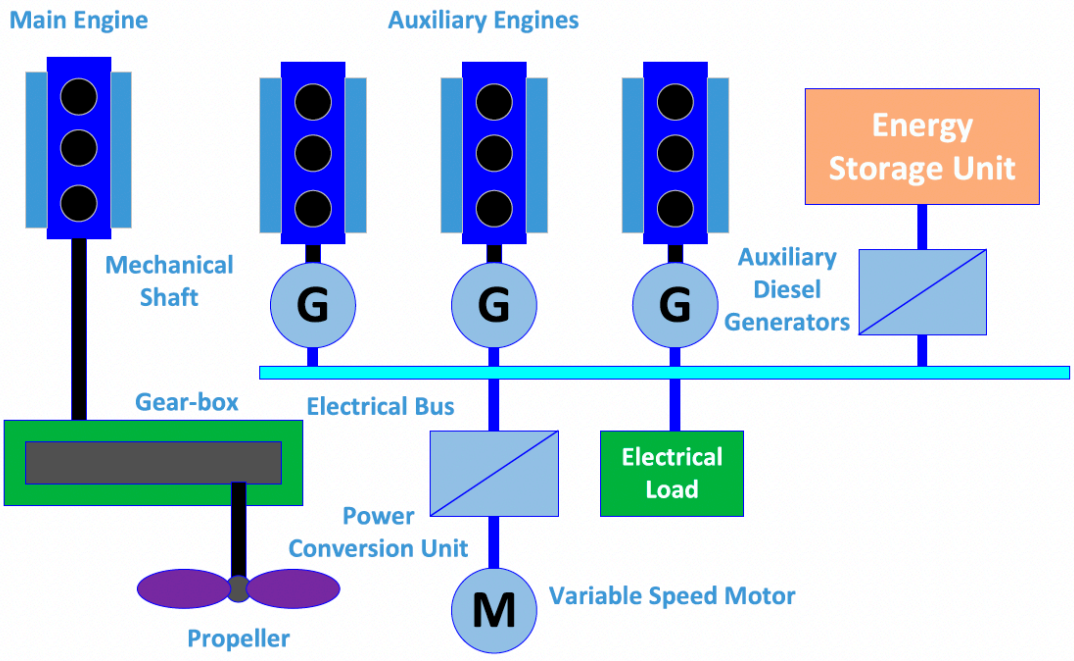

Figure 3-2: Traditional diesel–mechanical powertrain configuration

3.2.2 Diesel – Hybrid Propulsion System

With advancements in frequency converter drives for electric motors and reduced cost of power electronics that include AC-DC rectifiers and DC-AC inverters, there has been an increasing motivation to hybridise vessels. Some early adopters of this technology include ferries, cruise vessels, drilling and, pipe-laying vessels [92-94]. Hybrid vessels incorporate a shaft generator (i.e. motor generator) as an interface between the diesel engine and the main switchboard as seen in Figure 3-3. Essentially, this architecture allows for the main diesel engines to provide electrical power for distribution to all consumers throughout the vessel. This bi-directional motor generator, as the name suggests, can perform the task of a motor, whereby the power is drawn from the switchboard or as a generator when the power is supplied to the switchboard. This configuration provides added flexibility for the vessel's operational demands and improves the overall efficiency of the vessel as the auxiliary engines are now not required to solely provide electrical power to the onboard consumers independently.

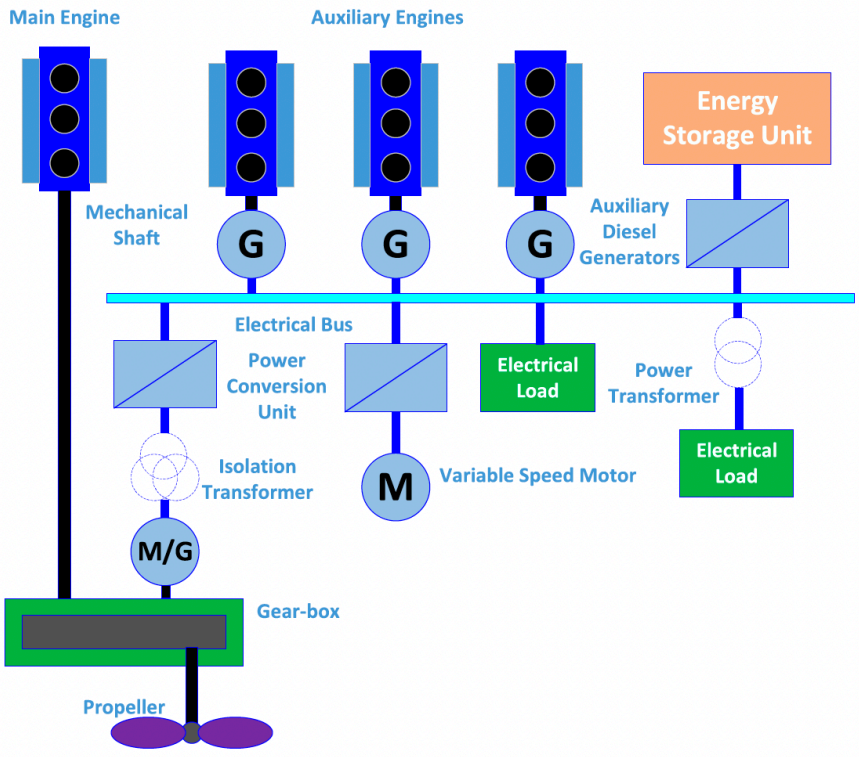

Figure 3-3: Diesel – hybrid propulsion architecture

3.2.3 Diesel – Electric Propulsion System

A full-electric vessel has received the attention of the shipping industry in recent years as an opportunity to reduce the carbon footprint and environmental impact of its operations. This solution provides benefits that include (i) renewable energy integration (ii) flexibility brought by an energy storage system (iii) shore-to-ship charging integration [95-97]. The main architecture of this system comprises auxiliary engines providing electrical power to the switchboard for distribution to the electrical consumers including a variable-speed electric motor which is used to move the propellor. This powertrain is further supported by the inclusion of marine batteries. As illustrated in Figure 3-4. This configuration ensures that the operational load demands of the vessel are met instantaneously with a smaller equipment footprint. Furthermore, this design provides the required flexibility to allocate the load to the different auxiliary engines as needed. This architecture can be designed as either a DC or AC distribution. One significant advantage of using a DC distribution eliminates the need to synchronise the frequencies between the different generators that are put online. Consequently, variable speed generators can be used providing the benefit of fuel savings as operating an engine at fixed speed during low load conditions is inefficient. Typically, these engines operate optimally at approximately 60% to 80% of the MCR. The specific fuel oil consumption (SFOC), a measure of fuel consumption per kilowatt (kWh) of energy produced for both fixed-speed and variable-speed engines, is shown in Figure 3-5. This figure is illustrated in percentage against a basis of the SFOC at 50% engine loading.

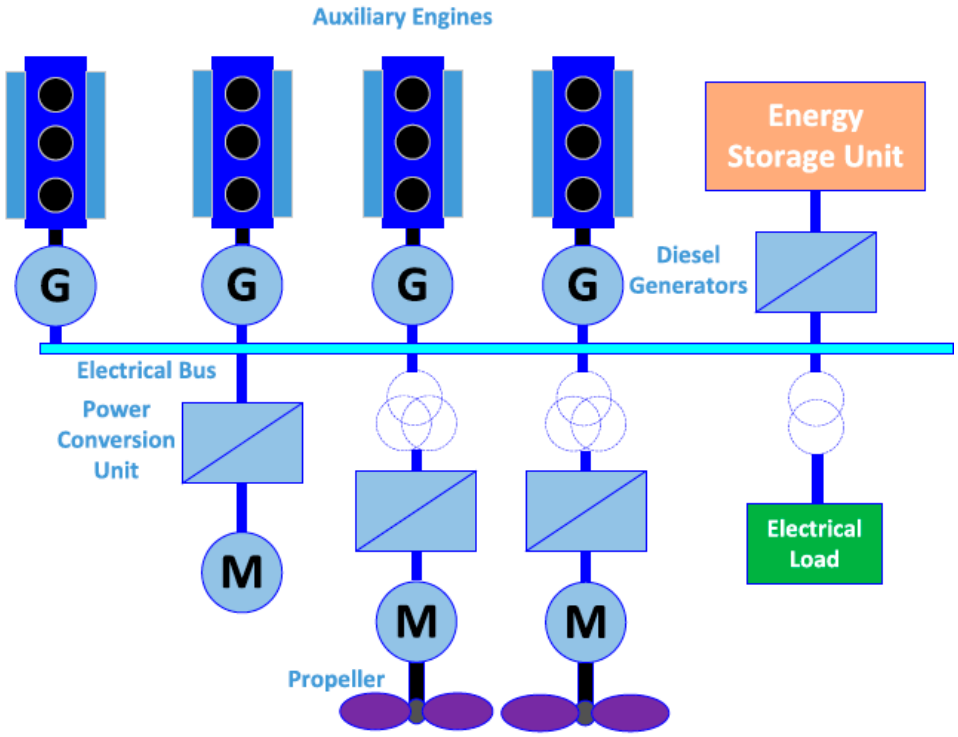

Figure 3-4: Diesel – electric powertrain

A DC distribution system also provides the required design basis for the seamless integration of renewable energy without the need for additional electrical equipment for DC-to-AC conversion. This includes the charging of batteries using green electrons generated by renewable energy such as solar or wind onshore via the DC switchboard. The DC architecture, as a baseline, will provide added motivation to retrofitting new technologies that consist of alternative energy conversion devices such as fuel cells, photovoltaic panels and wind sails as they operate on a DC bus.

The shift of power source for diesel-electric propulsion away from the use of engines to the use of batteries or alternate technologies would consequently reduce the engine's running hours and lengthen the maintenance intervals. During low load conditions, the batteries might be able to fully support the operation without having the genset come online eliminating emissions and reducing fuel costs, demonstrating this configuration's flexibility.

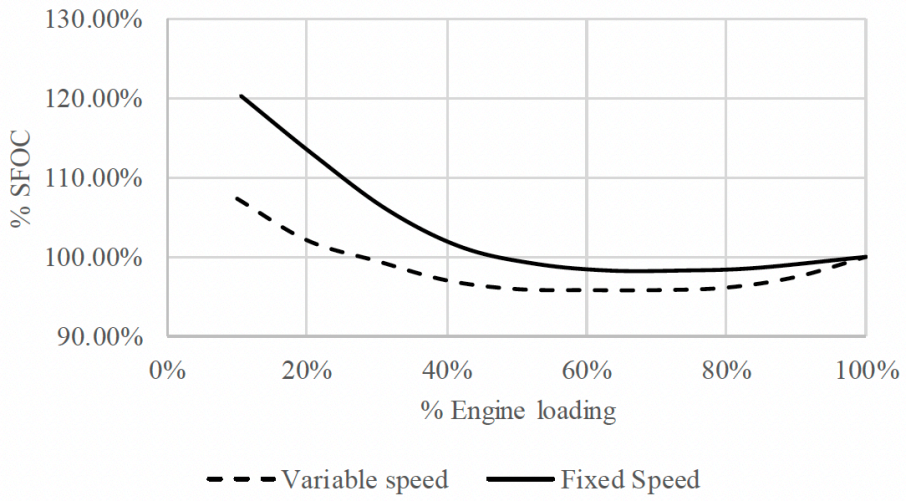

Figure 3-5: SFOC of a variable and fixed speed engine in % using 50% engine loading SFOC as basis

3.3 The Current State of Play for Hydrogen

Whilst it is novel to consider the use of hydrogen as a fuel, specifically as a marine fuel, hydrogen is currently widely used in several upstream industries, specifically in the petrochemical industry, albeit to refine long-chain hydrocarbons to synthesise higher value, lower sulphur products. Examples include gasoline, jet fuel, and petroleum gas. The process of hydrodesulfurization, a commonly used method to reduce sulphur content, requires a significant amount of hydrogen either via hydrogenation or hydrogenolysis [98]. In the industrial sector, hydrogen is an instrumental building block as feedstock in the production of ammonia and methanol. Figure 3-6 below, extracted from a 2021 report from the international energy agency, depicts the sector-specific demand for hydrogen, which has been steadily growing since the start of this century [99]. Omitted in Figure 3-6 is a small category of "others" which encompass grid injection, electricity generation, and the use in transport applications amounting to 0.02 wt.%. It is envisaged that the contribution from this sector to increase to approximately 30% by 2030 with the most significant change contributed by grid injection for consumption.

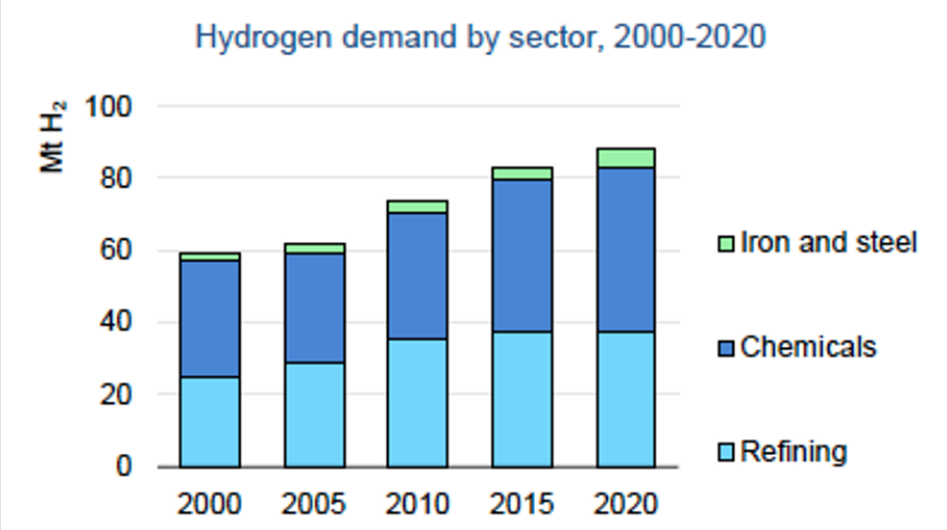

Figure 3-6: Hydrogen demand by industrial sectors (Extracted from IEA, 2021)

Distilling the data, the use of hydrogen for transport applications remains minuscule accounting for only 0.02% of the total hydrogen demand. In Singapore, a multi-agency committee (National Climate Change Secretariat (NCCS), Singapore Economic Development Board (EDB), and Energy Market Authority (EMA)) was commissioned in 2021 to study hydrogen imports and their downstream applications. The findings of this timely report were to substantiate the ambitious plans of the energy market of Singapore to reduce emissions of the electrical grid by 30% by 2035 [100]. The several pronged approaches to achieve this target include the use of other low carbon alternatives such as ammonia, and renewables as well as capitalising on technologies like carbon capture, utilisation, and storage (CCUS). This endeavour, admittedly for electrical generation, would provide the necessary infrastructure required for hydrogen handling and consequently spill over to adjacent industries.

3.4 Hydrogen Production

Hydrogen is the most abundant element in the universe and yet pure molecular hydrogen (H_2) only exists in small amounts. This is because of the high reactivity of pure molecular hydrogen with other elements such as atoms in water (H_2O) and methane (CH_4), oil, and coal which drastically reduces its occurrence. As a result, molecular hydrogen which is a flammable gas,

cannot be simply collected and burned as you would for traditional fuels. Instead, to use hydrogen as fuel, one would have to use energy to extract it from chemical compounds employing one of the three production pathways first. Industrially accepted colour bandings are used to denote how environmentally friendly these production pathways are. 'Grey' is the term used to describe hydrogen produced from fossil fuels [101], 'Blue' is the same as Grey but with carbon capture, where the carbon emissions produced during the extraction process are captured and stored. 'Green' is the term used when hydrogen is produced using renewable sources of energy through the electrolysis of water. Additionally, 'Turquoise' hydrogen uses methane (CH_4) as the feedstock whereby hydrogen is achieved through the methane pyrolysis process. This process also produces carbon as a by-product which can be used in adjacent industries. Lastly 'Pink' hydrogen can be seen as an offset of green hydrogen in which the eventual method of achieving hydrogen is still via electrolysis but with the use of nuclear energy as the source of energy [102]. A pictorial representation is illustrated in Figure 3-7 below.

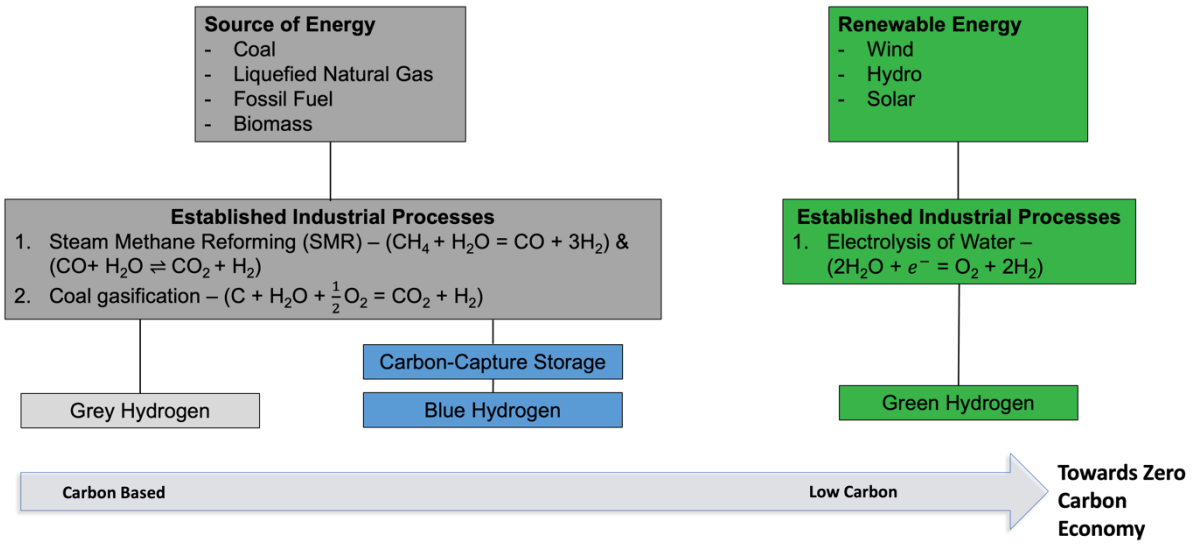

Figure 3-7: Hydrogen production pathways

Currently, over 90% of the hydrogen produced today is derived from a fossil-based source [103]. This is primarily achieved from the reforming of methane known as the Steam Methane Reforming (SMR) process. This process reforms methane into carbon monoxide and hydrogen, commonly referred to as syngas as products. Other methods used to produce syngas include the use of Auto Thermal Reforming (ATR) and coal gasification. SMR reaction is shown in equation (2-1) below:

$$C_xH_y + xH_2O \Leftrightarrow (x + y/2)\,H_2 + xCO \quad (3\text{-}1)$$

ATR combines steam reforming and partial oxidation. The reaction is given as:

$$2C_xH_y + (x/2)O_2 + xH_2O \rightarrow (x + y)H_2 + 2xCO \quad (3\text{-}2)$$

Coal can be used as a feedstock to produce hydrogen. Traditional uses of coal include the use of coking coal for steelmaking and thermal coal for electricity generation via steam turbines. The reaction for coal is given in equation (2-3) below:

$$C + H_2O \rightarrow H_2 + CO \quad (3\text{-}3)$$

To achieve a higher purity of hydrogen while reducing the carbon monoxide concentration, syngas undergoes a water-gas shift reaction to produce carbon dioxide and hydrogen. This reaction is given as:

$$CO + H_2O \Leftrightarrow H_2 + CO_2 \quad (3\text{-}4)$$

The production of hydrogen through this pathway is dependent on a commodity subject to political insecurity. As we pivot towards alternative feedstock such as water, we decouple the energy system from dependence on geopolitical forces.

As the ocean covers 70% of the earth's surface, this source of hydrogen can be perceived as effectively infinite. The ready availability of water, albeit over 90%, is saline, providing the last and possibly the most crucial feature of a future energy system. Increasingly, several proposals have been made to build large-scale water electrolysis plants to produce hydrogen

from water with the primary energy, electricity, coming from a renewable source. These initiatives attempt to extract hydrogen with net zero emissions and characterise the hydrogen produced as green. Hydrogen produced via this pathway could also be used as an energy storage medium to complement the inherent limitations of renewable energy, which are the mismatch in supply versus demand and fluctuations in the generating capacity due to unfavourable environmental conditions.

The majority of the world's demand for hydrogen is almost entirely met by grey hydrogen, with 60% using natural gas as the preferred feedstock. The other fossil-based hydrogen production feedstock includes coal and the reforming of naphtha, contributing 19% and 21%, respectively [104]. The reliance on fossil-based feedstock for hydrogen production has resulted in the release of 2.5% of global CO_2 emissions from the energy industry, approximately 900 metric tonnes [99]. This dominance promotes favourable economies of scale, resulting in a unit price point of roughly 1.60 USD/kg of hydrogen produced. The competitive pricing is prohibitive for alternative clean technologies that attempt to produce hydrogen with a lower carbon footprint. One such technology is using electrolysers for the electrolysis of water using renewable energy. The electrochemical process and its equation can be seen in Figure 3-7. Electricity is used to split water molecules into their constituent hydrogen and oxygen. Several types of electrolyser technologies with alkaline electrolysis dominate the market share as a mature commercial technology [105]. Geographically, 40% of the global installed electrolyser capacity is centred in Europe with an uneven distribution across the rest of the region with Canada being the largest country at 9% [99]. This resonates proportionally with political motivation and support given by European governments to expedite the energy transition by funding and enabling the research, development, and commercialisation of cleaner technologies. Collectively, efforts to increase the baseline project size, knowledge acquisition, and technical know-how would culminate in reducing the cost of electrolysis and providing a

competitive solution for hydrogen production. Figure 3-8 below shows the 2018 price gap in unit cost between the fossil-based traditional hydrogen production process and electrolysis of water. The minimum cost is determined theoretically using the cost of the feedstock (natural gas for SMR and water for electrolysis), together with the capital costs of the equipment required to produce hydrogen. By 2030, the planned execution and delivery of installed electrolyser capacity could climb to 54 GW from 290 MW, signalling an ambitious push towards the realisation of a lower hydrogen production cost via economies of scale [106].

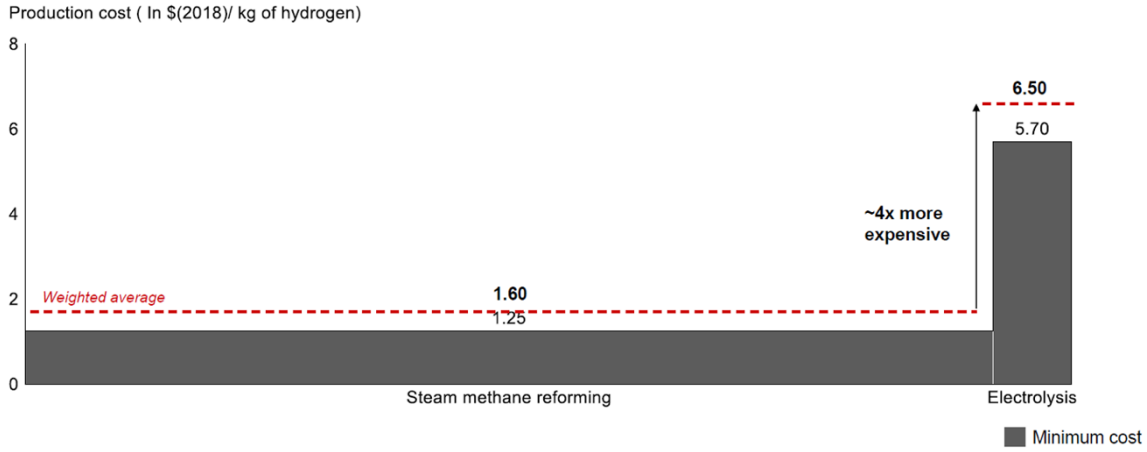

Figure 3-8: Hydrogen production cost (SMR vs. Electrolysis)

Furthermore, a significant number of planned projects would encompass the integration of a dedicated renewable energy input source. This direction is envisaged and would further accelerate the adoption of green energy. This spillover effect could provide the crucial track record and capability demonstration required for continued investment and deployment of renewable energy assets into the market.

Hydrogen production costs are inherently dependent on the production pathway employed. According to the International Energy Agency's 2024 global hydrogen review, green hydrogen production costs range between USD 3.00 and USD 6.00 per kilogram, influenced by electrolyser capital costs, electricity input price, capacity factor, and plant scale. The report projects that with continued technological innovation and expansion of renewable energy,

production costs could decline to USD 2.50/kg by 2030 and reach USD 1.80/kg by 2040. These projections align with forecasts from various national hydrogen strategies (e.g., Germany, Japan, and Australia), which emphasise declining levelised costs of hydrogen as electrolyser efficiencies improve and renewable energy becomes more accessible.

3.5 Hydrogen Infrastructure

The success criteria for the large-scale deployment and acceptance of hydrogen as a fuel to decarbonise the energy system would ultimately rely on a well-established infrastructure's robustness, cost-efficiency, and effectiveness. This infrastructure would need to satisfy the overall safe handling of hydrogen as it transits through the various stages of containment, transfer, and transportation to the end-user, and it is discussed in detail below.

3.5.1 Hydrogen Containment – Compressed

The type of hydrogen containment system depends on the state in which hydrogen is stored. Hydrogen's intrinsic chemical and physical properties differ vastly with phase changes. Hydrogen can either be stored as a gas in its compressed form or as a liquid at cryogenic temperatures. Correspondingly, the containment system would need to be designed to handle the high pressures of 150-700 bar or cryogenic temperatures of -253°C.

Hydrogen is widely used in its compressed form for several industrial applications, employing cylinders packaged in pallets. These hydrogen cylinders or bottles typically have a storage pressure of 150 bar. These cylinders are designed no differently from other compressed gases and follow well-established ASME pressure vessel standards. Compressed hydrogen containment instruments are classified into four major categories: Type I to Type IV [107]. The main difference lies in the structural integrity, whereas the above example would fall into Type I – all metal. Together with type II, these vessels are inherently heavy and have a low energy density with approximately 1 wt.% hydrogen availability [108]. As such, the applications are

limited to land-based stationary applications. The fundamental design of this containment system makes it susceptible to hydrogen embrittlement and permeation due to the high pressure and small molecular size of hydrogen. To mitigate this and reduce the overall weight of these vessels, Type III and Type IV containment systems comprise composite materials such as carbon fibre with liners made from either aluminium or plastic. These containment systems are also non-load bearing (i.e., self-supporting), ideal for marine applications as they circumvent additional stresses to the ship's structure [109, 110]. Furthermore, the motivation to increase storage pressure results in a longer operational endurance with gravimetric storage capacity increasing by 3.6 wt.% from 300 to 700 bar [111].

3.5.2 Hydrogen Containment – Liquified

Liquefying hydrogen introduces opportunities for cost-efficiently transporting and storing large quantities of hydrogen at low pressures. The motivation to liquefy hydrogen is to innovatively increase the gravimetric energy density considerably whilst reducing the volumetric space required for the containment [112].

The hydrogen liquefaction process relies on well-established, centuries-old, proven technologies. The two most common liquefaction cycles are the 1895 Linde-Hampson cycle and the 1902 Claude cycle [113, 114]. These cycles are still relevant in today’s context as the approach is technically sound, with research identifying gaps to improve the overall efficiency of the process with the current exergy efficiencies at 50%. The Linde-Hampson cycle uses liquefied nitrogen to pre-cool the highly compressed hydrogen gas as part of a two-stage heat exchanger before undergoing a Joule-Thompson expansion. The rapid expansion of compressed hydrogen cools the overall system further to yield liquified hydrogen as the product. The main difference in the Claude cycle, which partly contributes to the observed improvement in exergy efficiency, is the inclusion of an expander as part of the pre-cooling process [115]. This approach allows hydrogen to serve as the sole refrigerant. This is achieved

by connecting a branch from the 'hot' liquefying stream as feed to the expander, which leaves at a reduced temperature to be connected to the refrigerant line. To maximise the benefit of the expansion work, the tee connection to the refrigerant line is ahead of the heat exchanger. Both cycles are illustrated in Figure 3-9.

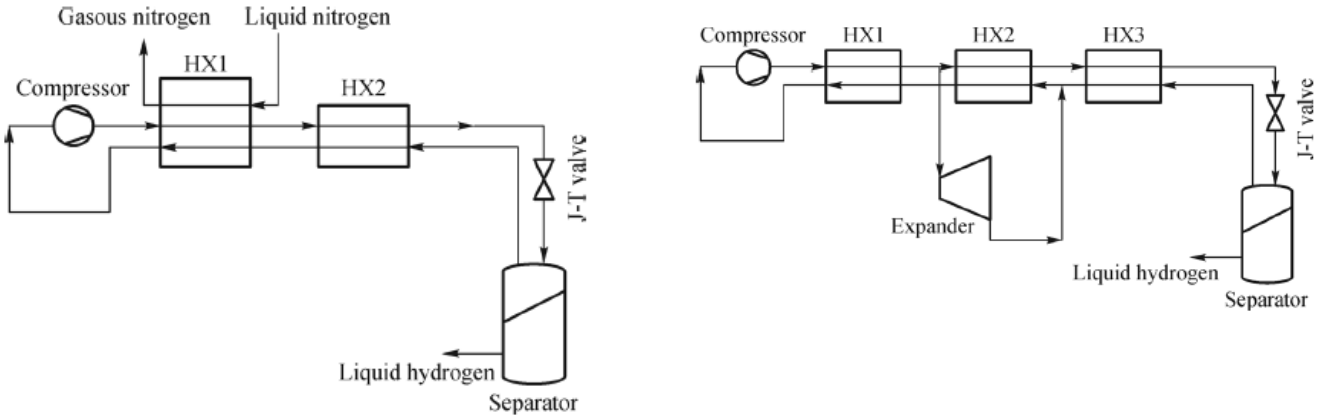

(a) (b)

Figure 3-9: Liquefaction process flow diagram for hydrogen (a) Linde-Hampson Cycle (b) Claude Cycle

The current state-of-the-art liquefaction plants require approximately 10 kWh/kgLH_2, which amounts to an energy shrink of about 30% of the available energy output deliverable from the use of liquefied hydrogen. Table 3-2 summarises the possible containment approaches that can be undertaken to store and transport hydrogen.

Table 3-2: Liquefied and compressed hydrogen physical properties

Characteristics	**Liquefied Hydrogen**	**Compressed hydrogen**
Containment	IMO Type C	4 Types (Type 1 to Type IV) Type III and Type IV – For Marine Applications
Storage Temperature (°C)	-253	Ambient temperature
Pressure	< 4 bar	350-700 bar
Volumetric Energy Density	8.5 MJ/L	2.99 – 4.92 MJ/L
Gravimetric Energy Density	118.8 MJ/kg LHV	
Energy Penalty/ Shrink (% of available energy)	28.8 – 36 MJ/kg (25% to 33%)	3.78 – 4.9 MJ/kg (0.8% to 1.3%)
Ability to be used as a fuel	Yes	Yes

Benchmarking hydrogen against other widely discussed alternative fuel options is also prudent. This illustration would provide valuable insights into the value proposition of hydrogen and is shown in Table 3-3.

Table 3-3: Alternative liquid fuels' physical properties

Types of fuel	**Auto-ignition Temperature (°C)**	**Boiling Point (°C) (1 atm)**	**Energy Content (MJ/L)**	**Flammability Range in Air (%)**	**Lower Heating Value (MJ/kg)**
Liquid Ammonia	651	-33	12.65	15-28	18.6
Liquefied Natural Gas	595	-162	22.32	5-15	49.6
Methanol	470	64.7	14.89	6.7-36	19.9
Liquefied Hydrogen	571	-253	8.5	4-75	118.8

When liquefied hydrogen is compared to a set of metrics, it is evident that it has intrinsic shortcomings from an energy delivery perspective. A poor volumetric energy density, low boiling point, and wide flammability range illustrate this.

Marine vessels are typically constrained by space and are designed to meet restrictions imposed by shore facilities such as cargo handling and bunkering. Also, certain voyages, primarily

through man-made infrastructures such as the Panama and Suez Canal, have limitations regarding how long and wide a ship can be to transit safely [116]. As such, should there be a need to increase the space allocated for fuel storage, the corresponding effect would be on the permissible cargo-carrying capacity. Ideally, earnings from sea trade are to be maximised for each voyage, depending on the quantity of the commodity it carries. Figure 3-10 represents the equivalent fuel tank size required for alternative fuels based on the energy content of 1000 m^3 of traditionally used marine gas oil.

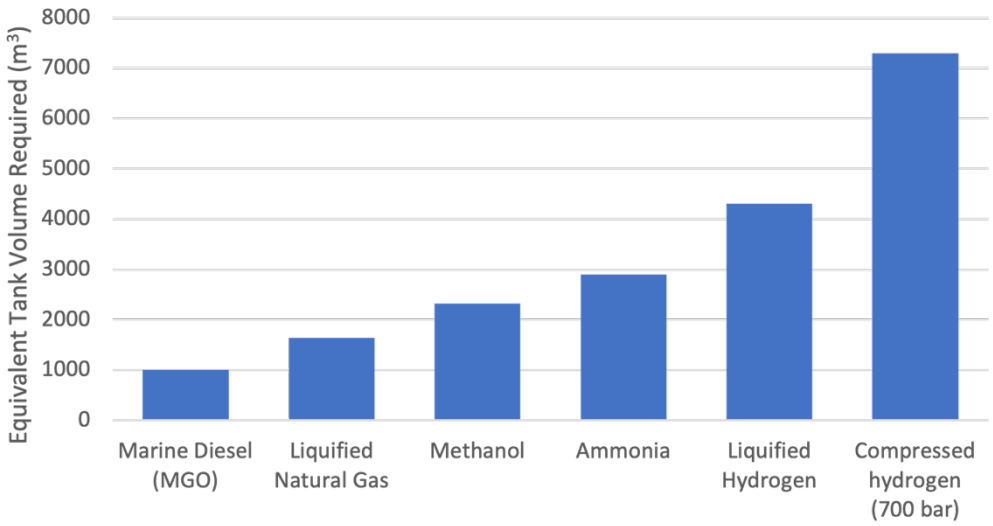

Figure 3-10: Equivalent fuel tank volume for 1000 m^3 MGO

3.5.3 Hydrogen Transfer – Liquefied

Hydrogen transfer from ship to shore can be conducted using pipes or hoses for liquid or compressed hydrogen. Liquid hydrogen transfer is significantly faster, with a rate of about 3,000 kg per hour, compared to compressed hydrogen's 220 kg per hour. Due to this, compressed hydrogen refuelling often involves swapping tanks or containers. Hydrogen bunkering locations are limited, predominantly in Northern Europe, and mainly consist of compressed hydrogen filling stations operating at 300 or 700 bar pressures. Liquid hydrogen transfer to ships is currently available at three locations: Kobe in Japan, Hastings in Australia,

and Hjelmeland in Norway—the facilities in Kobe and Hastings feature fixed infrastructure, including storage tanks. Norled's system in Hjelmeland is a mobile setup designed for use at any quayside, with liquid hydrogen delivered by truck. Another mobile liquid hydrogen refuelling system is planned for Aberdeen as part of the HI-FIVED (Hydrogen and Ammonia Fuels Inclusive to Value-Chain Energy Development) project.

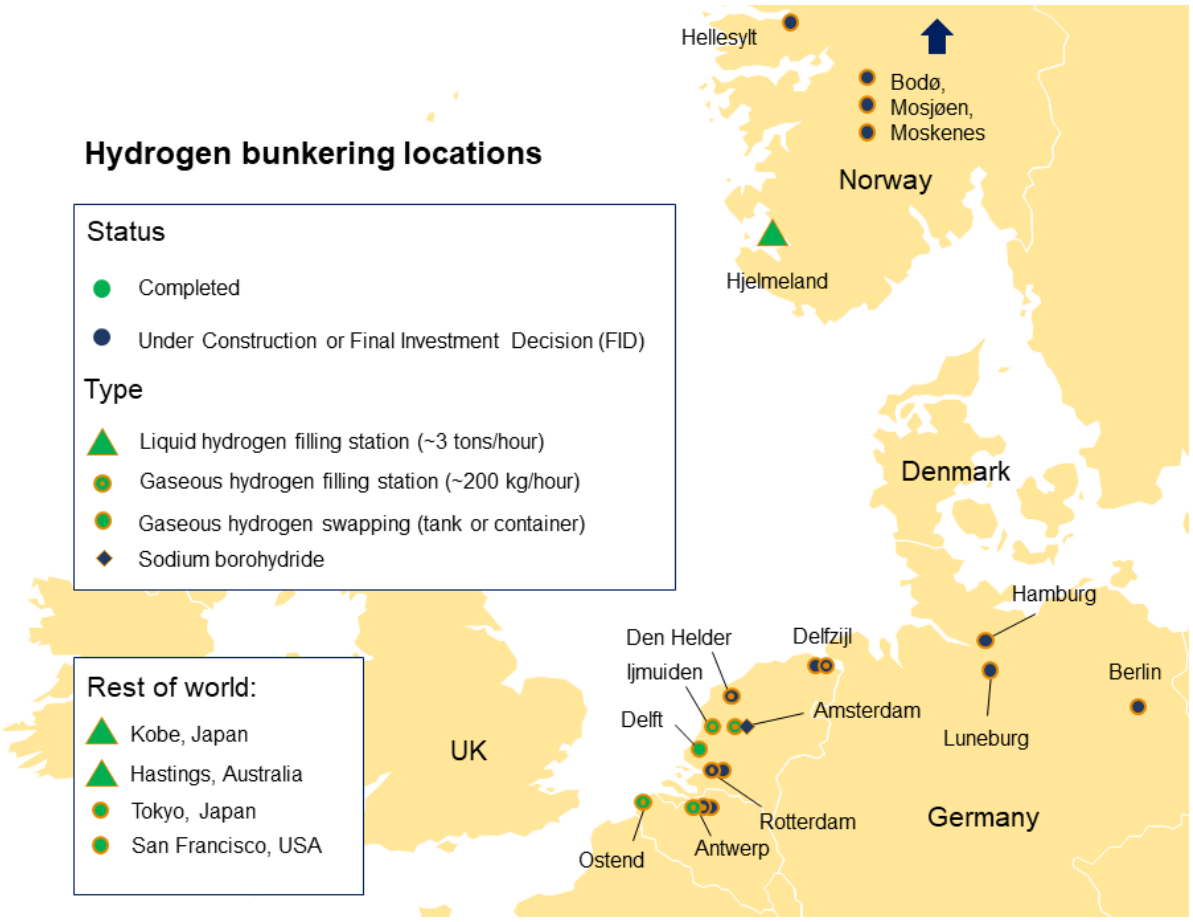

Figure 3-11: Hydrogen bunkering locations globally

Liquid hydrogen bunkering is at TRL/CRL9, with commercial operations refuelling the Hydra passenger ferry in Hjelmeland. Fixed systems, like those in Kobe and Hastings, are at TRL8, having successfully demonstrated shore-to-ship transfer. Mobile systems have been developed to address the challenges of large-scale liquid hydrogen supply and infrastructure by using lightweight, standalone setups that receive hydrogen via truck delivery. This approach ensures

that bunkering can be performed without needing fixed quayside infrastructure or a nearby fuel supply. Companies such as Norled and Unitrove are leading the development of these systems. Norled's liquid hydrogen bunkering system, designed for the Hydra passenger ferry, delivers liquid hydrogen directly to the ship. Although the "bunkering tower" is mobile, it can be adapted into a fixed port structure if space permits. Boil-off losses have been minimised to around 10-15 kg per liquid hydrogen load of 3.2-3.5 tonnes per truck, with plans for future system iterations to capture and utilise the gas locally, similar to onboard practices. With a loading rate of 3 tonnes per hour, it takes approximately 1 to 1.5 hours to fill the MF Hydra's 5.7-tonne storage capacity.

Liquid hydrogen bunkering can be conducted using either pressure difference or pumps. Systems that use pressure difference, such as Norled's, rely on the temperature difference between liquid and compressed hydrogen to create pressure as the hydrogen warms and gasifies. This pressure is then used to deliver the fuel to the consumer, with any excess pressure being fed back into the system. On the other hand, pump-based systems, like those from Unitrove, have been established for decades and are commercially available under the guidelines of manufacturers such as Linde, Air Products, and Air Liquide.

Figure 3-12: Mobile bunkering tower for LH2 transfer to MF Hydra ferry

Fixed bunkering systems are more permanent structures with associated storage tanks, like the liquid hydrogen terminal at the Port of Kobe, Japan. This terminal features a Rigid Type Loading Arm System (LAS) for ship-to-shore transfer. Successful testing of liquefied hydrogen cargo handling was completed in March 2023, placing the technology at TRL8. Currently, there is no specific standard for marine liquid hydrogen bunkering, but it is anticipated that the established LNG bunkering standards will guide liquid hydrogen bunkering practices. ISO TC197 is responsible for developing standards for hydrogen services, and current cryogenic bunkering practices are based on LNG protocols until specific ISO or CEN standards for liquid hydrogen are established.

ISO and CEN are actively working on creating standards for liquid hydrogen that will likely draw from accepted LNG bunkering practices. For instance, Unitrove Innovation's liquid hydrogen bunkering facility adheres to recognised codes such as NFPA2, BGCA, EIGA, and

other standards like BS EN 10079 for explosive environments, ensuring compliance with HSE requirements. All equipment, including high-pressure pumps, sensors, and metering systems, meet these standards.

Although NFPA2 "Hydrogen Technologies" references other NFPA codes like NFPA 52 "Vehicular Natural Gas Fuel Systems Code" and NFPA 55 "Compressed Gases and Cryogenic Fluids Code," these are generic and not specific to marine applications. However, they currently serve as the foundation for the ongoing development of liquid hydrogen bunkering standards in the maritime industry.

It is imperative to ensure that safety is never compromised during the bunkering operations of liquefied hydrogen. Safety measures and system redundancies are incorporated to ensure the highest level of operational excellence to mitigate risk. This can be achieved through (i) hazard identification, (ii) hazard and operability study, and (iii) qualitative risk assessments. These workshops and studies will address some examples of identified hazards listed below and provide mitigating measures that would effectively address them as shown in Table 3-4 below:

Table 3-4: Safety nodes and mitigating measures for liquefied hydrogen bunkering

Guideword	**Hazardous Event**	**Potential Causes**	**Potential Consequences**	**Risk Reducing Factors**
Mechanical damage	Damage of bunkering hoses	Wear and tear Lack of maintenance	LH_2 leakage when bunkering starts	Bunkering boom maintenance plan with hose replacement
Ship motion	Mooring line breakage	Strong wind and swell Draft and list ship variation Winch failure	Bunkering boom rupture Damage to bunkering boom LH_2 leakage	Mooring safety patrol and mooring tension monitoring Emergency release coupling on bunkering boom
Temperature hazards	Excessive boil off from receiving vessel tanks to recover	Bunkering with LH_2 colder/hotter than the receiving ships tanks	Overpressure in the bunker vessel tanks Venting of hydrogen into mast Flammable environment	Procedures including tank cooldown and flow rate ramp up

3.5.4 Hydrogen Transfer – Compressed

Compressed hydrogen filling stations have operated since 2010 and are now available in various locations, offering a crucial infrastructure component for hydrogen-powered maritime vessels. These stations are similar to those used for road transport, which are extensively deployed worldwide. A notable example is the compressed hydrogen multi-modal refuelling station operated by CMB.Tech in Antwerp, Belgium. This facility offers two different hydrogen bunkering pressures for vessels—200 bar and 350 bar—and also includes a tube trailer filling station capable of handling hydrogen at 500 bar. In addition to the fixed station, two mobile hydrogen refuelling trailers are deployed, each capable of refuelling vessels at 200 and 350 bar using 950 kg of hydrogen stored at 500 bar. These trailers offer flexible refuelling options that can be transported to where needed.

The technology employed in these hydrogen filling stations has been directly adapted from the road transport sector, adhering to existing land-based standards. This transfer of technology has facilitated the rapid deployment of these stations. Still, it has also meant that the limitations of road transport refuelling systems have carried over into the maritime sector. One significant technical limitation is the relatively low flow rate of hydrogen refuelling—currently about 220 kg per hour. This flow rate is sufficient for many land-based applications but falls short when applied to the demands of larger vessels, which require much more hydrogen in a shorter period. Efforts are underway to increase this flow rate significantly, with flow rates of up to 1,000 kg per hour or more currently being developed. However, these technologies are still at Technology Readiness Levels (TRL) 5-6.

An alternative approach has been developed to overcome the limitations of direct filling with compressed hydrogen: swapping pre-filled, containerised compressed hydrogen tanks with empty ones. These containers, typically housed in standard 20' or 40' ISO frames, are also known as Multiple-Element Gas Containers (MEGCs). This method offers several advantages, including reduced bunker times and greater flexibility in infrastructure requirements. Because the containers can be filled and stored away from the bunkering site, the associated storage and filling infrastructure can be located at a different port, reducing the complexity and cost of setting up bunkering facilities. Argo-Anleg GmbH has successfully demonstrated this method for the inland push-boat Elektra, and it is expected to be applied to other inland vessels such as the FPS Maas, Antonie, and those involved in the RH2IWER project, which includes six inland ships. For the Elektra push boat, the containers are swapped using an onboard crane, showcasing the practicality and efficiency of this approach. The standards governing the off-loading of these containers are currently covered by ISO 10855.

Norway is at the forefront of developing and investing in mass-produced containerised hydrogen for ship refuelling and trade. A significant project is underway in Mosjøen, where

planning consent has been granted for a facility producing 18,250 tonnes of hydrogen per year using a 100 MW electrolyser. This facility will also handle the filling, storing, and transporting of large hydrogen containers. The site will include a quay designed for seaborne transport, enabling the distribution of these hydrogen containers to markets in Norway and Europe. Another project in Bodø has reached a final investment decision (FID). It will focus on a facility with a daily bunker fuel capacity of 5 tons and an annual production capacity of 1,875 tons of hydrogen. These projects are part of a broader effort to create a robust infrastructure for hydrogen bunkering, supporting the maritime industry's transition to cleaner energy sources.

Despite these advancements, there currently needs to be a specific standard for the bunkering of compressed hydrogen for marine use. However, several existing facilities, such as CMB's compressed hydrogen bunkering facility, have been adapted to meet current needs. Tech in Antwerp adheres to the land-based fuelling station standard ISO 19880-1. This standard covers the design, installation, commissioning, operation, inspection, and maintenance of gaseous hydrogen fuelling stations. It provides a framework for ensuring the safety and reliability of hydrogen refuelling operations in the maritime sector. While this standard is not specifically tailored to marine applications, it is a helpful guideline until more specialised standards can be developed.

In addition to the challenges associated with establishing standardised practices for compressed hydrogen bunkering, there are also logistical and technical hurdles to overcome. The relatively low flow rates of current compressed hydrogen refuelling systems mean that larger vessels may need longer refuelling times, which could impact their operational efficiency. Moreover, the lack of widespread hydrogen production, storage, and distribution infrastructure presents another significant challenge. To address these issues, ongoing research and development efforts are focused on increasing the flow rates of hydrogen refuelling systems, improving the

efficiency of hydrogen production and storage, and developing new technologies that can streamline the entire hydrogen supply chain.

The future of compressed hydrogen bunkering in the maritime sector will likely involve a combination of direct refuelling and containerised hydrogen swapping, supported by a growing network of hydrogen production and distribution facilities. As standards are developed and infrastructure expands, the maritime industry will be better positioned to adopt hydrogen as a primary fuel source, helping to reduce greenhouse gas emissions and promote sustainability in shipping. The successful deployment of these technologies will depend on continued collaboration between industry stakeholders, regulatory bodies, and technology providers to ensure that the necessary infrastructure and standards are in place to support the widespread adoption of hydrogen-powered vessels.

3.5.5 Hydrogen Transportation

Hydrogen transport and distribution have evolved significantly, both on land and at sea, leveraging technologies that range from traditional pipeline systems to advanced cryogenic storage and delivery methods. These advancements support the growing demand for hydrogen as a clean energy source, particularly in maritime industries where decarbonisation is a high priority.

On land, hydrogen pipelines have long been a staple for transporting compressed gaseous hydrogen to heavy industrial users. These pipelines, which currently extend over approximately 4,500 kilometres globally, represent a mature and reliable infrastructure for the distribution of hydrogen. The technology for hydrogen pipelines closely parallels that of natural gas pipelines, allowing for the efficient and safe carriage of pure hydrogen over long distances. This method is particularly advantageous for regions with a high hydrogen production and consumption concentration, as it enables continuous and large-scale supply directly to industrial facilities, reducing the need for intermediate storage or road transport.

The maritime transport of hydrogen has seen groundbreaking developments, especially with introducing the Suiso Frontier, a specialized carrier designed to transport bulk liquid hydrogen by sea. Since its debut in 2021, the Suiso Frontier has demonstrated the viability of long-distance liquid hydrogen transport, marking a significant milestone in the hydrogen economy. The vessel has a double-shielded and double-insulated cryogenic tank capable of storing 90 tonnes of liquid hydrogen in a 1,250 m^3 tank. This sophisticated storage system ensures the hydrogen remains liquid, even during extended voyages.

One of the key challenges in transporting liquid hydrogen is managing boil-off gas, which occurs as the hydrogen slowly warms and transitions back to a gaseous state. On the Suiso Frontier, boil-off is expertly managed using a cylindrical pressure accumulator storage tank. This system allows the internal pressure within the tank to increase, effectively storing the boil-off gas without the need for immediate venting, much like the systems used on LNG carriers. While utilizing boil-off gas as a fuel for the ship's propulsion system—similar to practices on LNG carriers—has been proven on smaller vessels like the Hydra passenger ferry, it has not yet been implemented on large hydrogen carriers like the Suiso Frontier. However, this represents a potential area for future innovation, offering a way to enhance further the efficiency and sustainability of hydrogen transport by sea.

The future of hydrogen transport looks promising, with several new projects set to push the boundaries of what is possible. One such project is the HyEkoTanker initiative, which aims to retrofit an 18,600 DWT product tanker with 4,000 kg of compressed hydrogen storage. This project, expected to demonstrate bulk transportation of compressed hydrogen by 2024, also includes installing a 2.4 MW fuel cell system to provide auxiliary power. This dual-purpose approach not only enables the transport of hydrogen but also showcases its potential as a direct energy source for ship operations.

While maritime transport is vital for long-distance international trade, road transport remains essential for shorter distances and flexible supply chains. The transport of liquid hydrogen by road has been operational since the 1950s and has reached a high level of commercial maturity (CRL 10). Companies like Linde Gas, Kawasaki Heavy Industries, and Hylium are at the forefront of this industry, offering liquid hydrogen transport solutions using specialized trucks. These vehicles typically carry between 2.5 and 3.5 tonnes of liquid hydrogen in ISO 40-foot container-sized tube trailers. The trailers are designed with vacuum lamination and thermal insulation to maintain the hydrogen at cryogenic temperatures, ensuring minimal loss during transport.

A notable example of road-based liquid hydrogen transport is the supply chain established to refuel the Hydra passenger ferry in Hjelmeland, Norway. This system involves transporting green hydrogen over 1,000 kilometres by truck from a 24 MW electrolyser in Leuna, Germany. This long-distance supply chain highlights the feasibility and effectiveness of road transport for liquid hydrogen, especially in cases where pipeline infrastructure is unavailable.

In addition to liquid hydrogen, compressed hydrogen is transported by road, reaching the same level of commercial readiness as its liquid counterpart (CRL 10). Companies such as NPROXX, Air Liquide, BayoTech, and Linde Gas provide high-purity compressed hydrogen at various pressures, typically using standard 20- or 40-foot ISO containers. These containers can hold up to 1,100 kg of hydrogen per trailer, making them versatile for hydrogen distribution. Compressed hydrogen transport is especially useful for delivering hydrogen to locations not directly connected to a pipeline network or smaller-scale applications where liquid hydrogen transport might be impractical.

One of the advantages of compressed hydrogen transport by road is its flexibility. Unlike pipelines, which require significant upfront investment and are limited to fixed routes, road transport can deliver hydrogen to various locations, including remote or with variable demand.

This flexibility is particularly important in the early stages of hydrogen infrastructure development, as it allows for the gradual build-up of demand and supply without requiring extensive new infrastructure.

Hydrogen storage and distribution represent a significant portion of the overall supply chain cost and face unique challenges due to hydrogen's low volumetric energy density. According to the IEA's Global Hydrogen Review 2024, storage costs vary considerably depending on the method employed—compressed gaseous storage, cryogenic liquid storage, or conversion into carriers such as ammonia or liquid organic hydrogen carriers (LOHCs). For maritime applications, liquefied hydrogen and ammonia are currently the most researched vectors due to their higher energy densities and compatibility with existing bunkering infrastructures.

Distribution costs are similarly dependent on transport distance, carrier form, and port-side infrastructure. Hydrogen transported via pipelines is cost-effective over short distances but becomes prohibitively expensive internationally unless reconverted into derivatives. The IEA report notes that investment in distribution infrastructure is lagging production but is expected to increase significantly as pilot marine projects scale up and international hydrogen corridors (e.g., EU–Japan, Australia–Asia) begin deployment.

3.6 Hydrogen Utilisation

The entire value chain of hydrogen, or by extension any fuels in general, culminates in the eventual utilisation to perform useful missions required for the intended purpose. In this study, hydrogen will be used either in a fuel cell or burned in a heat engine via an internal combustion engine or a gas turbine. These two technologies have a proven track record in land-based applications, marine environments, or both. Each energy conversion powertrain would contain its respective balance of plant peripherals to provide an overall integrated solution.

3.6.1 Fuel Cells

A fuel cell is an efficient electrochemical device, which can directly convert the chemical energy of a fuel into electrical energy in a single step. The electrochemical reaction occurs as long as the reactants (i.e., fuel) and oxidants (i.e., air) are available at the anode and cathode, respectively, as illustrated in Figure 3-13. The unit cells are modularly connected to achieve the desired output capacity, known as a fuel cell stack. A balance of plant electrical peripherals supports the fuel cell stack to ensure desired performance as well as to ensure overall operational safety. Examples of auxiliary equipment include (i) hydrogen fuel supply system consisting of hydrogen containment, pressure regulators, and valves, (ii) ventilation systems for safety and oxidant supply, (iii) cooling systems for thermal management of fuel cell stacks and electrical components, and (iv) startup/shutdown systems including nitrogen purging systems.

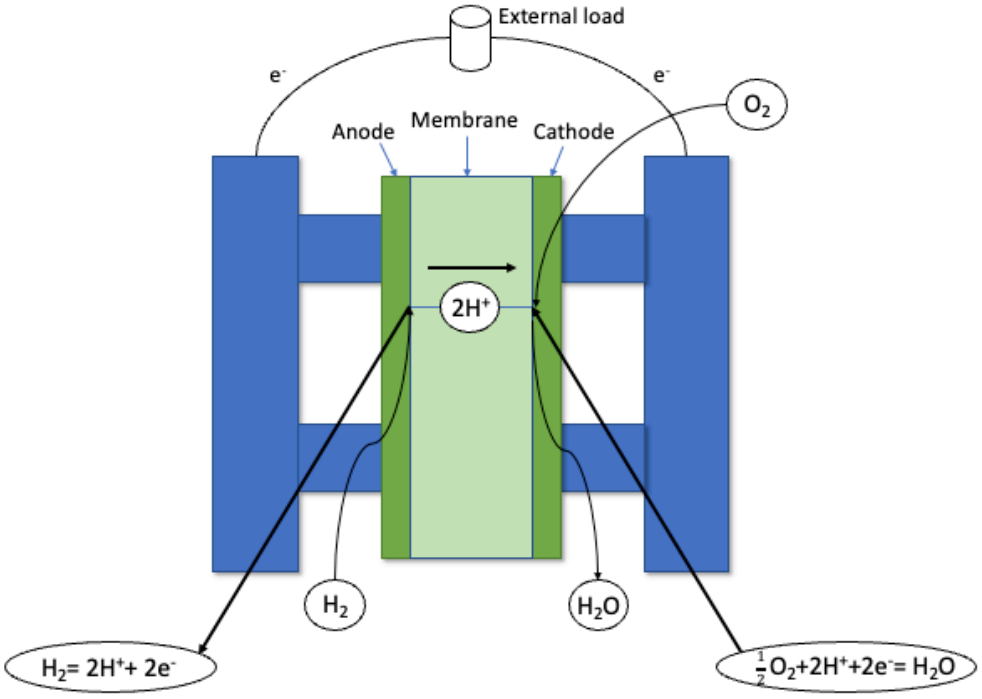

Figure 3-13: Fuel cell schematic diagram

Fuel cells can be deployed in a wide variety of applications, and they can be broadly categorised into three sectors: Portable, Stationary and Transport. In 2020, the total fuel cell capacity delivered is 1.3 GW across all three sectors [117]. Examples of specific applications within these categories include unmanned aerial vehicles and drones, combined heat and power systems for residential and industrial usage, fuel cell vehicles, forklifts, and maritime vehicles for portable, stationary, and transport. A fuel cell implementation roadmap as shown in Figure 3-14 adapted from European and ASEAN contexts depicts the progressive roll-out plan for multiple transport applications starting with exploration and feasibility studies [118-121]. This is followed by industrial and experimental development as a proof of concept, with the final stage being demonstration and market introduction.

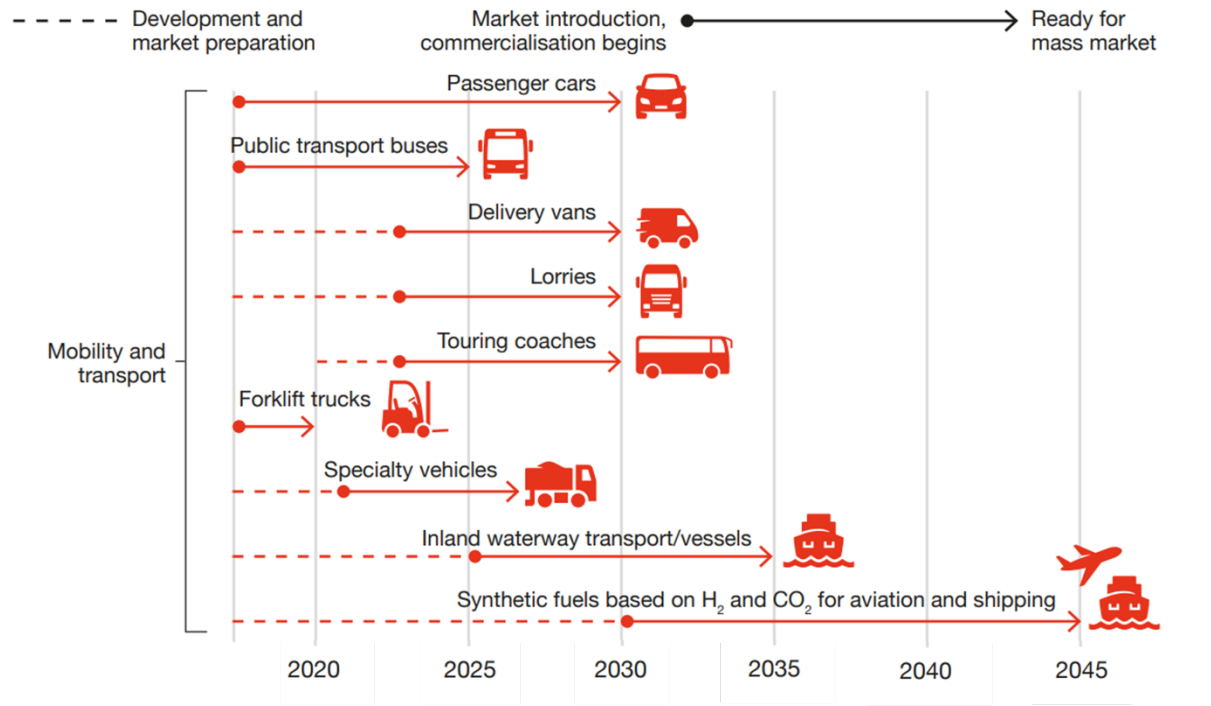

Figure 3-14: Fuel cells for mobility applications roll-out roadmap [122]

There are several well-established fuel cell technologies with varying degrees of market acceptance and commercialisation. Table 3-5 attempts to summarise the various fuel cell technologies highlighting key characteristics and operational requirements.

Table 3-5: Fuel cell technologies overview

Fuel Cell Technology	**Fuel Used**	**Module Size (kW)**	**Electrolyte**	**Operating Temperature (°C)**	**Electrical Efficiency / Combined Heat & Power**
Alkaline fuel cell (AFC)	Hydrogen	Up to 500 kW	OH- ions in aqueous KOH solution	50-90	60%
Molten carbonate fuel cell (MCFC)	Hydrogen, Hydrocarbon	Up to 500 kW	CO_3^{2-} aqueous $(NAK)_2CO_3$	600-700	45% (80% with CHP)
Phosphoric acid fuel cell (PAFC)	Hydrogen, LNG, Methanol	400 kW	H^+ ions in aqueous H_3PO_4	200	40% (80% with CHP)
Polymer Electrolyte Membrane fuel cell (PEMFC)	Hydrogen	200 kW	H^+ ions in solid polymer electrolyte	50-100 160-200 (High temperature PEMFC)	50-60%
Solid Oxide Fuel cell (SOFC)	Hydrogen, LNG, Methanol	20-60 kW	O^{2-} ions in porous ceramic (e.g., zirconia)	600-1000	40% (85% with CHP)

Whilst ongoing land-based development of fuel cells has been widely extensive, the use of fuel cells in a marine environment has been relatively nascent. This can be attributed to an indirect translational lag caused by the different perspectives of consideration when evaluating fuel cell technologies for marine applications. The parameters of importance and relevance can be listed as such:

- Power levels (kW) for the largest module
- Lifetime
- Technological maturity
- Physical size
- Emissions
- Safety

- Efficiency
- Sensitivity to fuel impurities

Forerunning fuel cell technology for marine applications with promising attributes that encompass the unique requirements is shown in Table 3-6.

Table 3-6: Fuel cell technology for marine applications

Fuel Cell Technology	**Justification**
PEMFC (Low temperature)	PEMFC is a mature technology that has been successfully used in land-based and marine applications. The maturity of the technology has also resulted in competitive pricing. The low operational temperature minimises safety concerns. The use of high purity hydrogen fuel results in water as the only emission
SOFC	SOFC is highly efficient and moderately sized. SOFC's efficiency can be further enhanced when combined with heat recovery. The track record for marine usage is limited and still in the R&D stage resulting in higher prices compared to PEMFCs. Fuel flexibility is permitted but the use of LNG or methanol will result in the release of CO_2 and NO_x
PEMFC (High temperature)	HT-PEM addresses the sensitivity to fuel impurities that is intolerable to LT-PEMFC. This potentially results in a cheaper upstream fuel reforming process. The higher operating temperature (200°C) also allows for heat management strategies to be in place which could increase overall efficiency

As described in detail, PEMFCs have been increasingly considered an appropriate candidate for mobile applications including marine vessels. The high Technology Readiness Level (TRL) coupled with a proven track record on land-based applications have catalysed the development of a marinized PEMFC capable of adhering to the stringent safety requirements for shipboard installation. Currently, PEMFCs are categorised into their operating temperature with the low temperature (LT-PEMFC) being the forerunner due to its maturity ahead of its high temperature (HT-PEMFC) counterpart. For marine applications, thorough environmental testing is necessary to ensure operability under adverse conditions. This favours LT-PEMFC as it eliminates the leaching of phosphoric acid commonly used in HT-PEMFC. The low-quality

heat produced by LT-PEMFC also prohibits complex waste heat management strategies resulting in a more straightforward integration to the vessel. LT-PEMFC requires 99.97% hydrogen purity to operate at the design output, whereas the HT-PEMFC is less sensitive to fuel impurities and consequently provides the opportunity for onboard fuel reforming to be explored [123, 124].

In marine environments, the performance and longevity of fuel cells are characterised by their beginning-of-life (BOL) and end-of-life (EOL) conditions, which are critical for assessing their operational viability and lifecycle costs. Marine settings pose unique challenges, different from land based installations that can influence fuel cell degradation over time. Factors such as constant exposure to salt-laden air, humidity, temperature fluctuations, and vibrations. High humidity can affect membrane hydration levels and accelerate corrosion, thermal cycling due to fluctuating ambient temperatures and load demands, and exposure to airborne contaminants such as sulfur compounds from surrounding marine air or fuel sources, which can poison fuel cell catalysts and reduce overall efficiency. At BOL, fuel cells typically deliver high efficiency and stable power output.

Throughout the operational life of the fuel cell, these environmental stressors contribute to the gradual degradation of key components, including the membrane electrode assembly (MEA), catalyst layers, and gas diffusion layers. As the system approaches EOL, performance metrics such as power density, efficiency, and responsiveness begin to decline. Structural wear, catalyst deactivation, membrane thinning or cracking, and contamination build-up all contribute to reduced output and increased maintenance requirements. These issues are particularly pronounced in maritime applications, where the operating conditions are more severe and less predictable than in stationary or land-based systems.

To mitigate these effects, fuel cell systems designed for marine use must incorporate robust thermal and humidity management strategies, corrosion-resistant materials, and advanced filtration systems to prevent contaminant ingress. Furthermore, monitoring systems that track degradation in real time can help operators better plan for maintenance and component replacement, extending the useful life of the system. As marine fuel cell adoption grows, a comprehensive understanding of how environmental conditions influence the BOL-to-EOL transition will be essential for ensuring operational reliability, economic feasibility, and environmental performance.

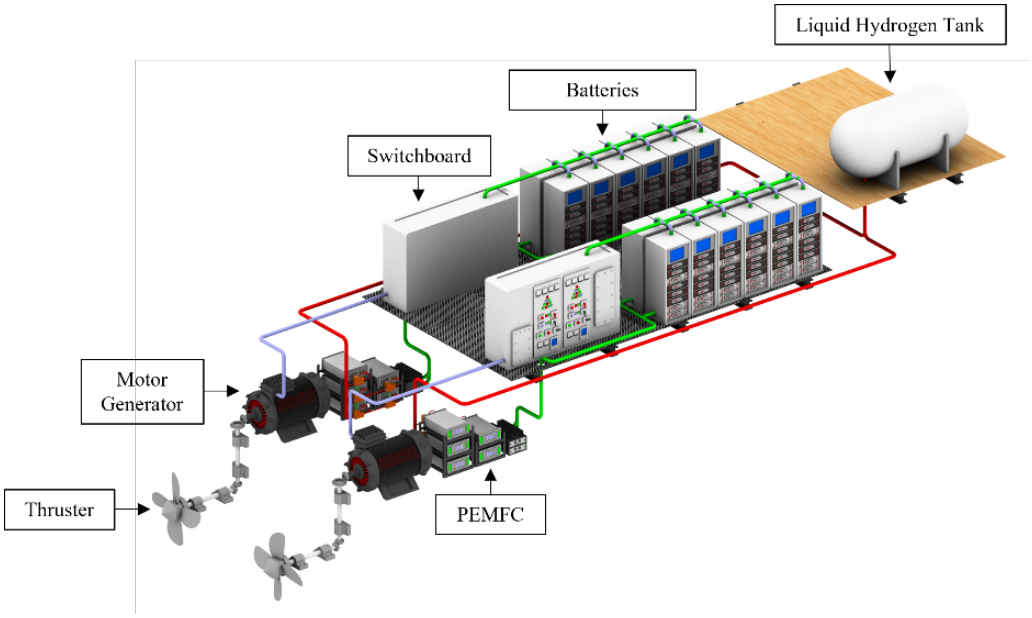

Figure 3-15: Fuel cell powertrain model for marine applications

A key performance criterion for vessels operating near shore and within the harbour is to be able to handle transient loads spontaneously. To ensure the vessel's responsiveness to these loads as well as to provide the necessary power during start-up, an energy storage system such as lithium-ion battery bank is proposed as seen in Figure 3-15. The batteries are charged by a motor-generator, which can operate either in a Power Take-In (PTI) or Power Take-Off (PTO)

mode. During the PTO mode, excess power is channelled to the battery management system for storage. Certain operational manoeuvres would require additional power to be supplied to the drive shaft. In such instances, the required boost will be delivered by the batteries through PTI mode. The charge cycles would be monitored by the battery management system to ensure sufficient energy storage and to preserve the longevity of the battery. The load sharing between the fuel cell and batteries and the electrical Balance of Plant (BoP) is automated through a control system designed to prolong the lifespan of the equipment. In such an electrical architecture, whereby a Direct Current (DC) based energy storage system (i.e., batteries) is used, a DC switchboard is favoured as it eliminates the need for additional converters. Furthermore, it is common practice for a DC-DC converter to be connected to both the battery bank as well as the fuel cell to ensure a quick response to meet any fluctuating load requirements.

3.6.2 Internal Combustion Engines

The use of combustion engines for marine propulsion is well established. Marine engines have been developed considerably, driven by regulatory requirements by the Marine Environment Protection Committee (MEPC) to ensure safety and reliability without compromising on their performance. The proven track record is exhibited in recent compliance to the 0.5% sulphur cap as well as nitrogen oxide (NO_x) limits when operating in emission control areas. Marine engine manufacturers have redesigned the power plant by incorporating technologies such as Exhaust Gas Recirculation (ECR) and Selective Catalytic Reduction (SCR) to reduce harmful NOx emissions to allow compliance with IMO tier III requirements. This hard limit, which is a function of the vessel's engine-rated rpm and year of construction ensures that NOx emissions are between 2 and 3.4 g/kWh for engine speeds between 130 and 2000 rpm.

A hydrogen ICE powertrain configuration is no different from a conventional ICE, by injecting hydrogen gas instead of diesel fuel into the combustion chamber to generate the thermal energy,

which is in turn converted to mechanical energy via the movement of the pistons [125]. This continuous process rotates the shaft to provide the propulsive power required by the azimuth thrusters to manoeuvre the tug as shown in Figure 3-16. To power electrical loads such as lights, motors and pumps, an auxiliary generator is used.

However, as the intrinsic energy content and combustion properties of the type of fuel used differ, a key performance index of a hydrogen engine is its ability to provide power and handle transient loads comparable to longstanding diesel engines.

Current R&D development includes hydrogen blends, which incrementally increase the percentage composition of hydrogen to access the viability and design consideration required [126-129]. The use of hydrogen blends as an intermediary step towards a 100% pure hydrogen-fuelled engine is promising as it provides the necessary validation and track record desirable for the use of hydrogen as a fuel. Notwithstanding the benefits of immediate albeit marginal GHG reduction, the carriage of hydrogen in addition to a primary fuel brings about challenges and impracticalities in the management of fuel tanks, especially for low volumetric energy density fuels.

When examining the combustion characteristics of hydrogen, distinctive features set it apart from other commonly used marine fuels. To achieve a power output comparable to diesel engines, attention to the air-fuel ratio and the fuel injection method is critical. Hydrogen has a stoichiometric air-fuel ratio of 34:1, which translates to 29.4 vol% of the combustion cylinder displaced by hydrogen. Typically, a lean-burn Otto cycle is preferred to reduce the oxides of nitrogen emissions, overcome the high auto-ignition temperature, and prevent pre-ignition caused by hydrogen's low ignition energy [130-132]. Consequently, hydrogen engines require a larger combustion cylinder to achieve a similar power output to a diesel engine.

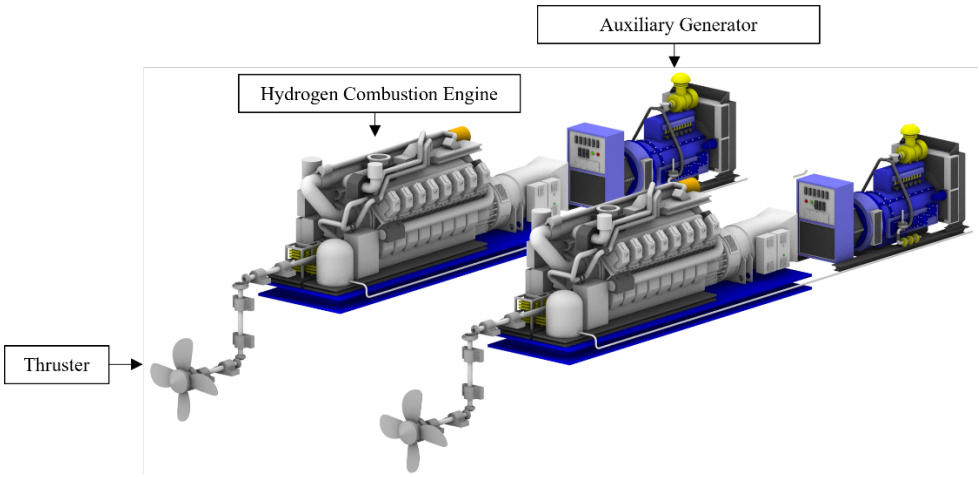

Figure 3-16: Internal combustion engine powertrain model for marine applications

In recent years, there have been developments to couple ICE with electrical motors for marine applications following successes observed in other hybrid mobility sectors. In this configuration, the ICE is coupled with a motor-generator to conserve energy and minimise wear on the engines brought about by frequent fluctuations in RPM. This scenario is a common occurrence observed and benefits vessels with a dynamic load profile where the power required by the thrusters changes regularly. Several power management system designers now offer an integrated solution that encompasses this hybrid powertrain facilitating the uptake of such systems. Typically, this setup would result in a change in the engine size as the maximum capacity rating would decrease due to the addition of the motor-generator, which provides the additional power boost as required. This power-sharing model not only provides Capital Expenditure (CAPEX) savings for the engine but also proposes to reduce emissions as fuel consumption decreases. The trade-off, however, would be an inclusion of a battery system, which has impacts on the increased cost, weight, and space on the vessel.

3.7 Hydrogen Economy

The overarching consensus of using hydrogen as a fuel of the future is strongly motivated by sustainability. This multi-layered buzzword is essentially supported by three pillars (i.e., economic opulence, social responsibility, and environmental protection). Immediately, the strong alignment and similarities are glaring when considering a hydrogen economy. Different actors provide a multi-dimensional perspective of the varying contributing factors that impact the overall techno-economic and environmental viability of hydrogen as a source of marine fuel. This can be visualised using Figure 3-17.

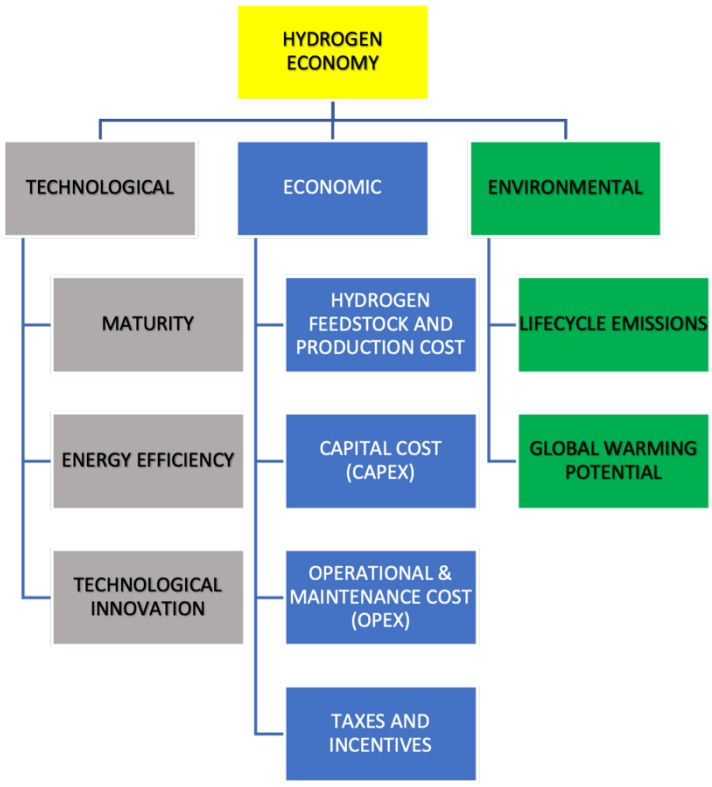

Figure 3-17: Hydrogen economy - A techno-economic and environmental representation

Whilst most of the identified matrices for each pillar above are self-explanatory, clarity on the definition and understanding is important to minimise ambiguity.

- Maturity: Technological maturity refers to the stage at which the technology is currently in (i.e., conceptual, proof-of-concept, demonstration, etc.)

- Energy efficiency: This refers to the optimisation of energy use to achieve the desired output with minimal energy waste, enhancing sustainability and reducing environmental impact.
- Technological innovation: This refers to the diversification and assessment of energy sources and prospects of innovative solutions to realise the desired outcome
- Hydrogen feedstock and production cost: This refers to the cost recognised from the selected pathway model in which hydrogen is manufactured
- Capital cost: This refers to the cost recognised in establishing a facility for manufacturing and the associated supply chain network required.
- Operational and maintenance cost: This refers to the cost recognised from the day-to-day running of the facility
- Taxes and incentives: This 'carrot and stick' approach refers to the framework in which a carbon tax is levied on emissions resulting from the use of fossil fuels while defraying the investment needed to encourage the use of green technology.
- Lifecycle emissions: This refers to the 'well-to-wake' emissions from cradle (i.e., exploration) to grave (i.e., utilisation)
- Global warming potential: This refers to the severity of a pollutant in warming the earth relative to carbon dioxide

Chapter 4

Techno-economic and Environmental Assessment

This chapter introduces the concept development of HyForce, the first-of-its-kind hydrogen-fuelled tugboat. It discusses the design basis, powertrain options, and fuel containment system. The objective is to establish this concept's value proposition against the baseline of a fossil-based equivalent counterpart. This is achieved through a techno-economic and environmental assessment. Finally, the breakeven point under different scenarios is considered

4.1 Conceptualisation of HyForce – A Hydrogen-Powered Tugboat

Leveraging on the knowledge acquired through the extensive literature review carried out on the various powertrain models, a paper has been published in the International Journal of Hydrogen Energy detailing the findings of a techno-economic and environmental study carried out on a hydrogen-fuelled harbour craft. This study provided valuable insights into the use of hydrogen as a source of fuel and the highlights are listed below:

- Feasibility assessment of a hydrogen-fuelled harbour tug
- The use of hydrogen PEM fuel cells and an internal combustion engine for marine tug application
- The total cost of ownership comparative analysis against a traditional diesel tug for 2030 and 2040
- Signposts for hydrogen landing cost breakeven point for commercial viability
- Well-to-wake GHG emissions for different sources of hydrogen

This study resulted in the design of a hydrogen-fuelled harbour tug, which can be seen in Figure 4-1. The tug is designed to carry 50m^3 of liquefied hydrogen in a type C tank at the AFT section of the vessel.

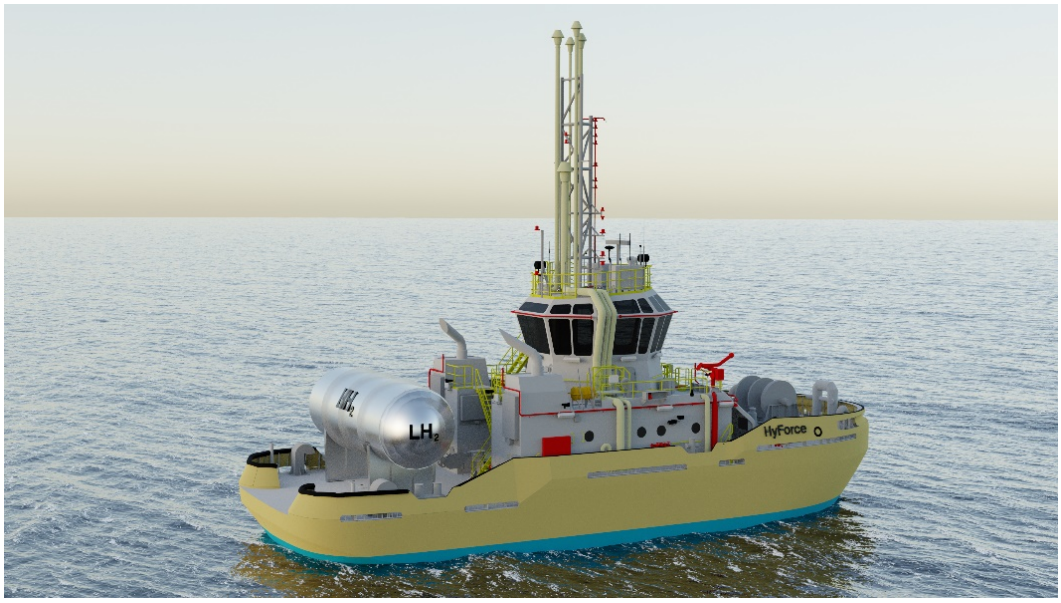

Figure 4-1: Render model of LH2 tugboat - HyForce

4.1.1 Design Basis

This harbour craft, specifically referred to as a tugboat is an instrumental asset in the overall port infrastructure. She facilitates the berthing and unberthing of vessels to a shore or floating structure to perform a range of activities. These might include but are not limited to cargo operations, bunkering, ship-to-ship transfer, crew change, and the loading of stores and provisions. These vessels are small by design but carry a heavy payload with propulsion power. This is essential as it aids in the manoeuvrability of very large vessels up to 10 times her size. Key design parameters of HyForce are given in Table 4-1:

Table 4-1: Design parameters of HyForce

Length Overall (LOA)	20 meters
Beam	7 meters
Bollard Pull Capacity	45 tonnes
Speed	12 knots
Propulsion	2 x 1 MW Internal Combustion Engine (ICE), or 10 x 200 kW Proton Exchange Membrane Fuel Cell (PEMFC)

The design and general arrangement was selected from canvassing the Singapore harbour tug registry to suit the intended outcomes of this study. The various components for the powertrains were identified through product brochures and discussions with tug designer and builders based in Norway and the Middle East.

Figure 4-2 shows the general arrangement of the main equipment. The fuel cell stack and electrical cabinets are designed to be near the motor generator to minimise cable length, comply with ventilation requirements, and mitigate the risks of a hydrogen leak entering the battery room. The proposed layout also considers the ease of access for maintenance and monitoring of the fuel cell stacks.

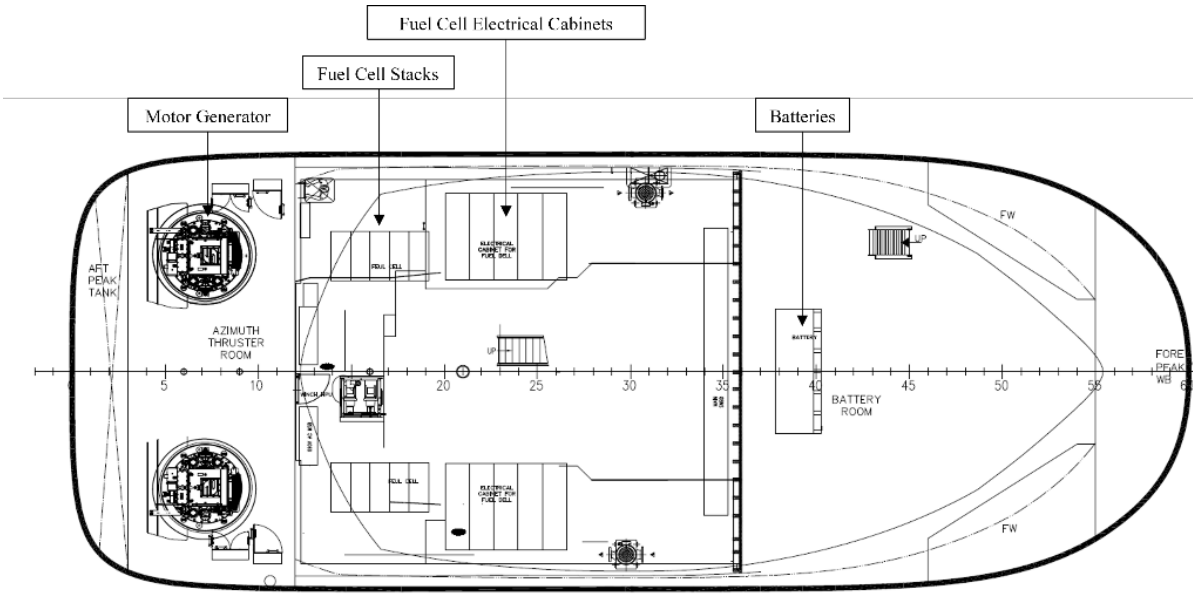

Figure 4-2: General arrangement for HyForce engine room

4.1.2 Onboard Electrical Distribution

A single-line diagram is an engineering drawing that illustrates the main electrical distribution on a vessel. It provides important information such as the (i) size and type of the power-producing equipment (ii) the different consumers that tie into the main switchboard (iii) operating voltage and current (iv) electrical components such as breakers, transformers and converters. The single-line diagram for HyForce is shown below in Figure 4-3.

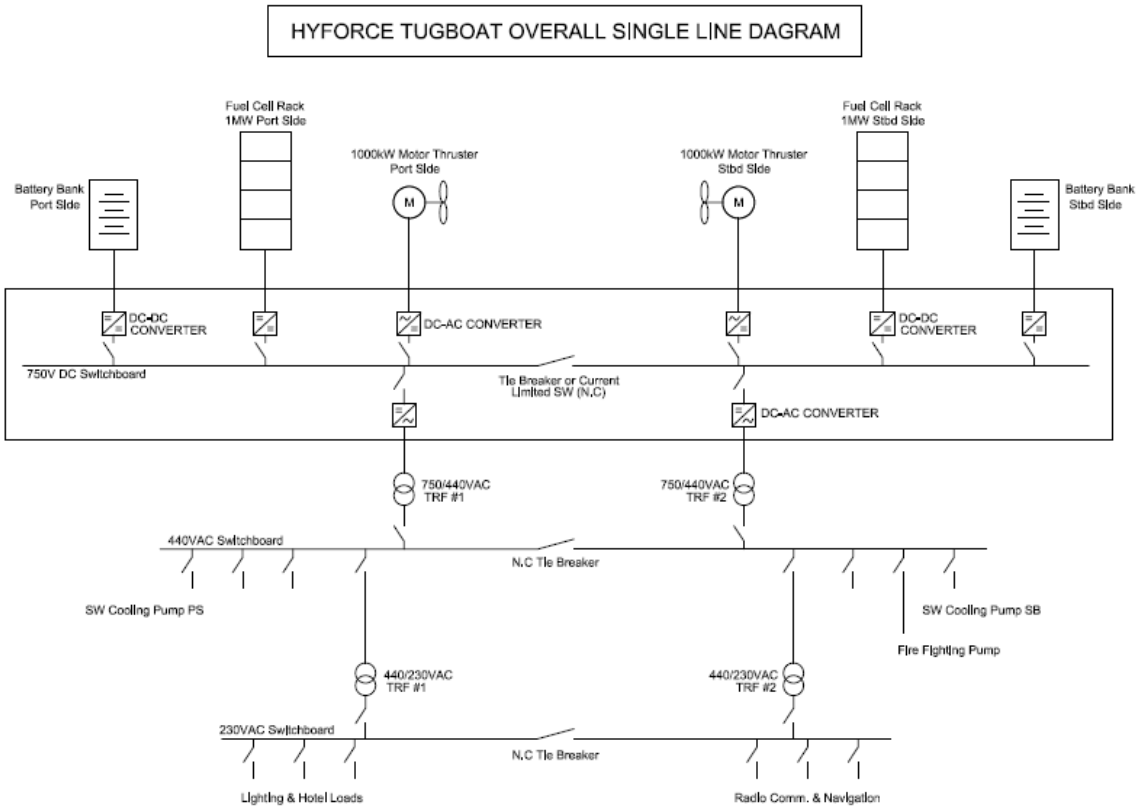

Figure 4-3: HyForce Single Line Diagram

4.1.3 Operational Profile

A comparative study was performed with two distinctive powertrains, a PEM fuel cell and hydrogen-fuelled ICE to determine their respective baselines with the above-mentioned performance indicators. The different powertrains were benchmarked against a fixed set of operating profiles derived from Jurong Marine Services' fleet of tugboats to ensure a realistic representation. The design load profile, which ultimately affects the power requirements of the tug is also shown in Table 4-2. The time spent in each operational profile is formulated based on a daily 12-hour shift the tugboat will be working.

Table 4-2: HyForce operational profile

Operational profile	Time in hours (%)
Idling – Hotel loads	7.2 (60%)
Transit	1.8 (15%)
Standby	1.2 (10%)
Towing	1.8 (15%)

For each operating profile, its corresponding efficiency and fuel consumption are given in Table 4-3. The fuel consumption for the different powertrains together with the inclusion of upstream exploration and processing of hydrogen would set the premise as part of the holistic lifecycle overview of the well-to-wake emissions expected. The efficiencies of the fuel cells are given as a function of the caloric value of hydrogen, fuel consumption, and the corresponding power delivered.

Table 4-3: HyForce power requirement and fuel consumption

Operation Profile	Power requirement (kW)	PEMFC consumption (g/s)	Fuel cell efficiency (%)	Hydrogen ICE consumption (g/s)
Idling	400	6.3	53.44	9.52
Transit	800	12.5	53.87	19.05
Standby	600	9	56.11	14.28
25% bollard pull	700	10	58.92	16.66
50% bollard pull	1086	17	53.77	25.85
75% bollard pull	1428	23	52.26	33.99
100% bollard pull	1940	35	46.65	46.17

4.2 Well-to-Wake Emissions

The two identified hydrogen powertrains are further compared against a traditional diesel-powered ICE, which dominates the current energy mix for this harbour craft application. The motivation to do so is to benchmark against an existing solution to determine and dimension the gap that needs to be overcome. Similarly, the entire lifecycle of GHG emissions for diesel is quantified to ensure a levelled comparison. From Figure 4-4, one may notice that the GHG emissions for the PEMFC and ICE for a 12-hour daily operation amount to 5.4 and 8.2 tonnes of CO2 equivalent (tCO2e), respectively. Retrospectively, the traditional diesel-powered tug emits approximately 7.4 tCO2e. There is a 66% reduction in emissions when hydrogen is

produced via electrolysis using renewable energy. The emissions associated with the use of a high-speed 4-stroke hydrogen ICE are given by a 35% overall energy efficiency across all load profiles. The production and transportation of MDO call for 0.06 kWh/MJ of energy, which is significantly lower than the 0.25 kWh/MJ required for hydrogen.

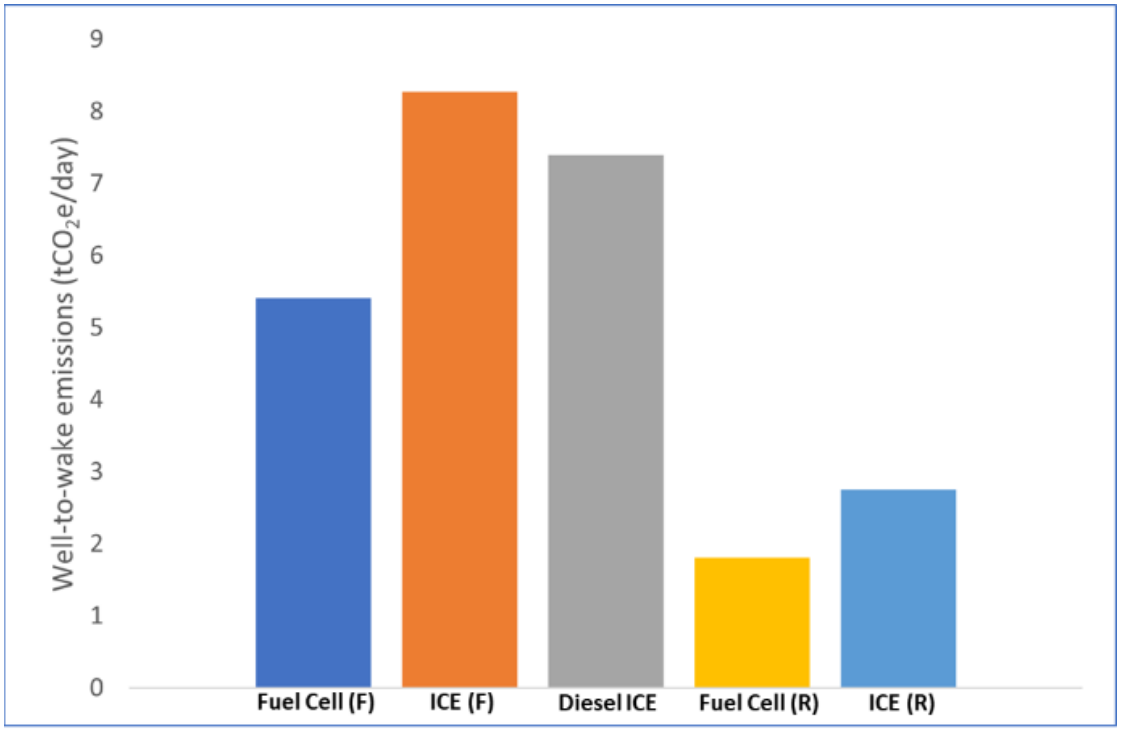

Figure 4-4: HyForce well-to-wake emissions

4.3 Economics

The boundary of the costing estimate of HyForce begins at the conceptual design stage and encompasses the basic and detailed engineering, procurement, construction, and commissioning before delivery from the shipyard. This study, given in US dollars, also includes the operational costs associated with her day-to-day deployment. To provide greater clarity, the cost of safety studies, classification society and insurance fees have also been included. It is noteworthy to highlight that many of these expenditures are expected for any given ship, but a significant disparity arises when contemplating the use of novel technology with a lower Technology Readiness Level (TRL). The difference can be attributed to the cost of the main

equipment, engineering, commissioning, and fuel used. Typical strategies used to mitigate this commercial impact are through the marginal cost of production to achieve desirable economics of scale or using skilled and experienced engineering consultants familiar with the risk-based approach during the conceptual and design phases. Moving forward, the cost of engineering can be alleviated when prescriptive rules are available.

In the conceptual design stage, much of the work is similar to this study whereby a design approach is conceived, and different permutations of system architecture are developed. The intent is to establish the feasibility of the design to meet the operational demands satisfactorily whilst adhering to safety guidelines. Furthermore, the conceptual design would provide valuable insights for the ensuing stages of engineering. This one-off cost is only applicable to 'first of its kind' vessels. It is common for the Final Investment Decision (FID) to be made at this point.

4.3.1 Engineering and Construction Costs

The detailed design and construction phases typically proceed concurrently, with engineering drawings guiding the fabrication and assembly process. The costs in this stage include raw materials (steel cost), production consumables for cutting and welding, production activities such as lifting and transporting (production cost) and labour cost (man-hours). Costs have also been accounted for the conduct of Hazard Identification (HAZID) and Hazard and Operability Analysis (HAZOP) workshops, hydrogen dispersion studies in the event of a leak and classification society fees for design appraisal and approval, which can be seen in Table 4-4.

The engineering costs will generally be higher for novel purpose-built projects such as HyForce, given its unique nature. In the absence of established rules from classification societies, a risk-based approach is often adopted. The costs given for this study is given from costs extrapolated from a hydrogen pilot project designed and built by a Singapore shipyard in 2022. The capital expenditure (CAPEX) estimates for key main systems are derived from

several sources, including quotations, cross-references to similar technologies, and extrapolation. These systems include the PEMFC system, including batteries, hydrogen containment with associated processing units, and the ICE. In this study, the PEMFC is priced at $2,000/kW, whereas the ICE is $379/kW. The cost of the PEMFC is steadily expected to decrease with increased adoption of this technology.

The main contributor to the operational expenditure (OPEX) of HyForce undoubtedly comes from the cost of hydrogen. In this study, the shore-side infrastructure to produce, transport and bunker hydrogen is assumed to be established. The hydrogen landed cost for Singapore is derived from the summation of activities leading to the eventual bunkering onto HyForce. This includes hydrogen production, liquefaction, storage, and transportation. The landed cost price sensitivities fluctuate according to the primary energy source used to produce hydrogen. The feedstock price of natural gas influences the cost of fossil-based hydrogen while the electricity and land costs have a significant impact on the price of hydrogen from renewable sources. It is also noticed that the liquefaction process contributes significantly to the overall cost of hydrogen. In this study, it is assumed that the landing cost of hydrogen is $8.50/kg$LH_2$ for fossil-based (F) hydrogen and $12.50/kg$LH_2$ for renewable (R) hydrogen.

Table 4-4: Cost estimates for the development and construction of HyForce

Steel weight	550 tonnes
Steel cost	$355,7000
Production cost	$275,000
Liquefied hydrogen fuel landed cost in 2022	$8.50/kg$LH_2$ (F) and $12.50/kg$LH_2$ (R)
Engineering costs	$828,948
Production labour cost (Shipyard)	$814,000

4.3.2 Commercial Assessment

An important metric used in this study to assess the economic viability of this project is the breakeven point in which the scale will tip over in favour of HyForce over a traditional diesel tug. The breakeven point takes into consideration both the CAPEX and OPEX to provide better visibility on the bottom-line purchase price of liquefied hydrogen. As the lifespan of the tugboat is between 20 to 25 years, the breakeven point projection is limited to 15 years of operation. Figure 4-5 plots the projected landed cost of liquefied hydrogen against the time horizon of 10, 12 and 15 years starting from 2021. This is benchmarked against the required purchase price of hydrogen to break even at a given point in the operation. For example, for HyForce to break even within 12 years of operation, liquefied hydrogen needs to be purchased at approximately \$4/kgLH_2. It can be seen from Figure 4-5 that the HyForce with a PEMFC system is not cost-competitive after 15 years of operation as the required purchase price is lower than the projected landed cost of hydrogen in 2036.

Figure 4-5 also illustrates the effect of a carbon taxation regime on the purchase price of hydrogen. The magnitude of the tax is based on the expected emissions associated with the traditional diesel ICE. A \$50/tCO_2 tax incentivises the adoption of hydrogen as the required breakeven price increases by 25% to \$4.55/kgLH_2 for a breakeven point of 10 years and a \$100/tCO_2 would allow HyForce with a PEMFC system to breakeven after 15 years from 2036 at a hydrogen purchase price of \$6.39/kgLH_2

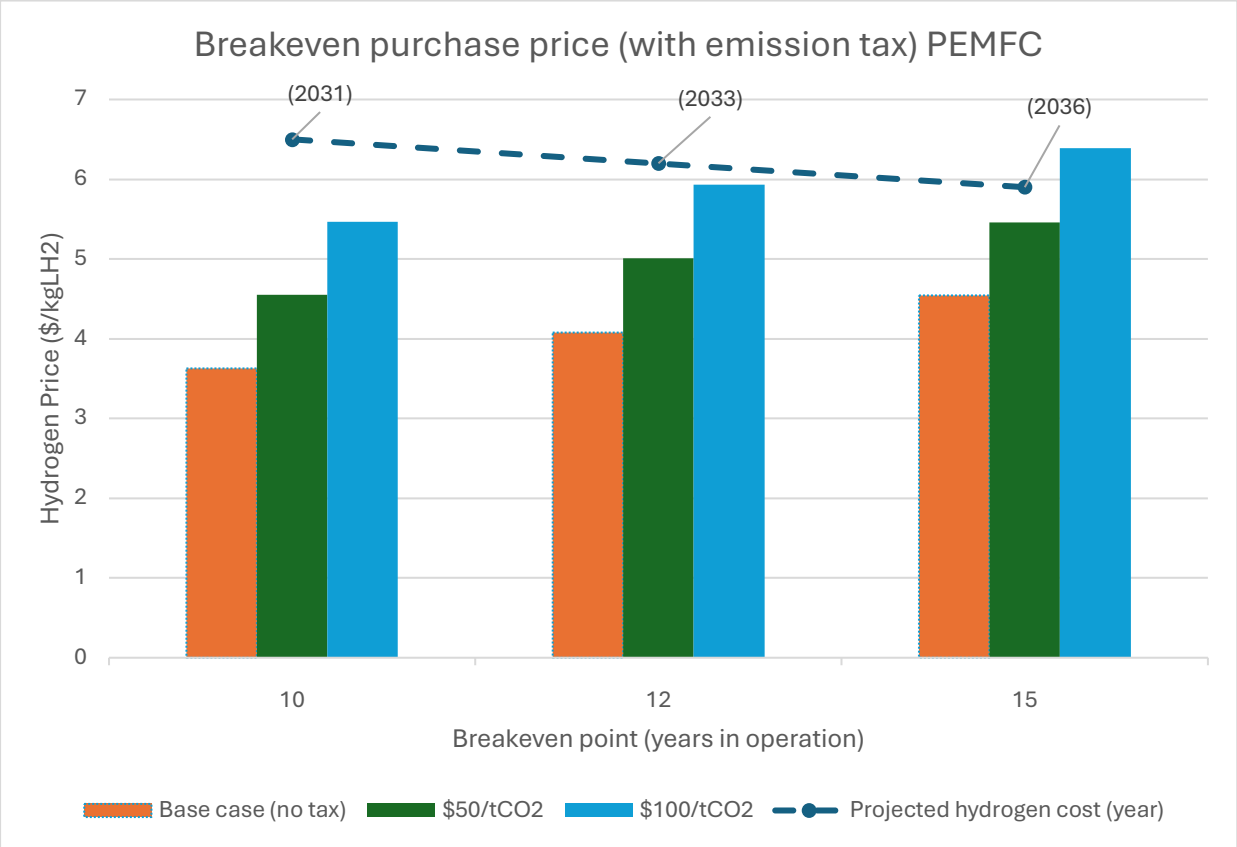

Figure 4-5: Hydrogen purchase price for the use in PEMFC under different emission tax scenarios levied for diesel ICE

Similarly, Figure 4-6 shows the hydrogen purchase price should a hydrogen ICE be used instead. The lower breakeven hydrogen purchase price signals that the ICE system is more cost-prohibitive compared to the PEMFC system. Taking a 15-year breakeven point as an example, hydrogen would need to be purchased at 3.86 USD/kgLH_2 to break even compared to 4.54 USD/kgLH_2 for a PEMFC system. As the initial CAPEX required for an ICE system is lower than the CAPEX of a PEMFC system, the results show that the OPEX is a significant determinant in the overall economics of HyForce. The inferior powertrain efficiency coupled with higher fuel consumption, which ensues from minimising NO_x emission contributes negatively to the economics of this option. Based on the projected landed cost of hydrogen cost within the time horizon of this study, the results show that it will be challenging for HyForce powered by an ICE to achieve an acceptable breakeven point.

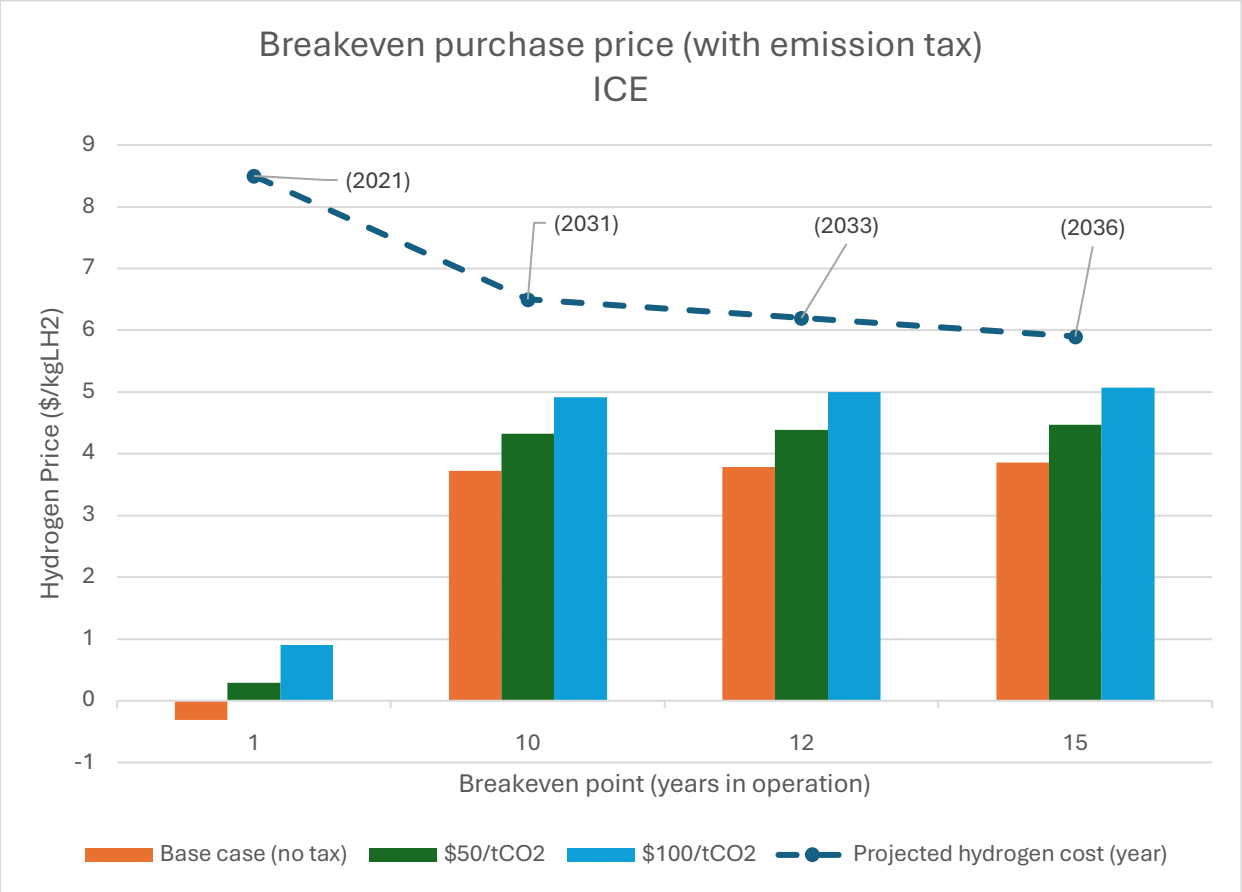

Figure 4-6: Hydrogen purchase price for the use in hydrogen ICE under different emission tax scenarios levied for diesel ICE

Figure 4-7 attempts to illustrate the effect of CAPEX reductions because of technology maturity and acceptance within the maritime industry. A 15% or 25% reduction in CAPEX increases the purchase price of hydrogen by 28% to \$4.65/kgLH_2 or by 47% to \$5.34/kgLH_2 for a 10-year breakeven point, respectively. CAPEX reduction is understandably a signpost for better economics, and one can see the adoption of this technology as a catalyst for this change.

.

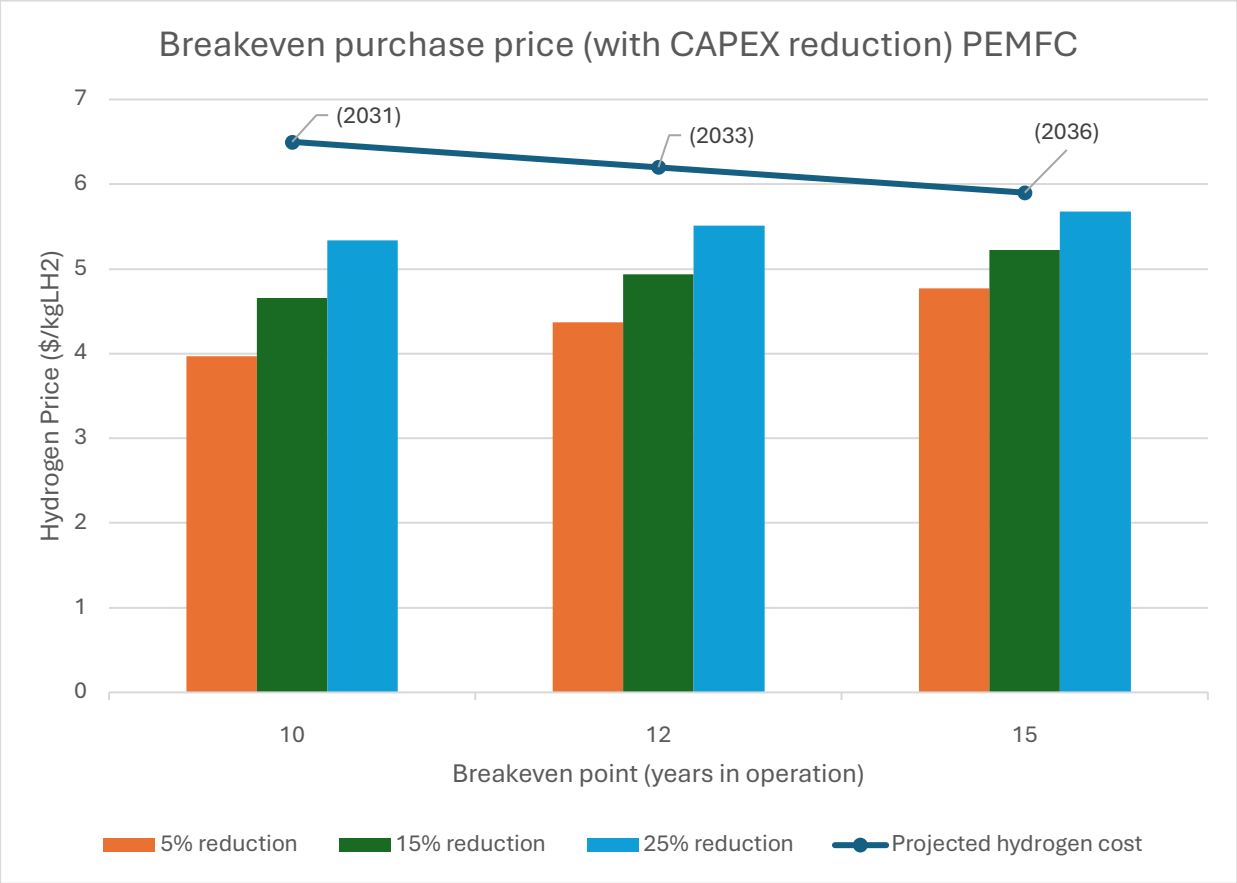

Figure 4-7: Hydrogen purchase price at different PEMFC CAPEX reduction percentages

However, with the rising cost of raw materials and labour, the effect of technology maturity on CAPEX reduction might be diluted. Nonetheless, this shortcoming could be compensated with an improvement in performance and efficiency. The current PEMFC efficiency at different operating load conditions given in Table 4-3 returns an average value of 53.57%. Figure 4-8 illustrates the impact of improved PEMFC efficiency on the overall breakeven price of hydrogen.

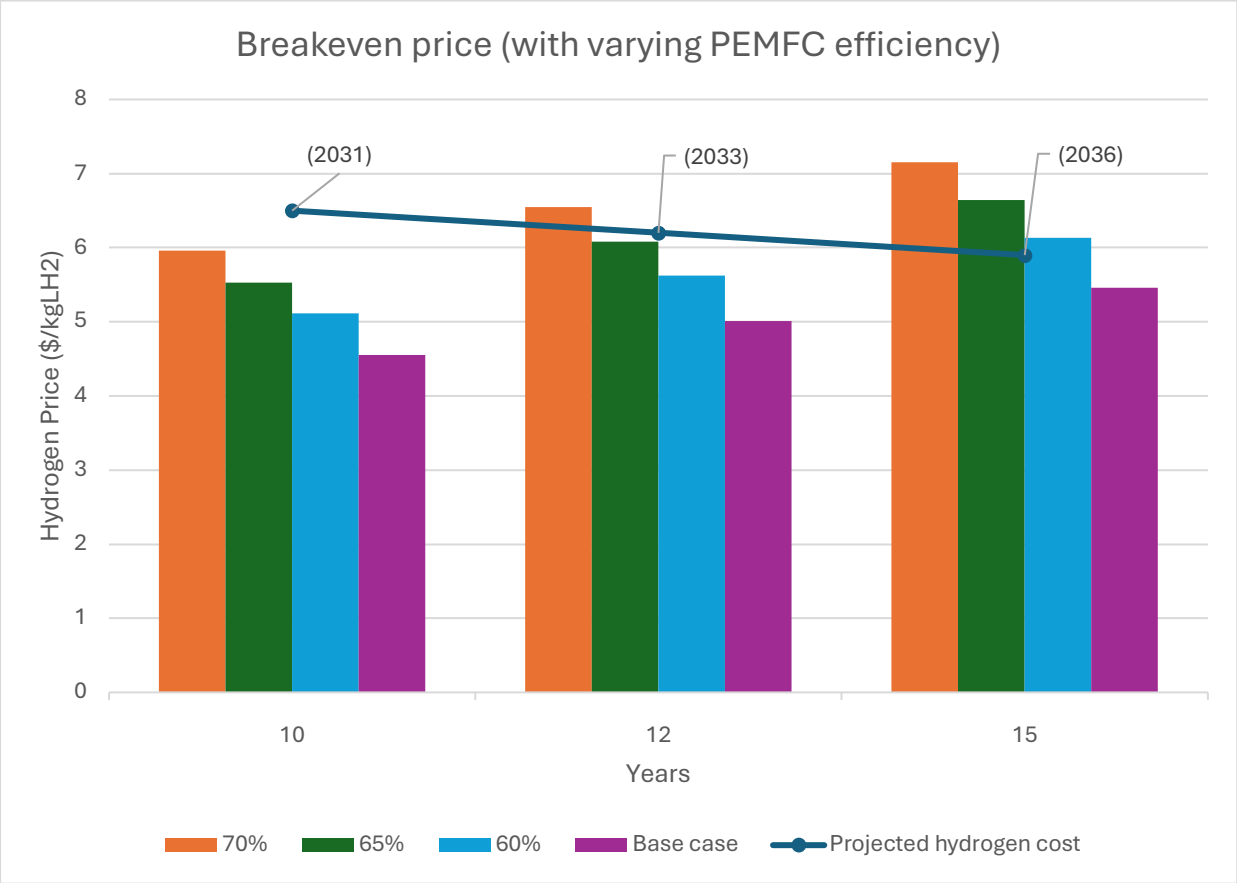

Figure 4-8: Hydrogen purchase price at different PEMFC efficiency percentages

The effect of cumulating CAPEX improvement and a carbon tax levy is shown in Figure 4-9, whereby a 15% reduction and a \$50/tCO_2 tax would allow a PEMFC-based HyForce to be cost-competitive from 2036 with a breakeven point within 15 years.

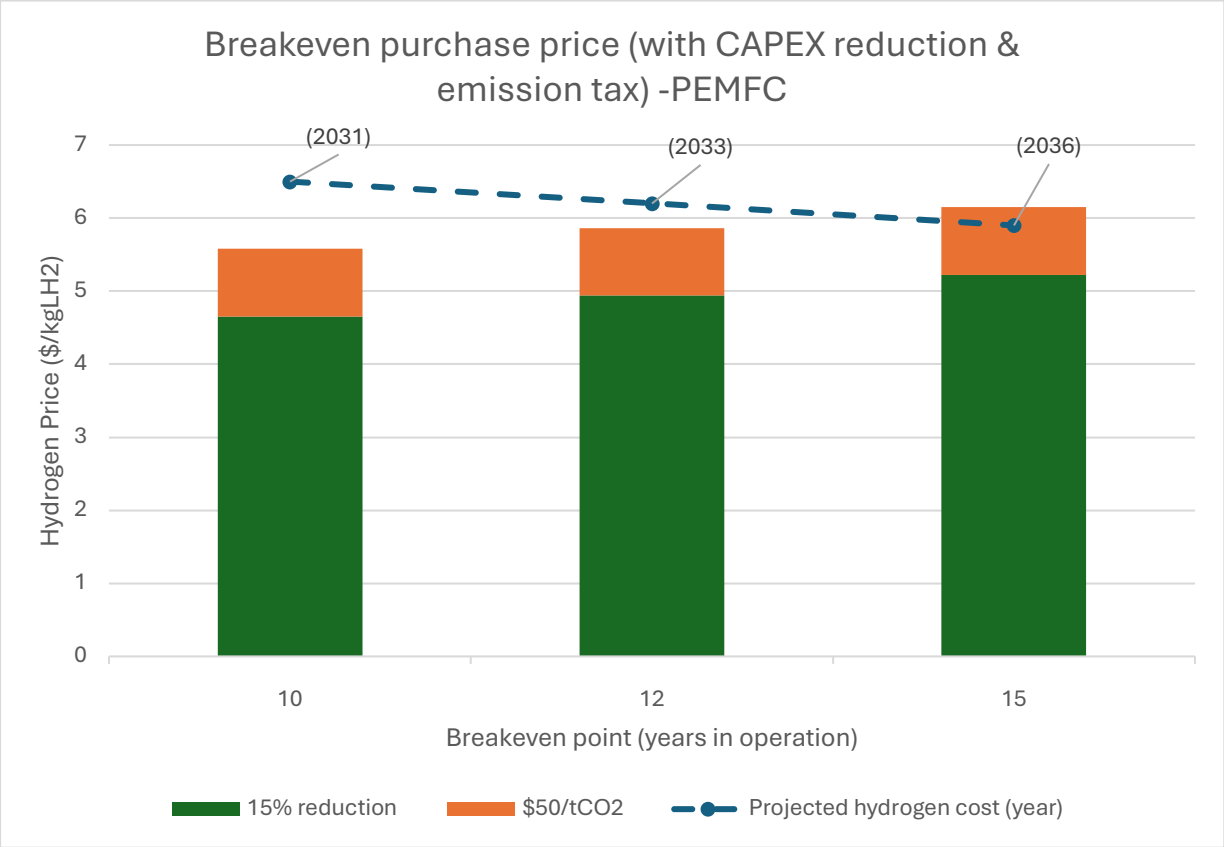

Figure 4-9: Hydrogen breakeven price with 15% CAPEX reduction and $50/tCO2 tax levied on PEMFC

4.4 Total Cost of Ownership

The annualised Total Cost of Ownership (T_{CO}) as shown in Figure 4-10 illustrates the expected cost at different time horizons till 2050 for each of the powertrain options. The cost involved in owning and operating a diesel-powered tugboat is also included as a base case for visibility. The T_{CO} is calculated using equation (4-1), which takes into consideration the capital cost as well as the costs associated with operating the asset.

$$T_{CO} = (Cost_{Fuel} \times Consumption_{Fuel}) + Capex_{Propulsion} + Capex_{Storage} + OPEX + CO_2\ cost \quad (4\text{-}1)$$

The cost of ownership for the hydrogen powertrains takes into consideration the projected downward trajectory of landed cost for liquefied hydrogen till 2050, which is estimated to be

$4.10 per kg. The cost of owning a diesel ICE tugboat increases if she were levied with a $50/tCO$_2$ tax in 2030, $75/tCO$_2$ in 2040 and $100/tCO$_2$ in 2050. Should there be no tax levied on the diesel ICE, the annualised T_{CO} is $1,230,749, which is similar to the cost of ownership of a hydrogen PEMFC powertrain in 2040. The CAPEX of the PEMFCs and ICE are kept constant intentionally to provide a worst-case scenario visualisation of the cost incurred during the operational phase of HyForce. However, as technology for fuel cells improves and moves towards an industry goal of $1500/kW [133], HyForce powered by fuel cells, can be easily cost-competitive by 2040, even without taxes levied on diesel ICE tugs. Notwithstanding a smaller CAPEX compared to PEMFC, hydrogen ICE remains pricier to own in 2050 unless a tax of $50/tCO$_2$ is imposed on the diesel ICE, which as mentioned earlier, is a result of the energy penalty caused by lower efficiency and trace amounts of NO_x emissions produced.

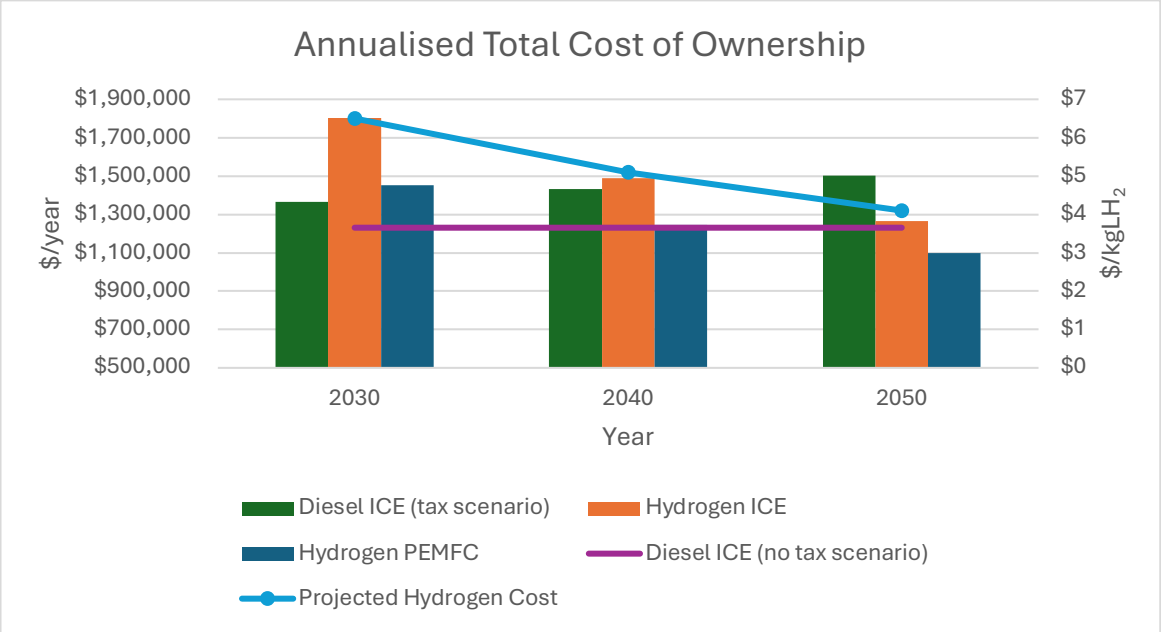

Figure 4-10: Total cost of ownership of different powertrain configurations

The (T_{CO}) calculations establish a baseline of the costs under varying scenarios including but not limited to a carbon levy on the emissions produced by similar vessels operating with a traditional fuel source. This study paves the way for a detailed assessment of the powertrain

used by HyForce and subsequent optimisation to extract her maximum potential. The accuracy and realistic development of this powertrain will be pivotal in ensuring the credibility of this assessment. Advanced simulation tools have the necessary fidelity and robustness to ensure this is ambition is attainable.

This is achieved by creating a digital twin of HyForce and subsequently placed in a virtual environment with real world conditions simulated. The following chapters will progressively introduce and evaluate her performance to meet this objective.

Chapter 5

Modelling Guided Energy Management System

In this chapter, a model of HyForce will be developed, transforming the harbour tug into a virtual environment primed for a range of simulations. The simulations quantify the total resistance exerted on the vessel during operation. This vital information would be instrumental in developing the power management system and subsequent optimisation works. The methodology is detailed and encompasses a holistic range of environmental factors.

5.1 Advanced Simulation for HyForce

Simulation tools such as Computational Fluid Dynamics (CFD) modelling are powerful instruments that provide highly accurate and representative outcomes for any desired function. CFD can identify and present areas of concern requiring further refinement when modelled with reliable data inputs and coherent system dynamics. In the case of HyForce, the main objective is to quantify and validate the viability of utilising hydrogen as a fuel source. A model of HyForce will be developed, transforming the harbour tug into a virtual environment conducive to a range of simulations. These simulations encompass various environmental conditions anticipated for HyForce's operation, such as wind speed, wave height, currents, seawater temperature, and salinity. There are current gaps in the literature surrounding the use of CFD tools for this intended application [134-138]. In [134], the authors have described in great detail the numerical analysis surrounding the manoeuvrability of a similar tugboat application albeit with an emphasis on the skeg of the vessel. This feature is not present in HyForce as it operates with twin azimuth thrusters. [135-137], which are high-level conceptual studies on using hydrogen fuel cells with batteries for marine vessels. Collectively, these

studies address different considerations surrounding the multi-faceted issue of the use of hydrogen in marine applications. This includes hydrogen availability, fuel consumption, bunkering requirements, safety and hazardous zones, electrical load analysis, and GHG emissions quantification. However, they exclude any investigation to rationalise or substantiate the required power to be delivered by the fuel cells. The current study's outcomes, which include the methodology and the framework, will address this gap to complement future studies. In [138], the CFD study performed was constrained to propellors and their interactions with the hull of the vessel was not investigated. Essentially, the power delivered by the propellor will need to compensate for the additional loads experienced on the vessel during operations. The absence of this integration will make it challenging to holistically evaluate the performance of the vessel. The modelling simulations conducted on HyForce, coupled with the theoretical model of the power trains, will yield essential inputs for power requirements under different operating conditions. These inputs are instrumental in managing operational power variations, facilitating outcomes such as (i) reduced fuel consumption (ii) optimised battery charge cycles (iii) improved battery charging scenarios, and (iv) setting a lower hard limit for the reserve 'take-me home' power.

5.2 Digital Twin Development

HyForce is a liquid hydrogen (LH_2) fed fuel cell-powered harbour craft with batteries designed to operate within coastal waters. HyForce is equipped with a 45-ton bollard pull winch to perform the necessary pull and/or push towing scenarios. The towing winch is strategically placed at the vessel's forward section to accede to the placement of a $50m^3$ LH_2 containment system, containing approximately 3.6 tonnes of hydrogen at the stern as seen in Figure. 5-1. Overall technical geometry configurations of the HyForce vessel are shown in Table 5-1.

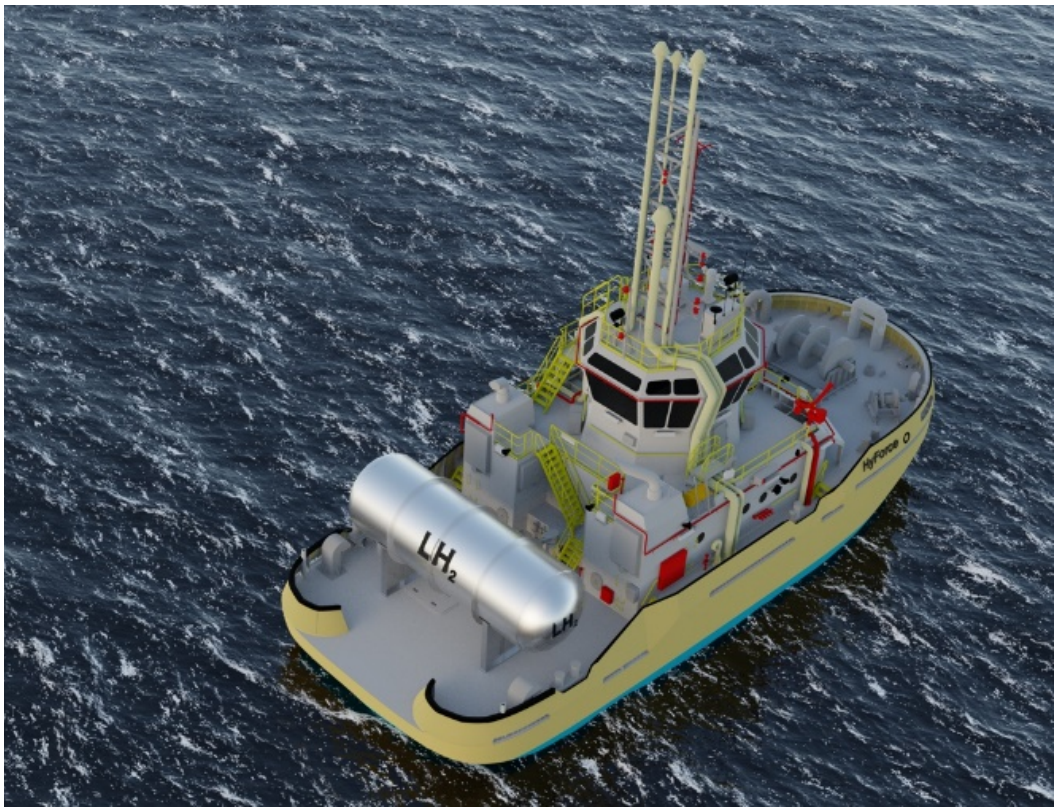

Figure. 5-1: Bird's-eye view of HyForce with liquid hydrogen storage tank

Table 5-1: HyForce vessel parameters

Parameter	Symbol	Value	Unit
Overall length of the tugboat	L	30	m
Width	W	12	m
Wetted surface of bare hull	S_{BH}	401	m^2
Length of water line	L_W	28.22	m
Breadth of water line	B	12	m
Draft	T	3.30	m
Displacement	∇	661	m^3
Wetted surface area of appendages	S_{APP}	5	m^2
Waterplane coefficient	C_{wp}	0.851	-
Midship section coefficient	C_m	0.854	-
Block coefficient	C_b	0.576	-
Form factor	$(1 + k_1)$	0.57	-

As the tugboat transitions through the different operational scenarios, the corresponding power demand from the propulsion system changes. As no two missions are alike, the inherently dynamic nature of tugboat operations makes it challenging to accurately estimate the combined power output the propulsion systems are required to produce. In the unlikely scenario that the tugboat performs identical missions (i.e., same load demand), environmental conditions might differ, resulting in variations in the power required to sustain vessel speed and heading or towing force. Nonetheless, a basis of design needs to be established to right-size the propulsion system capable of fulfilling the operational demand rigour. For HyForce, the operational profile was curated through close collaboration with an existing tugboat operator in Singapore to best harmonise the different potential mission scenarios that can be anticipated. This collaboration provided the opportunity to have more granularity on the operational profile which can be seen in Table 5-2. The transition between the load points will be instantaneous as defined in the operational requirement of tugboat. This is made possible with the ESS providing the necessary transient power.

Table 5-2: Operating scenarios for HyForce

Operating Scenarios	
In port – Mainly hotel loads (e.g., HVAC, lighting, pantry, etc.)	7.2 hrs (60%)
Movement to mission location	1.8 hrs (15%)
Awaiting mission start (i.e., hooking up of tow line etc)	1.2 hrs (10%)
Mission execution	1.8 hrs (15%)
Auxiliary loads	400.0 (kW)
Transit 6 knots	103.25 (kW)
Transit 10 knots	770.01 (kW)
Transit 12 knots	1601.90 (kW)
Towing 50% (bollard pull)	765.5 (kW)
Towing 100% (bollard pull)	2082.5 (kW)
Maximum speed	12.0 (knots)
Maximum pulling load	45.0 (ton)

5.3 Methodology for Power Evaluation

For optimal operation of the designed operating scenarios, an accurate power evaluation tool is developed. This section describes the methodology for the optimal power evaluation to achieve operational profile setting with the effects of the environment. Particularly, the effects of current and water depth directly affect the speed of the HyForce, while the surface roughness, water temperature, water properties, wind, wave, displacement, and trim directly contribute to the total resistance of the tug. The required total power is needed to overcome the total resistance and maintain the HyForce performance. Figure 5-2 shows the evaluation workflow for power and tugboat performance considering the environmental effects. Details of each component are analysed in the subsequence subsections.

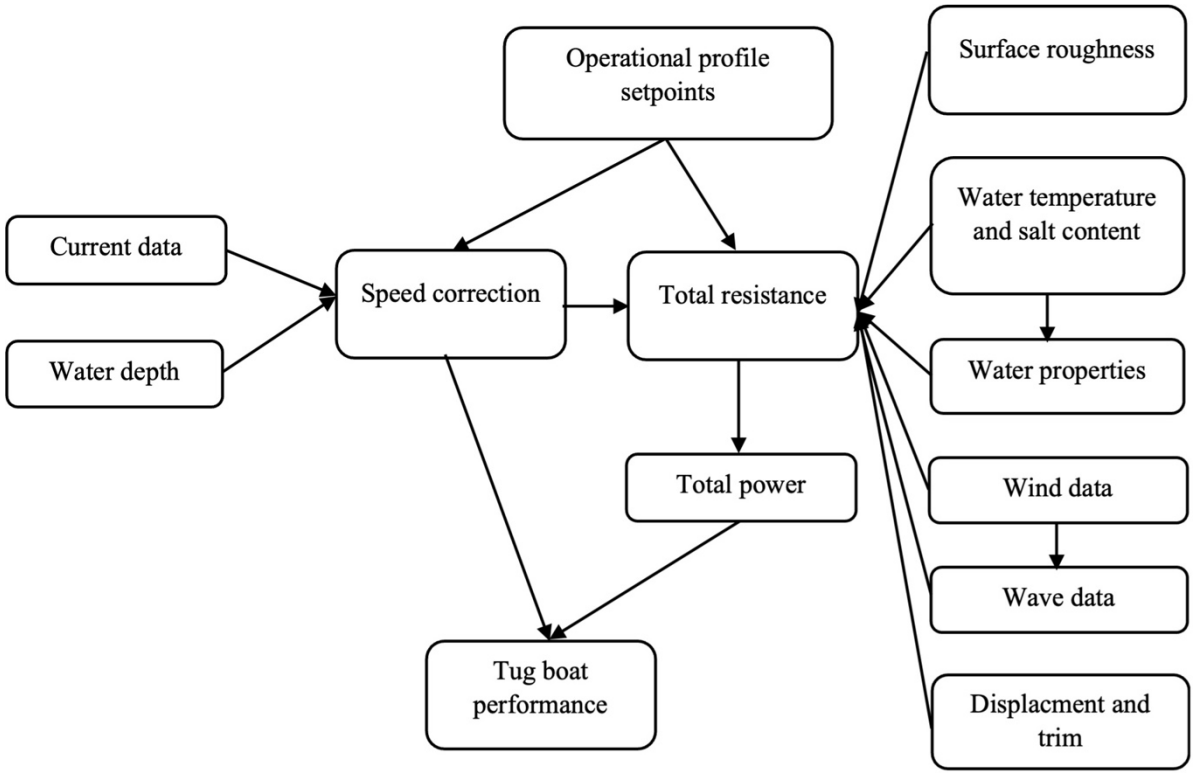

Figure 5-2: Power evaluation workflow for the operational profile of HyForce with environmental effects

5.4 Speed Correction

Both current speed and the depth of seawater directly influence the HyForce speed. To obtain the actual speed of the tug, the correction speed must be accurately evaluated. The effect of the water depth can be evaluated via empirical formulation [139] , while the effect of the sea current can be evaluated through vector summation theory and the relative direction of the current and the tugboat. Thus, the actual speed of the tug can be expressed as

$$V_{actual} = V_{set}\left(1 - \Delta V_{depth}\right) + \Delta V_{current} \quad (5\text{-}1)$$

In this expression, V_{set} is the setting speed that engine(s) can deliver in calm and depth (>20 m) water. ΔV_{depth} is speed reduction caused by the depth of the seawater. $\Delta V_{current}$ is the change in tugboat speed caused by the current of the sea. V_{actual} is the corrected speed of the tugboat. This actual speed of the tug will be implemented and integrated into the programme for the toral resistance and power evaluation.

5.4.1 Effect of Water Depth

HyForce, a harbour craft, operates in coastal water at varying depths. The depth of water has an impact on the actual speed of the water and this speed reduction is calculated using the formulation proposed by Lackenby [140]:

$$\frac{\Delta V}{V} = 0.1242\left(\frac{C_m}{H^2} - 0.05\right) + 1 - \sqrt{\left(tanh\frac{gH}{V^{\frac{2}{3}}}\right)} \text{ for } \frac{C_m}{H^2} \geq 0.05 \quad (5\text{-}2)$$

where (C_m) is the midship section coefficient underwater, (g) is the gravity acceleration, (H) is water depth, (V) is the tugboat speed, and (ΔV) is the decrease of the tugboat speed due to the shallow water. From the above, water depths exceeding 20 meters do not have any considerable effect on the speed reduction of the vessel.

5.4.2 Effect of Seawater Current

The corrected speed of the HyForce is evaluated based on the relative angle of the current direction and the tug direction (Θ_c), the current velocity (V_c), and the relative velocity (V_s) of the tug and the seawater. Which, the corrected angle and corrected speed are calculated using the following formulations.

If ($90^o < \Theta_c < 270^o$):

$$\Theta_{corrected} = 180 - tan^{-1}\left(\frac{V_c \times sin\left(\frac{\pi}{180}\times\Theta_c\right)}{V_s + V_c \times cos\left(\frac{\pi}{180}\times\Theta_c\right)}\right) \times \frac{180}{\pi} \quad (5\text{-}3)$$

$$\Theta_{cal} = tan^{-1}\left(\frac{V_c \times sin\left(\frac{\pi}{180}\times\Theta_c\right)}{V_s + V_c \times cos\left(\frac{\pi}{180}\times\Theta_c\right)}\right) \quad (5\text{-}4)$$

$$V_{corrected} = V_s - \frac{V_c \times cos\left(\frac{\pi}{180}\times\Theta_c\right)}{cos\,(abs(\Theta_{cal}))} \quad (5\text{-}5)$$

else:

$$\Theta_{corrected} = 180 - tan^{-1}\left(\frac{V_c \times sin\left(\frac{\pi}{180}\times\Theta_c\right)}{V_s - V_c \times cos\left(\frac{\pi}{180}\times\Theta_c\right)}\right) \times \frac{180}{\pi} \quad (5\text{-}6)$$

$$\Theta_{cal} = tan^{-1}\left(\frac{V_c \times sin\left(\frac{\pi}{180}\times\Theta_c\right)}{V_s - V_c \times cos\left(\frac{\pi}{180}\times\Theta_c\right)}\right) \quad (5\text{-}7)$$

$$V_{corrected} = V_s - \frac{V_c \times cos\left(\frac{\pi}{180}\times\Theta_c\right)}{cos\,(abs(\Theta_{cal}))} \quad (5\text{-}8)$$

5.5 Effect of Temperature and Salt Content on Seawater Properties

Seawater temperature varies according to geographical location and the spectrum is sufficiently wide to affect its viscosity and density. Together with temperature, salinity is also an important parameter which contributes to the change in the physical properties of seawater. These physical properties can be calculated based on the correlation of freshwater and salinity (S_A) and temperature (T) given by Sharqawy et al. [141]. The dynamic viscosity of seawater (μ_{sw}) can be evaluated using the following equations referencing freshwater (μ_{fw}) as below.

$$\mu_{sw} = \mu_{fw}(1.0 + A * S_A + B * S_A) \quad (5\text{-}9)$$

Where A and B are functions of temperature, T in (°C) is given below:

$$A = 1.541 + 0.01998T - 9.52 \times 10^{-5}T^2, \quad (5\text{-}10)$$

$$B = 7.974 - 0.07561T + 4.724 \times 10^{-5}T^2 \quad (5\text{-}11)$$

In which, the viscosity of the freshwater is the function of the temperature and be expressed as

$$\mu_{fw} = 0.0018 - 6.0 \times 10^{-5}T + 1.0 \times 10^{-6}T^2 - 8.0 \times 10^{-9}T^3. \quad (5\text{-}12)$$

The density of the seawater is expressed using the following correlation

$$\rho_{sw} = \rho_{ref} + B1 * S_A + 1.5 * C1 * S_A + d_0 * S_A^2 \quad (5\text{-}13)$$

where

$$\rho_{ref} = a_0 + a_1T + a_2T^2 + a_3T^3 + a_4T^4 + a_5T^5, \quad (5\text{-}14)$$

$$B1 = b_0 + b_1T + b_2T^2 + b_3T^3 + b_4T^4, \quad (5\text{-}15)$$

$$C1 = c_0 + c_1T + c_2T^2. \quad (5\text{-}16)$$

In these expressions, the coefficients a_i, b_i, and c_i are given as

$a_0 = 999.842594$, $a_1 = 6.793953e^{-2}$; a_2 =-*9.095290*e^{-3}, $a_3 = 1.001685e^{-4}$,

$a_4 = -1.120083e^{-6}$, $a_5 = 6.536332e^{-9}$, $b_0 = 8.2449e^{-1}$, $b_1 = -04.0899e^{-3}$,

$b_2 = 7.6438e^{-5}$, $b_3 = -8.2467e^{-7}$, $b_4 = 5.3875e^{-9}$, $c_0 = -5.7246e^{-3}$,

$c_1 = 1.0227e^{-4}$, $c_2 = -1.6546e^{-6}$, $d_0 = 4.8314e^{-4}$.

The calculated seawater properties as a function of temperature and salinity show that the seawater density is highest when the temperature is at 0°C with a corresponding salt concentration of 50g/kg seawater.

5.6 Total Resistance

This section studies all the key parameters contributing to the total resistance of HyForce. The implications of (i) wind (ii) water (iii) wave data (iv) friction on the total resistance acting on HyForce were investigated. The methodology is to isolate and quantify the impact of each

parameter on the total resistance applied to HyForce. The effects of wind and water are evaluated through computational fluid dynamics, while the effects of the wave and friction are computed using empirical methods. These environmental effects are anticipated to be observed on HyForce during operations and inevitably have an impact on the total power required. It is hence prudent to design any power management optimisation strategies against a realistic real-world scenario.

5.6.1 Wind Resistance

An environmental attribute that can contribute significantly to ship motions during operations is the presence of wind. This is more pronounced for smaller vessels and HyForce falls under this category. To this effect, CFD can play an important role in evaluating the impact of wind load on the vessel. The results generated from the CFD are useful to understand the complex airflow behaviour around the vessel. Through modelling and simulation, the wind resistance acting on HyForce can be quantified and analysed. A fit-for-purpose approach was taken to simplify the complex superstructure which otherwise require a detailed and locally very fine grid which might not necessarily add significant improvement to the accuracy of the results. A modified geometry of the model was used to identify any blockage effects. The physical dimensions of HyForce were the length (L_W) of 28.22 m, breadth (B) of 12.0 m, the frontal projected area (A_F) of 130.2 m^2, lateral projected area (A_L) of 253.5 m^2. Also, the reference wind velocity (U_{ref}) of 10.0 m/s was used with a Reynolds number of 7.76x10^6. The computational domain and direction of wind experienced on the vessel are given in Figure 5-3.

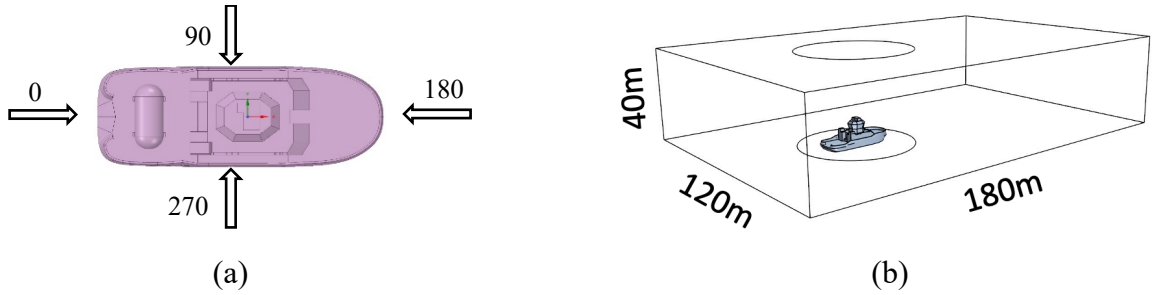

(a) (b)

Figure 5-3: Numerical setup and direction definition of the force: (a) Direction of wind acting on the vessel, (b) designed computational domain for CFD calculations

The CFD calculations were based on a geometry model that represented HyForce on a 1:1 scale where the wind loading coefficients, $C_{FX} = \frac{F_x}{\frac{1}{2}\rho V^2 A_F}$, $C_{FY} = \frac{F_y}{\frac{1}{2}\rho V^2 A_F}$ and $C_M = \frac{M_x}{\frac{1}{2}\rho V^2 A_F L_{OA}}$ are defined through the forces (F_x and F_y) in the x and y direction with the moment (M_x) on the tugboat in the z direction around the centre of the vessel. The top surface of the computational domain is 40 meters from the water surface which is sufficiently high enough to capture the full effect of wind flow over HyForce as illustrated in Figure 5-3.

The computational grids are constructed using Ansys Fluent and the higher-order unconstructed Quadratic Upstream Interpolation for Convective Kinematics (QUICK) numerical scheme is employed for the space discretization of the Reynolds-averaged Navier-Stokes (RANS) governing equations. The shear stress transport (SST) k-ω turbulence model [142] is used together with an automatic wall function approach for a full boundary layer resolution [143]. The velocity profile, $U(z)$, is specifically chosen to resemble best an atmospheric boundary layer profile observed in open seas [144]. The moment coefficients are calculated at different inflow angles from 0.0 degrees to 360.0 degrees with a step increase of 10.0 degrees. The wind speed is set at 10.0 m/s at the inflow boundary with constant pressure specified downstream of the computational domain. 36 simulations were performed to evaluate the moment coefficients with a total mesh count of about 3.5 million obtained from the mesh convergence study. The

results from the CFD calculations for both the longitudinal and lateral wind load coefficients are shown in Figure 5-4.

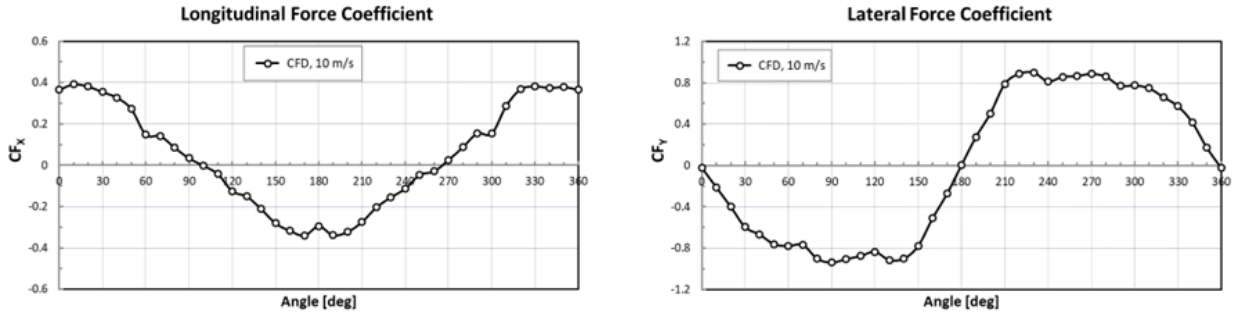

(a) (b)

Figure 5-4: Wind load coefficients at different wind heading directions (a) Longitudinal (b) Lateral

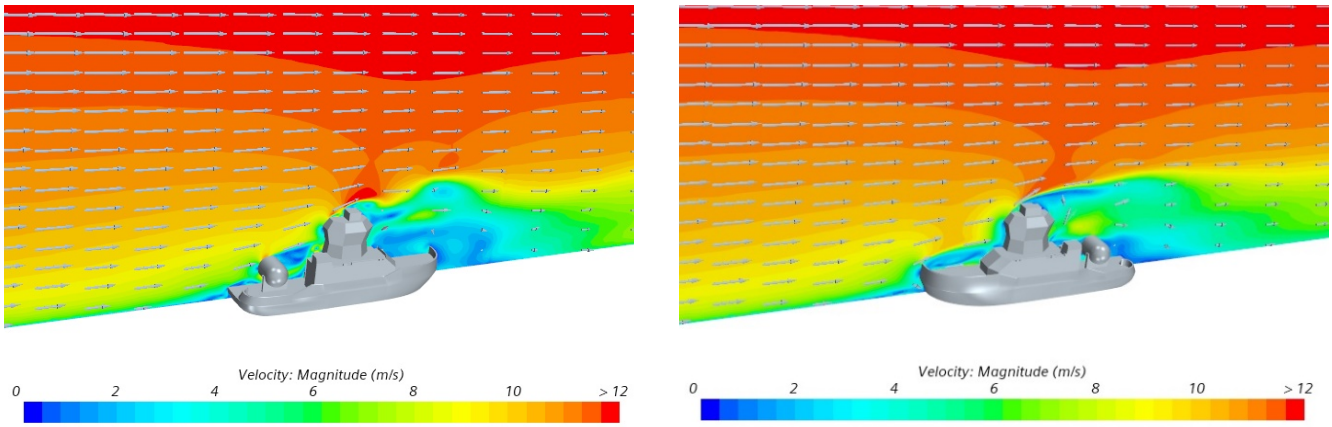

(a) (b)

Figure 5-5: Wind velocity contour including the wake for different wind heading directions (a) 0.0 degrees (b) 180.0 degrees

Figure 5-5 shows the velocity contours at the cross-section of HyForce at 0.0 deg heading (wind blowing from the back) and 180.0 deg heading (wind blowing from the front). The obtained results show that the wind speed slows down as it approaches the tugboat, and a wake is created as it leaves. This creates a high pressure in the frontal direction and a low pressure in the wake region which is illustrated in Figure 5-6.

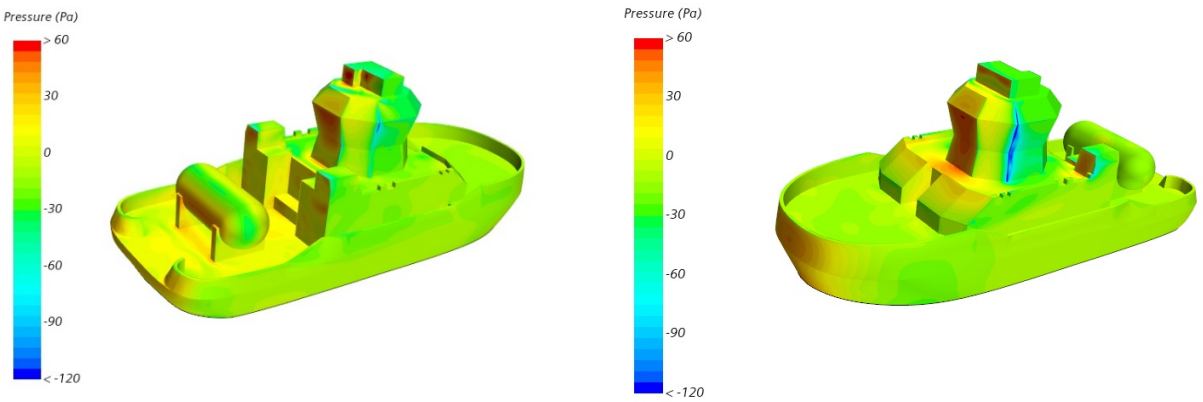

(a) (b)

Figure 5-6: Pressure contour acting on HyForce's walls for different wind heading directions (a) 0.0 degrees (b) 180.0 degrees

5.6.2 Water Resistance – Currents

Similarly, water resistance is an important factor contributing to the total resistance, which is also evaluated through the modelling simulation of the incompressible flow using computational fluid dynamics. The QUICK numerical scheme is employed for spatial discretization of the incompressible water flow, which is governed by RANS equations. The SST k-ω model is used for the turbulence model and details of the numerical method are extracted from Yuck et al [145]. A total of 36 CFD simulations were performed with varying seawater current headings from 0.0 degrees to 360.0 degrees in increments of 10.0 degrees using the finite volume method within Ansys Fluent. The computational domain is determined to ensure that the far-field boundary conditions do not affect the accuracy of the results. A mesh grid with a total of about 4.0 million cells obtained from mesh grid convergence studies was used in the simulation. The seawater properties that best represent Singapore's coastal waters were chosen, which set the temperature at 25℃ and salt concentration at 35 g/kg seawater, respectively. This simulation is performed at a speed of 1.0 knot, equivalent to 0.513 m/s at a

Reynolds value of 6.92x106. The water load coefficients of the longitudinal and lateral forces are calculated similarly to wind resistance and their results are shown in Figure 5-7.

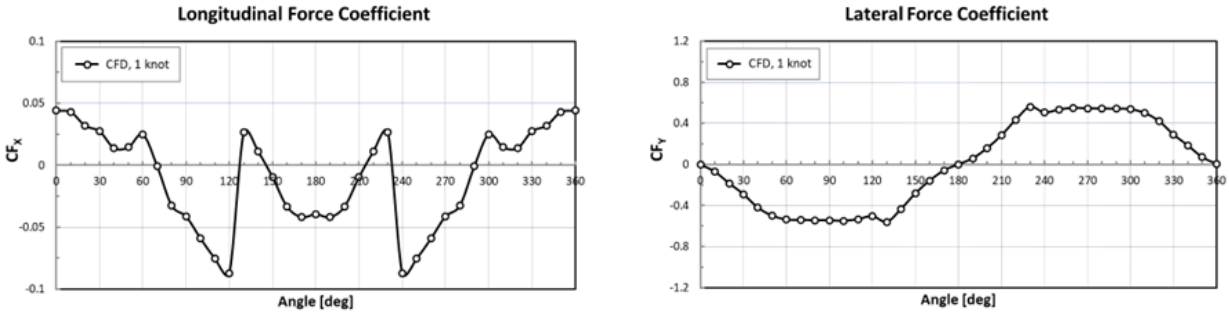

(a) (b)

Figure 5-7: Current load coefficients at different current heading directions; (a) Longitudinal coefficient and (b) Lateral coefficient

The simulations performed provided the velocity and pressure contours across HyForce and the results are shown in Figure 5-8 and Figure 5-9 respectively. Figure 5-8 shows the velocity contour at the middle cross-section of the tugboat for the different current heading directions. Figure 5-8 (a) shows the velocity contour of the 0.0 degrees, and Figure 5-8 (b) shows the velocity contour for the case of 180.0 deg. Figure 5-9 shows the pressure contour of the seawater on the surface of the tugboat for different current heading directions. Figure 5-9 (a) is when the current heading direction is at 0.0 degrees, and Figure 5-9 (b) is the case of 180.0 degrees.

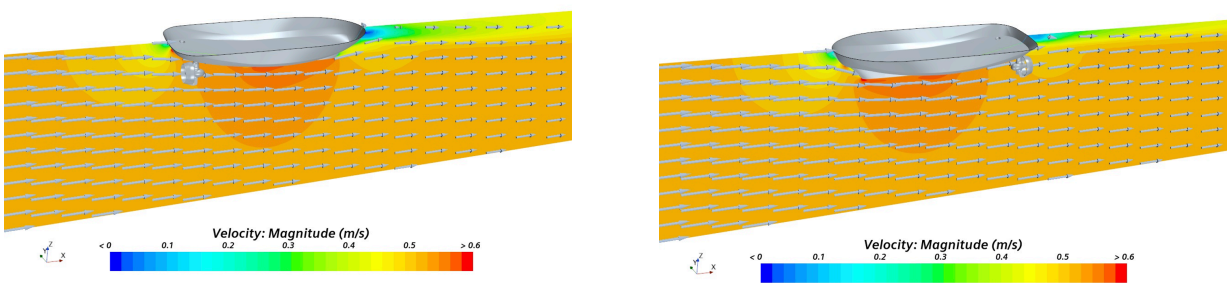

(a) (b)

Figure 5-8: Velocity contour at the cross-section along the centreline of HyForce at different current headings with a speed of 1 knot (a) 0.0 degrees (b) 180.0 degrees

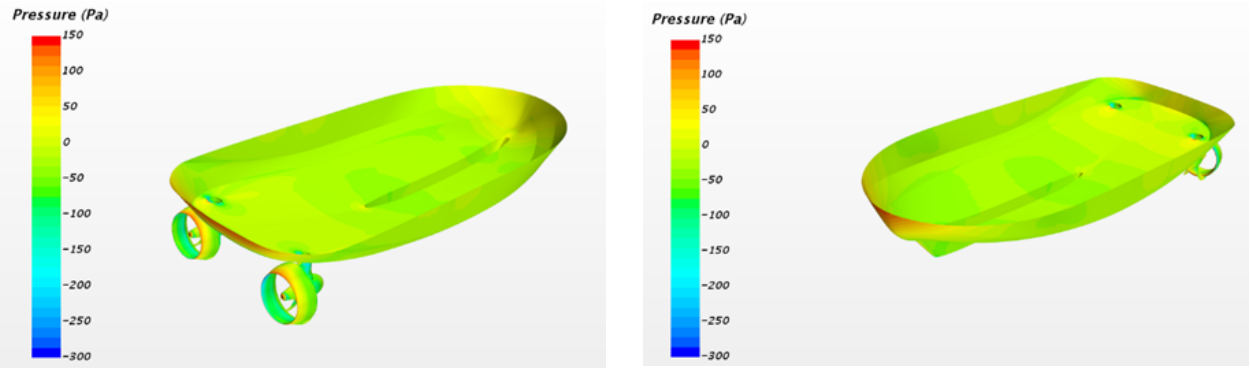

(a) (b)

Figure 5-9: Pressure contour at the cross-section along the centreline of HyForce at different current headings with a speed of 1 knot (a) 0.0 degrees (b) 180.0 degrees

5.6.3 Wave resistance – Heave and Pitch

To determine the added resistance that will be experienced by HyForce due to waves can be determined by model testing in a tank basin. This controlled environment is capable of artificially replicating waves accurately to capture and record the observations and results on the test model. Alternatively, an approximation formula which is limited to ±45.0 degrees off the bow can be used given in the equation below [146]:

$$R_{AWL} = \frac{1}{16}\rho g H_w^2 B \sqrt{\frac{B}{L_{BWL}}} \quad (5\text{-}17)$$

The resistance attributed to waves (R_{AWL}) is a function of the significant wave height (H_w), the breadth (B), and the length of the bow on the water line (L_{BWL}) of 7.4 m. The range of the wave height is selected through the actual condition of the wind and history measurement data for the Singapore Strait. Compared to the water resistance, waves contribute significantly less to the overall total resistance experienced by HyForce during operations.

5.6.4 Friction Resistance

The friction resistance is a function of seawater properties (density and viscosity) and the surface roughness of the hull. The estimated formulation of the friction resistance is given as:

$$R_F = \frac{1}{2}\rho(S + S_{APP})V_S^2 C_F \quad (5\text{-}18)$$

In this expression, C_F is the friction coefficient, ρ is the density of the seawater, S is the wetted area of the tugboat's hull, S_{APP} is the wetted surface area of the appendages, V_s is the velocity of the HyForce. The friction coefficient is calculated as

$$C_F = C_{F0} * (1.0 + k) + C_{SR} \quad (5\text{-}19)$$

The reference frictional resistance coefficient is calculated as

$$C_{F0} = \frac{0.075}{(log(Re) - 2.0)^2} \text{ with } Re = \frac{V * L_{WL}}{\mu} \quad (5\text{-}20)$$

The coefficient of the surface roughness is calculated as

$$C_{SR} = 0.001\left(105\left(\frac{ks}{L_{WL}}\right)^{1/3} - 0.64\right) \quad (5\text{-}21)$$

In this study, $k = 0.57$, $ks = 120 \times 10^{-6}$, and $\rho = 1025.9$ kg/m^3, $S = 408$ m^2, $L_{WL} = 28.2$ m, and $\mu = 1.831 \times 10^{-5} Pa.s$ (corresponding with the Singapore Strait seawater properties). The appendage resistance is largely contributed by the twin azimuth thrusters which provide both the power for propulsion and manoeuvrability. This results in higher friction as the vessel speed increases. The roughness is contributed by rust, buckling, welding beads, paint roughness, and marine growth. The assumptions to calculate the frictional resistance include a clean hull with no marine growth present. Also, the model excludes any silicon-based paint coating system on the hull, which is designed to reduce friction. The above assumptions are valid as marine growth is managed and mitigated through the application of antifouling paint, which is typical for most if not all marine vessels as well as drydocking of HyForce at regular intervals as prescribed by classification society requirements. It should be noted that the surface roughness of the hull will be changed during the operation time of the tug. The new hull often

has roughness around 120-160 mm, while it will be up to 300-400 mm before maintenance is needed.

5.6.5 Total Resistance Validation

The total resistance (R_{Total}) acting on HyForce is a summation of several mentioned contributing factors. As a vessel moves through the water, two evident characteristics are apparent from observation. The wave pattern that moves with the hull and the turbulent flow along the length of the ship becomes a wake at the stern. These water flow traits, therefore, contribute resistance to the moving vessel. Predominantly, the total energy dissipated concerning losses from resistance can be classified into two main contributing factors, (i) pressure and (ii) friction. Pressure, which accounts for the normal forces acting on the hull can be attributed to hydrodynamic components and the energy in wave breaking, wave pattern, and transom drag. The latter includes the viscous hull resistance resulting from skin friction against the hull of the ship and the appendages (e.g., the rudder, and azimuth thrusters which protrude out of the hull) [147]. Particularly, the wind also greatly contributes to the total resistance acting on the top structure of the tugboat, while the water contributes to the total resistance by both pressure and friction acting on the hull of the tug. The wave resistance acts on the hull and strongly depends on the wave height. The friction resistance value is the function of the hull's surface roughness and the seawater viscosity. Adding to the resistance acting against the vessel is given in the following equation [148].

$$R_{Total} = R_{wind} + R_{water} + R_W + R_F \quad (5\text{-}22)$$

For the validation of the current methodology, the current calculated resistance is compared with the predicted total resistance based on the measurement data of the model for the same operational and environmental conditions with the velocity of the vessel from 7 knots to 12 knots. Particularly, a model of the vessel with the appendages is tested in the calm water tank to determine the resistance characteristics. The hull model was manufactured according to the

requirement given in the ITTC recommended procedure 7.5-01-01-01 for the ship models [149]. The propeller(s) model was manufactured according to the requirements given in the ITTC recommended procedure 7.5-01-02-02 for propeller model accuracy [149]. The methods used to carry out the tank tests and to extrapolate the results for the actual vessel follow the general methodology given in the relevant ITTC recommended procedures [149]. The tests are carried out in the deep-water towing tank size of 270.0m x 12.0m x 6.0m corresponding with the length, breadth, and depth, respectively. The tests are carried out in the seawater properties of 3.5% salinity and temperature of 15°C. The modelling and simulations are carried out for the same operational and environmental conditions. The wind and current direction are $\theta_{wind} = 0$ and $\theta_{current} = 0$. The obtained results are plotted together in Figure 5-10 for the comparison. The observation indicates that our model is in good agreement with the measurement-based extrapolation result. A maximum difference between the current modelling method and measurement-based extrapolation value is about 6.5% on average is observed. It implies that our model can be used to accurately predict the total resistance acting on the HyForce to estimate the optimum power required for vessel operation.

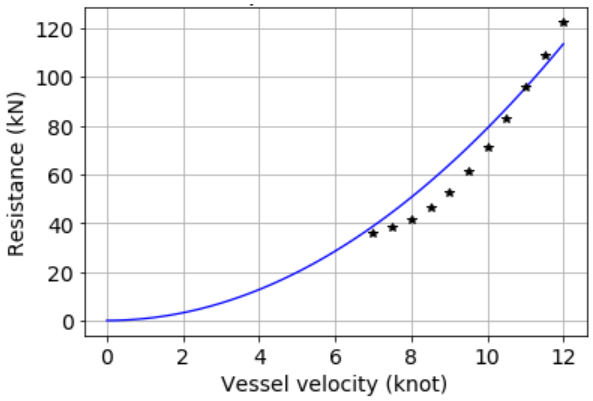

Figure 5-10: Validation of the current method (solid blue line) with measurement data (black stars) under the same operating and environmental conditions for different vessel speeds

For the total resistance, the approach to determining the various forces acting on HyForce is to first define the material parameters given in the above section. These input parameters provide the necessary estimation to investigate the total resistance acting on HyForce, which was validated in the previous section. It provides insightful information on the change in resistance and the various parameters contributing to it. This association allows for deeper analysis to inquire into the fundamentals governing the total resistance acting on a vessel. The calculated results show an increasing trend of resistance as the vessel increases in speed. Furthermore, the increment in resistance becomes more apparent as the vessel increases speed from 8 knots. This coincides with an increase in the Froude number which is a function of wave resistance. Wave resistance has a profound impact on the total resistance, and this can be attributed to the absence of a bulbous bow commonly present in larger marine vessels. The purpose of the bulbous bow, when designed optimally, reduces the total resistance and power requirement allowing for improved operational efficiency, reduced fuel consumption and better stability [150-152]. The frictional coefficient, which is a function of the Reynolds number decreases as the flow through the hull becomes more turbulent (i.e., higher Reynolds number and surface roughness of the hull). Within the turbulent region, the viscous hull resistance attributed to the boundary layer between the hull surface and moving water decreases, which results in a smaller frictional coefficient [153-155]. HyForce is a partially submerged vessel with a draft of 3.3 meters. At 5 knots, the Froude number exceeds the benchmark threshold of 0.25, which indicates a significant influence of wake-making and inertia of the fluid (i.e., seawater) on the total resistance [134, 156].

5.7 Total Propulsion

The propulsive forces that are required for HyForce to achieve the required operational requirement ($F_{Operational}$) are subject to several external factors that influence the overall power required to be delivered to the propeller. This interaction occurs between the hull and the propeller and includes components such as (i) wake fraction (ii) thrust deduction fraction (iii) relative rotative efficiency. Through the computation of these variables, the torque and thrust of each propeller, total delivered power, and the propeller efficiency can be determined. The wake fraction (ω) is a variable that predicts the efficiency and thrust of the propeller when operating in the ship's wake. The wake which has a complex flow form will inevitably result in a lower average speed of water flowing into the propeller compared to the speed of advance of the hull. The ratio of the advance coefficient of the propeller (J_p) and of the hull (J_h) will give the wake fraction as shown:

$$\omega = 1 - (J_p \,/\, J_h) \tag{5-23}$$

During the operation, the HyForce manoeuvres using her dedicated propulsion system, the spinning of the azimuth thrusters, located at the stern of the vessel, disrupts the pressure fields at the rear of the hull as the propellers accelerate the flow of water in this region. This causes an increase in shear force (i.e., frictional resistance) because of the increased movement of water molecules in the boundary layer between the hull and seawater. Therefore, the thrust generated will minimally need to exceed the bare hull resistance. The thrust deduction fraction (t) arguably can be described as a resistance augment instead of a propulsive force but not in practice. It can be calculated using equation 10.

$$t = 1 - (R_{Total} - F_D)/(N_p \times Th) \tag{5-24}$$

Most vessels are propelled using a single propeller designed sufficiently large to provide the necessary thrust (Th). HyForce, limited by her size, is propelled using twin screws to deliver the required power, which inadvertently has an impact on the pressure fields at the stern of the

vessel and hence necessitates the inclusion of the number of propellers (N_p) in the overall equation.

The propeller, which is connected via a shaft to the main engines or motors is supplied with the necessary torque to deliver the required thrust. To determine the intrinsic hydrodynamic performance of a propeller, model scale open water tests are performed. In these tests, the inflow of water to the model-scale propeller is uniform. The propeller efficiency (η_P) is determined by the advance coefficient of the propeller (J_p), torque coefficient (K_{Qo}), and thrust coefficient (K_T) given by:

$$\eta_P = J_p \times K_T/(2\pi \times K_{Qo}) \quad (5\text{-}25)$$

Where the torque coefficient is:

$$K_{Qo} = \frac{Q}{\rho n^2 D^5}, \quad (5\text{-}26)$$

and thrust coefficient is:

$$K_T = \frac{T}{\rho n^2 D^4} \quad (5\text{-}27)$$

However, in actual operation, the turbulent inflow of water (i.e., wake) to the propeller depends on the ship's design (i.e., hull form) to which it is fitted. Inevitably, the torque absorbed by the propeller in an open water test (K_{Qo}) differ from a similar operating condition under turbulent flow (K_{Qs}), which provides the relative rotative efficiency (η_R) and it is given by:

$$\eta_R = K_{Qo}/K_{QS} \quad (5\text{-}28)$$

Having derived the (i) wake fraction (ii) thrust deduction fraction (iii) relative rotative efficiency above, the torque, thrust and total delivered powered by the propellers can be determined.

The amount of thrust in kilonewtons (kN) that can be generated from HyForce because the propeller rates revolution (RPM) (n), and diameter (D) is given by:

$$T = J_p^2 \times \rho \times D^4 \times n \quad (5\text{-}29)$$

The thrust produced by the propeller is accredited to the torque supplied by the shaft to which it is connected. This shaft as highlighted earlier, is driven by power-producing equipment on board and in the case of HyForce, comes from large electrical motors energized by fuel cells. The torque produced by the shaft (Q) is given by:

$$Q = (\frac{K_{QS}}{\eta_R}) \times \rho \times D^5 \times n^2 \quad (5\text{-}30)$$

Finally, the total delivered power by the propellers (P_D) in kilowatts (kW) can be determined by:

$$P_D = N_p \times 2\pi \times n \times Q \quad (5\text{-}31)$$

The propulsion and power calculations require intrinsic properties of HyForce, which include the characteristics and performance of the propeller as well as the total resistance acting on the vessel. The characteristics of the propeller include the number of blades, diameter, and pitch ratio, while the performance of the propeller is given by its wake fraction, advance coefficient, and propeller efficiency respectively. This information is given in Table 5-3 and Table 5-4 respectively. The information is provided by the propeller's vendor, which is measured in the calm water tank tests for different vessel speeds (5.0-12.0 knots) and water properties ($\rho_{sw} = 1.025$ kg/m^3 and $\mu_{sw} = 1.0 \times 10^{-6}$ m^2/s).

Table 5-3: The design information of the propeller(s) used for HyForce

Parameter	Symbol	Value	Unit
Number of propellers	N_p	2	-
Number of blades	N_b	4	-
Propeller diameter	D	2.5	m
Propeller pitch ratio	R_{p_p}	0.95	-

Table 5-4: HyForce's propeller design performance

V [knots]	Wake fraction [ω]	Propeller Adv ratio [J_p]	Propeller Efficiency [η_P]
5.0	0.021	0.703	0.262
6.0	0.020	0.701	0.266
7.0	0.022	0.7	0.269
8.0	0.021	0.697	0.281
9.0	0.022	0.686	0.310
10.0	0.024	0.671	0.348
11.0	0.026	0.652	0.384
12.0	0.025	0.641	0.402

The dimensionless propeller's advance ratio is the distance moved by the vessel normalised by the propeller's diameter in one revolution. From Table 5-4, it is observed that the propeller's advance ratio decreases as the vessel's speed increases. This reduction can be rationalised by external factors restricting the forward movement of the vessel and it is corroborated by an increase in the vessel's total resistance with increasing speed.

The wake fraction remains relatively constant throughout the different speeds which indicates that the delta between the water velocity seen by the propeller, and the hull speed does not change significantly. The low wake fraction of 0.02 highlights the uniformity of water velocity across the vessel and this can be attributed to the low block coefficient of 0.576. The ample space within the rectangular block allows for the displaced volume of water to regain an even distribution eliminating any cross flows.

The propeller's efficiency is influenced by the thrust and torque coefficients and the propeller's advance ratio. It can be misconstrued that an overwhelmingly large contributor affecting the efficiency of the propeller will be the advance ratio (i.e., distance moved by the vessel per RPM). From Table 5-4, it is shown that there is an opposite trend between the propeller's advance ratio and efficiency as the vessel's speed increases. The improvement of the propeller's

efficiency as the vessel increases its speed is a result of bigger thrust and torque coefficients and this is validated in Table 5-5. The change in the thrust and torque coefficients indicates a large change in delivered thrust and torque, respectively, with a relatively smaller change in the propeller's RPM as observed from equations 13 and 14.

Table 5-5: Prediction of the total required power, thrust, and torque for the vessel operating at different speeds

V [knots]	P_D [kW]	n [rpm]	T [kN]	Q [kNm]
5.0	93	86.1	4.8	5.2
6.0	163	103.5	7.0	7.5
7.0	259	120.7	9.7	10.3
8.0	399	138.8	13.7	13.7
9.0	605	158.4	20.5	18.2
10.0	914	179.8	31.5	24.3
11.0	1353	202.9	47.5	31.9
12.0	1892	225.3	63.7	40.1

The total power delivered at various speeds, as detailed in Table 5-5 and visually depicted in Figure 5-11, reveals a noteworthy trend. The curve's gradient experiences a pronounced increase at speeds surpassing 10.0 knots, primarily attributable to the heightened power delivery by the propeller. This observation finds reinforcement in the concurrent rise of the thrust coefficient within a similar operational range. The evaluated results of power, thrust, and torque are suitable and fit well with the design purpose of the current propulsion system. Especially, the calculated 1892.0 kW delivered power robustly indicates HyForce's capability to meet the designated power requirement of 2.0 MW. To ensure the attainment of the desired propeller RPM across different speeds, a detailed analysis of a suitable gear reduction ratio becomes imperative. Typically, motor generators operate at RPMs exceeding 1000, and based on the insights gleaned from Table 5-5, a recommended gear reduction ratio of 6.3 emerges.

This strategic choice ensures a motor generator rating that sufficiently delivers the required power even under the most demanding load conditions.

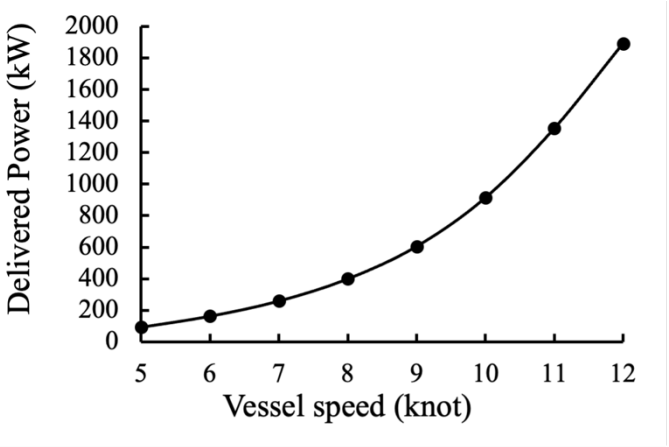

Figure 5-11: HyForce power prediction for different vessel speeds within the Singapore Strait

Chapter 6

Modelling and Simulation of HyForce's Power-Sharing Strategies

This chapter introduces HyForce's powertrain, which comprises fuel cells and batteries in a hybrid configuration. It discusses the theoretical framework for power-sharing strategies and identifies the desired cost functions. The objective is to ensure that the cost functions are representative of the desired outcome envisaged for HyForce. All major components are modelled for simulation and subsequent performance evaluation. The results are presented and discussed.

6.1 Powertrain Configuration

Tugboats, unlike several other marine applications such as ferries or ocean-going vessels, are designed to provide reliable and stable power throughout a dynamic range of operational scenarios. Their primary objective often entails the safe transit (i.e., towing) of larger marine vessels in a near-to-shore setting. The marine vessels under towage typically berth alongside a shore infrastructure for embarkation/disembarkation (passenger ferries) or the loading and unloading of cargo (containerships/bulk carriers). This specific operation requires the tugboat to perform a series of pushing or pulling operations (i.e., bollard pull) under the direction of the harbour pilot for the safe mooring of the vessel. Understandably, due to the proximity to shore, the associated risks to human life and property damage are higher in such a scenario as compared to the voyages in the open ocean. Hence, tugboats must be able to spontaneously meet the dynamic power demand. To ensure its reliability, extensive work on the simulation and validation of test scale models is required to ensure the manoeuvrability meets design and classification society standards [156, 157].

Traditionally, tugboats meet this power demand through diesel-driven ICE which relies on the torque of shaft power from the rotating engines to turn the propellors [158]. The powertrain on HyForce challenges this status quo and is designed to meet the power requirements through a combined power-sharing strategy of fuel cells and batteries [46]. The proposed powertrain configuration is shown in Figure 6-1 where ESS is the energy storage system of the batteries.

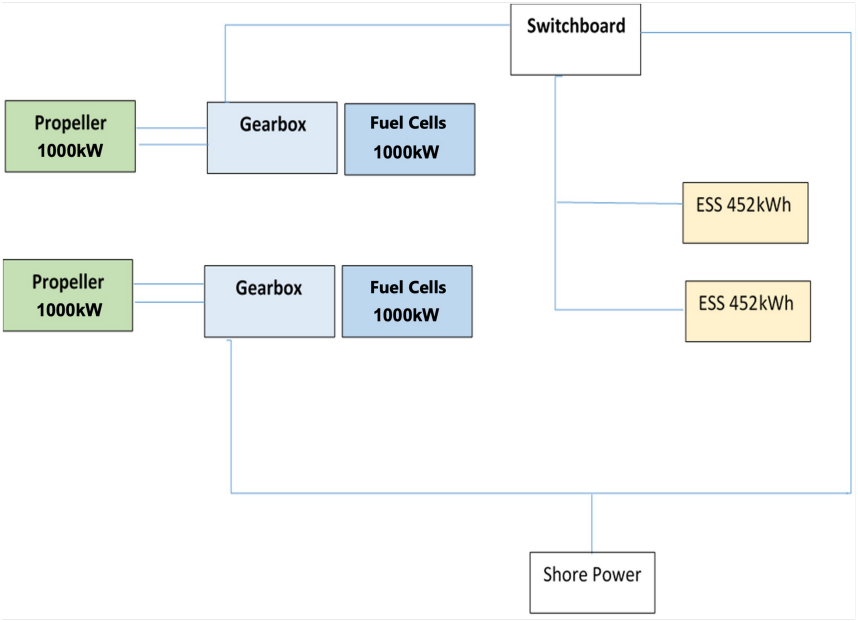

Figure 6-1: HyForce powertrain block diagram

The methodology used to design the power-sharing models is derived from the tugboat's load requirements in different operating scenarios. A reasonable assumption of the operational data to be used as inputs for the power-sharing model is the estimated and anticipated time spent at each load profile to best depict the tug's overall power requirement during a typical operational cycle (i.e., 1 day).

Both powertrains are capable of operating in 3 different distinct power modes. The first mode is either fuel cells or an internal combustion engine; the second mode is via battery power and the last mode is a combination of the first two (i.e., hybrid). At an individual equipment level, there are limited opportunities for optimisation as they are designed and operated at the

manufacturer's recommended setting. The first two, power from fuel cells/ICE and battery are individually limited in optimisation as these standalone pieces of equipment are sized and designed under the purview of the manufacturer. However, when integrated, opportunities arise to develop a robust power-sharing philosophy that fulfils the end objective of the desired cost function. Cost functions are variables, and examples include (i) reduced fuel consumption (ii) improved battery life by reducing charge cycles (iii) minimised excess power generation (iv) optimal reserve power allowable in the battery pack. Ideally, each optimised power-sharing strategy identifies a cost function's desired end outcome, and downstream measures are implemented correspondingly. Specific to this study, the cost function identified was to reduce fuel/energy consumption and consequently prolong the time intervals between each bunkering/charging operation to maximise the operational time of the tugboat.

6.2 Theoretical Model Development

To curate an accurate and viable representation of the power-sharing strategy, the topological hierarchy of the power schematic needs to be developed. The primary objective is to ensure that the nodes and their corresponding connections within the overall framework are aligned to (i) the design capabilities of the individual components (i.e., Fuel cells/Hotel load/Battery consumption) (ii) the cause and effect of the various nodes (i.e., Yes/No) (iii) the ability to produce the desired results at the end state (Hydrogen fuel consumption/battery's state of charge). Figure 6-2 illustrates the theoretical framework developed to govern the power-sharing strategy.

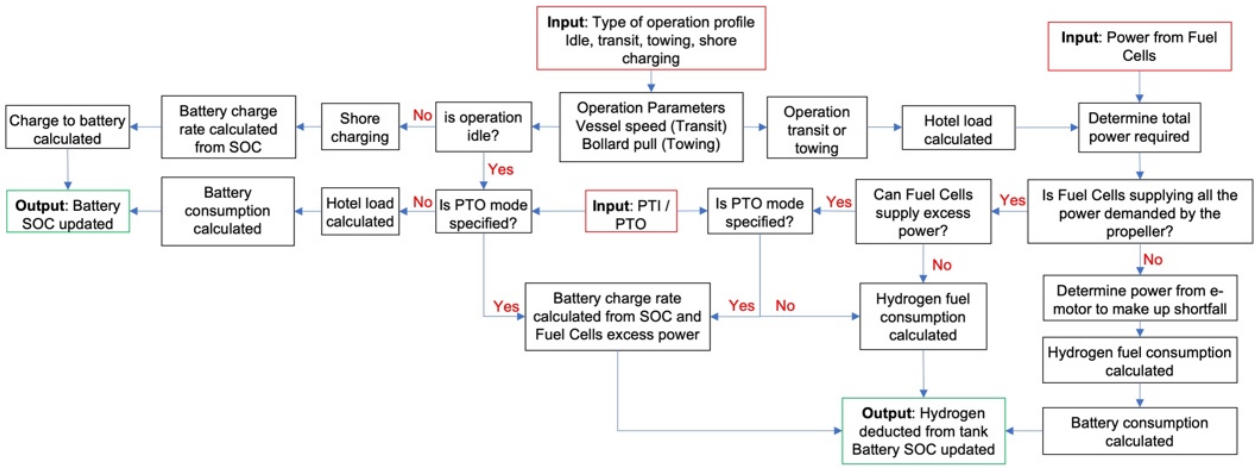

Figure 6-2. Theoretical model framework of the power-sharing strategy

The robustness of the theoretical model framework is verified against a series of potential operating profiles given in Table 6-1 to ensure completeness. Through these series of tests, the specific operating conditions in which the (i) battery would be providing 100% of the power (ii) fuel cells would be providing excess power in a Power Take Off (PTO) mode to charge the battery (iii) the battery would top-up the remaining power in a Power Take In (PTI) mode were identified. The theoretical model thus provides an overview of the pockets of opportunity and the basis for power optimisation to be explored. A summary of the power sources at various operating profiles is illustrated in Table 6-1.

Table 6-1. Power source inputs are different operating profiles

Operating Profile	**Fuel Cells**	**Electric Motor**	**Battery**
Idle	Off	Off	On (PTI)
Transit 6 knots	Off	On	On (PTI)
Transit 8 knots	Off	On	On (PTI)
Transit 10 knots	On	On	On (PTI/PTO)
Transit 12 knots	On	On	On (PTI/PTO)
Bollard Pull (25% to 75%)	On	On	On (PTI/PTO)
Bollard Pull (100%)	On	On	On (PTI)

6.2.1 Theoretical Model Simulation

The interfaces between the individual components in the powertrain can be mapped out using the theoretical model, allowing the overall operability of the envisaged powertrain to be simulated. The simulation provides clarity on the constraints and limitations surrounding the baseline operating scenario, which can be analysed graphically. It also provides the benchmark against which future optimisation strategies can be compared.

6.2.1.1 Electric Motor

To build the powertrain accurately in a virtual environment, statistical data on the individual components are gathered through the manufacturer's datasheets and literature sources that provide empirical data [159]. This data is selected as it is representative of the actual components and equipment used in JMS Sunshine, a Singapore registered tugboat operating with a hybrid control system with electrical motors. Using the propellor design shared in chapter 5, the propellor power requirements and RPMs are shown in Figure 6-3.

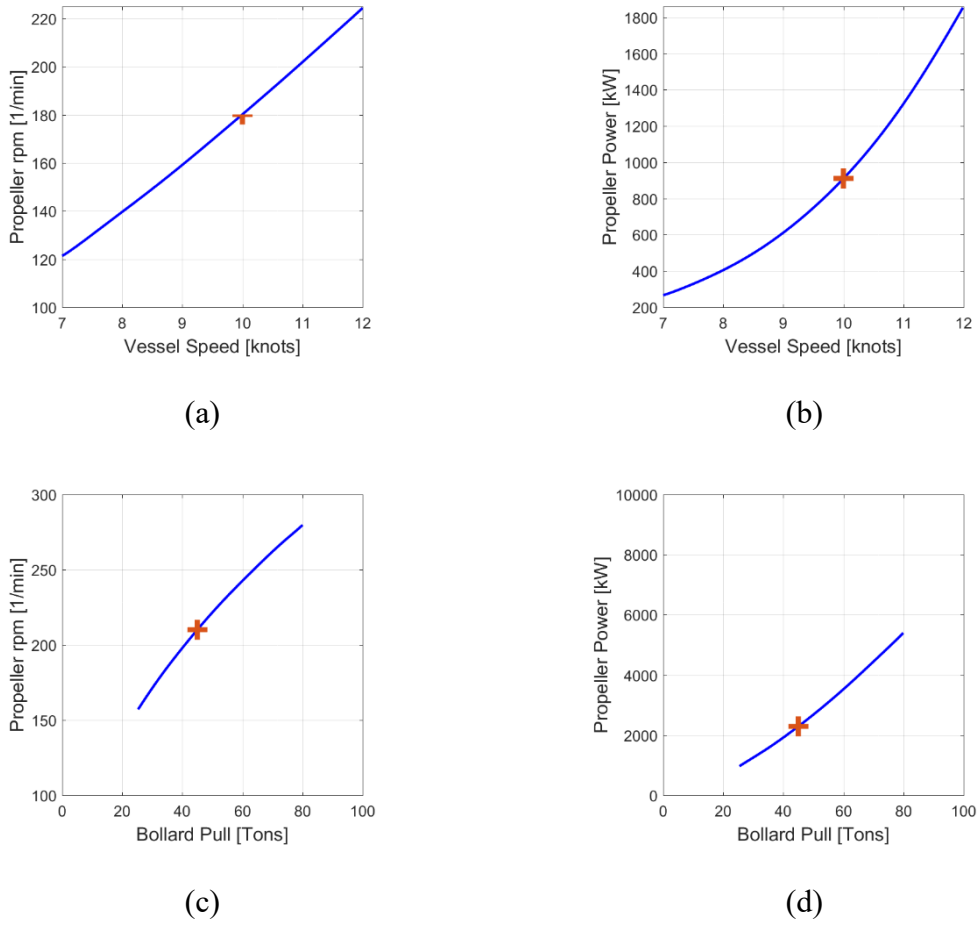

Figure 6-3: Propellor power requirements for HyForce

To ensure adequate power delivery to perform the required maximum bollard pull of 45 tonnes, the following key parameters needs to be achieved as shown in Table 6-2.

Table 6-2: HyForce at maximum bollard pull

Parameter	**Value**	**Unit**
Propeller RPM	210.097	1/min
Propellor Power	2291.192	kW
Propellor Power (each powertrain)	1145.596	kW
Hotel load (power)	110.710	kW
Hotel load (energy)	0.115	kWh

From Table 6-2 above, the electric motor will need to deliver a power output of 1200 kW. This requirement can be met by choosing the Marelli Motori B4J400LC6 [160] with the following parameters given in Table 6-3.

Table 6-3: Electric motor parameters

Values per phase (locked rotor, 20℃)	
Stator Resistance	0.0030Ω
Stator Reactance	0.0468Ω
Rotor Resistance	0.0100Ω
Rotor Reactance	0.0313Ω
Values per phase (running, 70℃)	
Stator Resistance	0.0036Ω
Stator Reactance	0.0511Ω
Rotor Resistance	0.0024Ω
Rotor Reactance	0.0612Ω
Magnetisation Reactance	1.4806Ω
Iron Loss Resistance	$0.0328k\Omega$

At the maximum bollard pull, the operating point, RPM and torque of the electric motor can be determined using the following equations, whereby 5.011 is the gear reduction ratio between the motor and the propellor:

$$RPM = 210.097min^{-1} \times 5.011 = 1052.8min^{-1} \quad (6\text{-}1)$$

$$Torque = \frac{1145.596kW}{\frac{1052.8}{60s}\times 2\pi} = 10391.23Nm \quad (6\text{-}2)$$

The torque-RPM curve is illustrated by the blue line while the propellor requirement as seen by the electric motor is illustrated by the red line in Figure 6-4. The intersection between the lines corresponds to the operating point at maximum bollard pull.

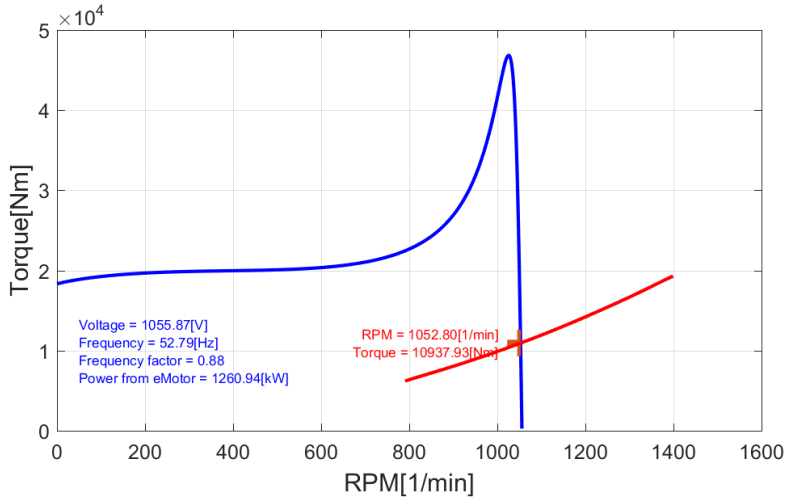

Figure 6-4: Torque vs. RPM curve for HyForce electric motor

6.2.1.2 Fuel Cell Module

The building blocks of a fuel cell module start with a single cell. The characteristic of this cell is given below:

$$T = 70°C$$
$$P = 101325Pa$$
$$P_{O_2} = 0.21 \times 101325Pa$$
$$\alpha_{cathode} = 1.0$$
$$i_{crossover} = 0.002A$$
$$i_{limit,cathode} = 1.6A$$
$$i_{exchange,cathode} = 3.0 \times 10^{-6}A$$
$$R_{i,ionic} = 0A$$
$$R_{i,electronic} = 0.15A$$
$$R_{i,contact} = 0A$$

Assuming flow-through mode with recirculation, the voltage of a single cell is given by:

$$E_{cell} = E_{r,cathode} - \frac{RT}{\alpha_{cathode}F} ln\left(\frac{i_{external}+i_{crossover}}{i_{exchange,cathode}}\right) - \frac{RT}{\alpha_{anode}F} ln\left(\frac{i_{external}+i_{crossover}}{i_{exchange,anode}}\right) - \frac{RT}{nF} ln\left(\frac{i_{Limit,cathode}}{i_{limit,cathode}-i_{external}-i_{crossover}}\right) - \frac{RT}{nF} ln\left(\frac{i_{Limit,anode}}{i_{limit,anode}-i_{external}-i_{crossover}}\right) - (i_{external} + i_{crossover})R_{i,ionic} - i_{external}\left(R_{i,electronic} + R_{i,contact}\right) \quad (6\text{-}3)$$

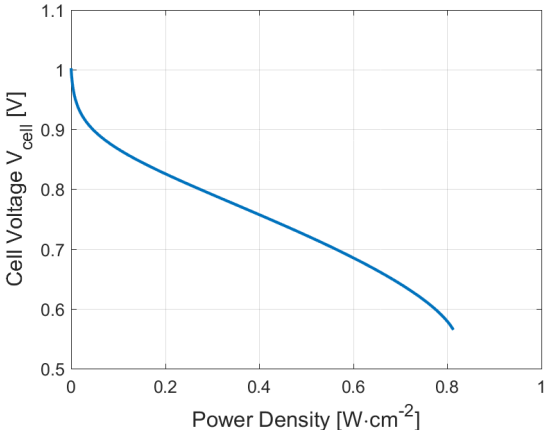
Cell Voltage V_{cell} [V]
Power Density [W·cm^{-2}]

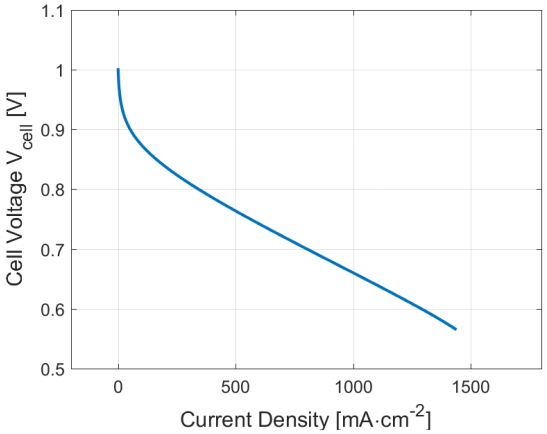
Cell Voltage V_{cell} [V]
Current Density [mA·cm^{-2}]

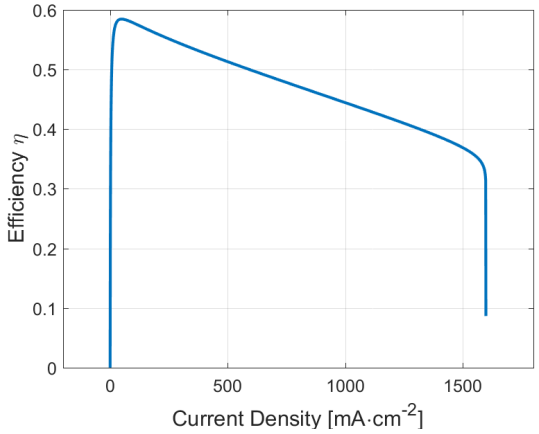
Efficiency η
Current Density [mA·cm^{-2}]

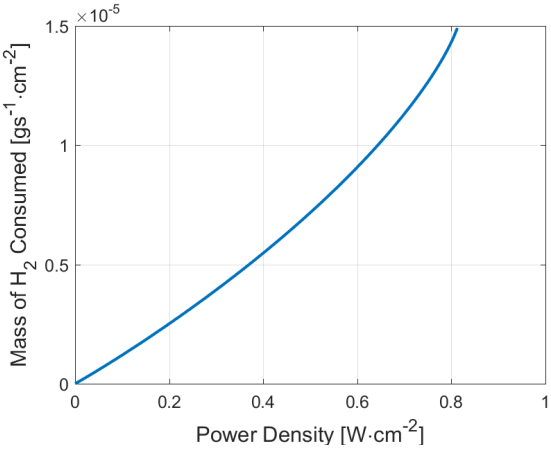
$\times 10^{-5}$
Mass of H_2 Consumed [gs^{-1}·cm^{-2}]
Power Density [W·cm^{-2}]

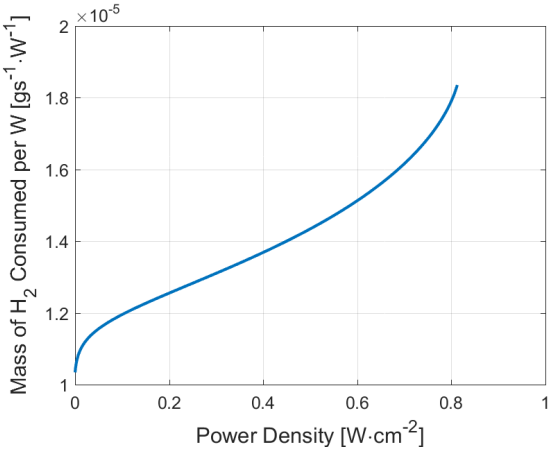
$\times 10^{-5}$
Mass of H_2 Consumed per W [gs^{-1}·W^{-1}]
Power Density [W·cm^{-2}]

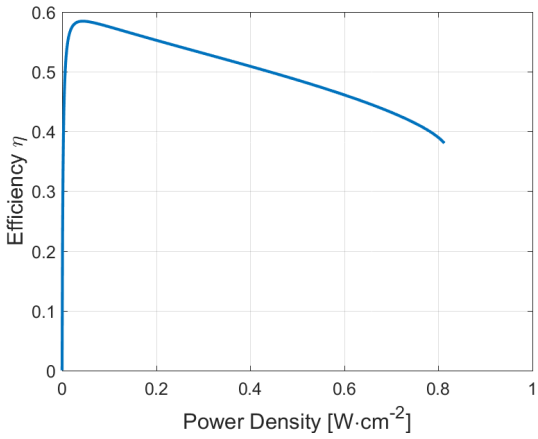
Efficiency η
Power Density [W·cm^{-2}]

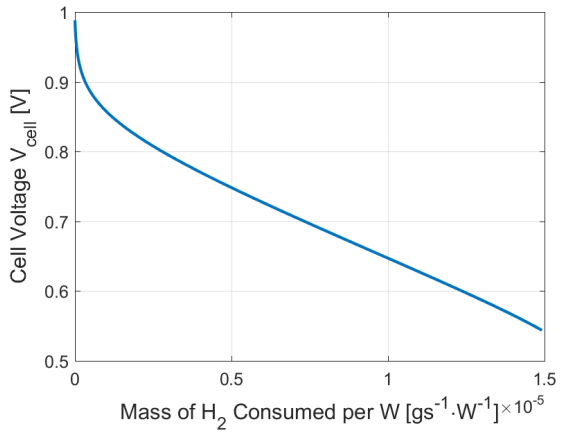

Figure 6-5: Fuel cell characteristics

Combining the characteristics of a single cell:

$$nStack = 2500$$
$$A_{electrode} = 500cm^2$$

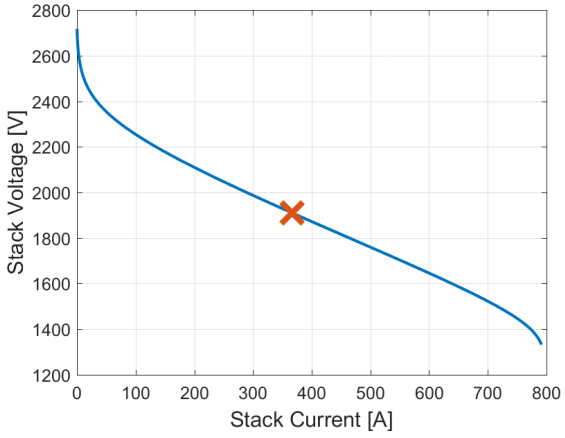

Figure 6-6: Fuel cell stack operating point

From Figure 6-6, the red cross corresponds to the rated operating point of the fuel cell stack. This gives the (i) stack current at 366.5 A, (ii) stack voltage at 1910.0 V, and (iii) stack power at 700 kW. Using a specific design operating profile as shown in Table 6-4, the total energy required to perform a job is 2033.97 kWh. Simulating this operation profile with a similar sized battery, the discharge profile is shown in Figure 6-7 (a). By revising the strategy into one where the propellor power required is provided by the fuel cell stack as practicable, and any shortfall in power is provided by the battery, the battery drawdown is illustrated in Figure 6-7 (b).

Table 6-4: HyForce operating scenario

Sequence	Operation	Task
1	Idle	8 minutes
2	Transit	5.556 km at 7 knots
3	Transit	3.074 km at 10 knots
4	Transit	8.889 km at 12 knots
5	Idle	8 minutes
6	Towing	45 tonnes b.p for 12 minutes
7	Towing	38.75 tonnes b.p for 12 minutes
8	Towing	32.5 tonnes b.p for 24 minutes
9	Idle	8 minutes
10	Transit	8.889 km at 12 knots
11	Transit	3.074 km at 10 knots
12	Transit	5.556 km at 7 knots
13	Shore Charging	60 minutes

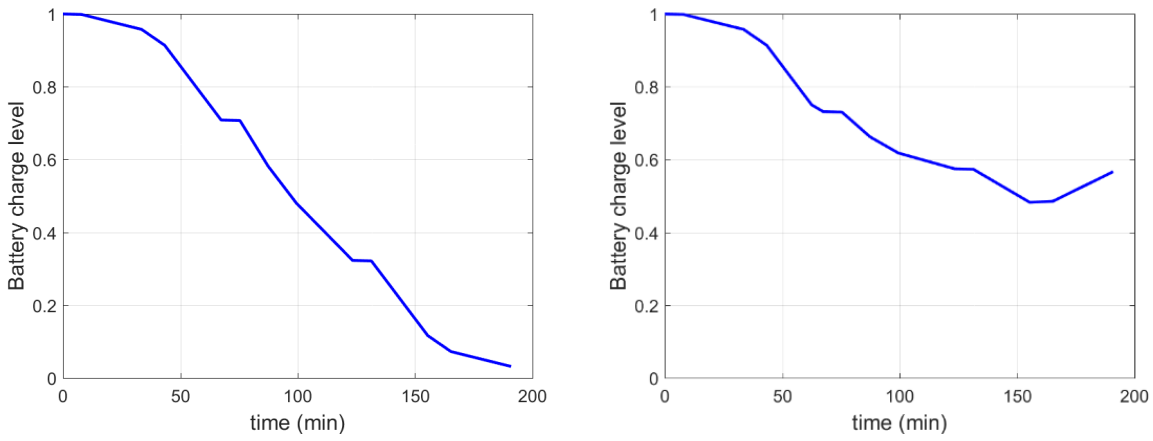

(a) (b)

Figure 6-7: (a) Battery discharge with no fuel cell support (b) Battery discharge with fuel cell support

The gentle gradient of change in the battery's State of Charge (SOC), as seen in Figure 6-7 (b), is attributed to the contribution of load sharing by the fuel cell to meet the power demands of HyForce as the operating profile changes. As the power demand exceeds the power available of the fuel cells, the battery will kick in to provide the difference in power. Furthermore, to quantify how the fuel cell operates at different loading points, the (i) fuel consumption rate, (ii) stack power (iii) stack current and (iv) stack voltage are shown in Figure 6-8.

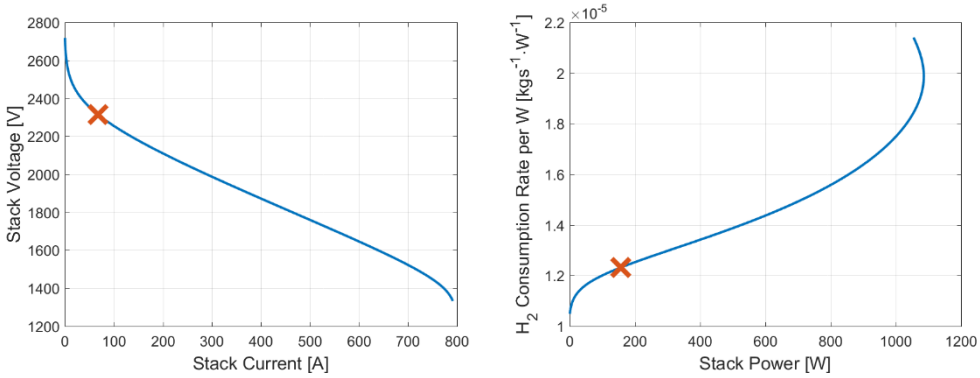

(a) 7 knots transit

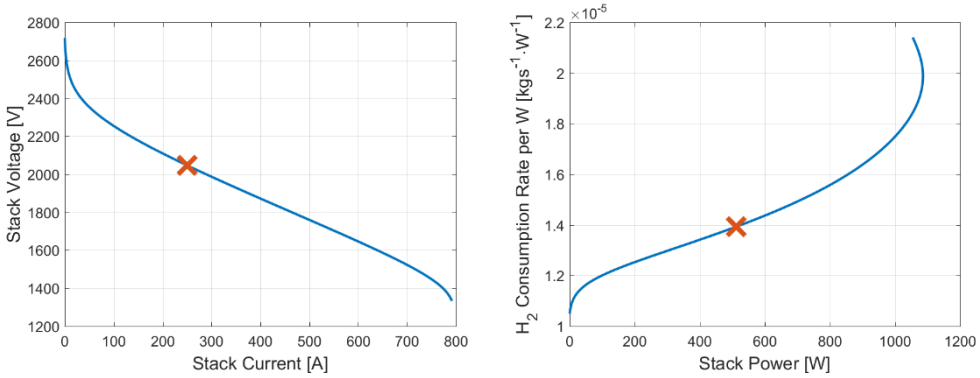

(b) 10 knots transit

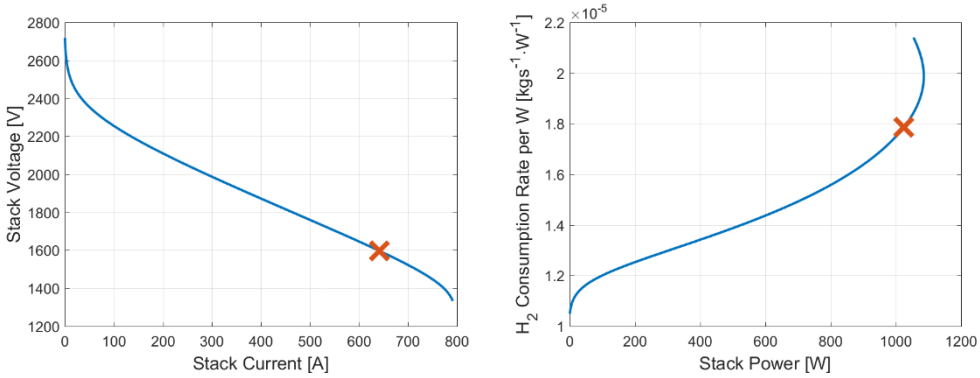

(c) 12 knots transit

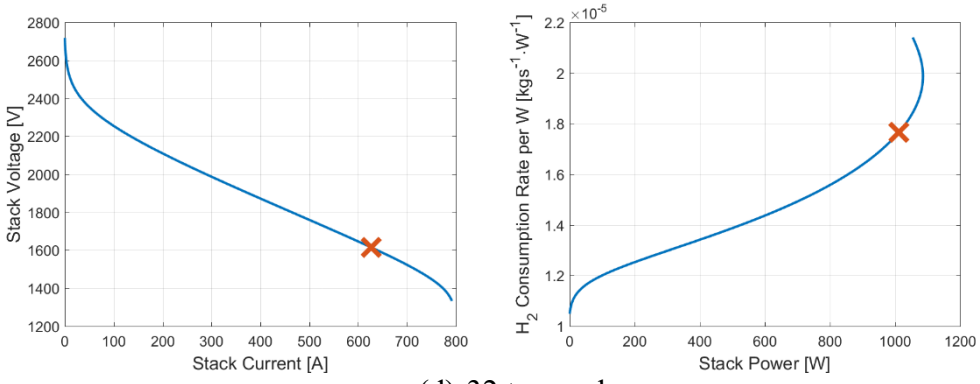

(d) 32 tonnes b.p

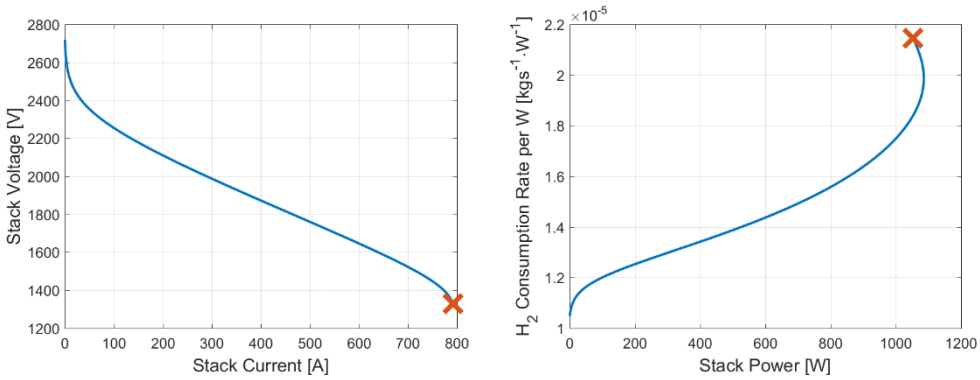

(e) 45 tonnes b.p

Figure 6-8: Fuel cell stack operating points at different scenarios

Similarly, the accuracy of the digitised data of the batteries were verified through a vigorous series of tests.

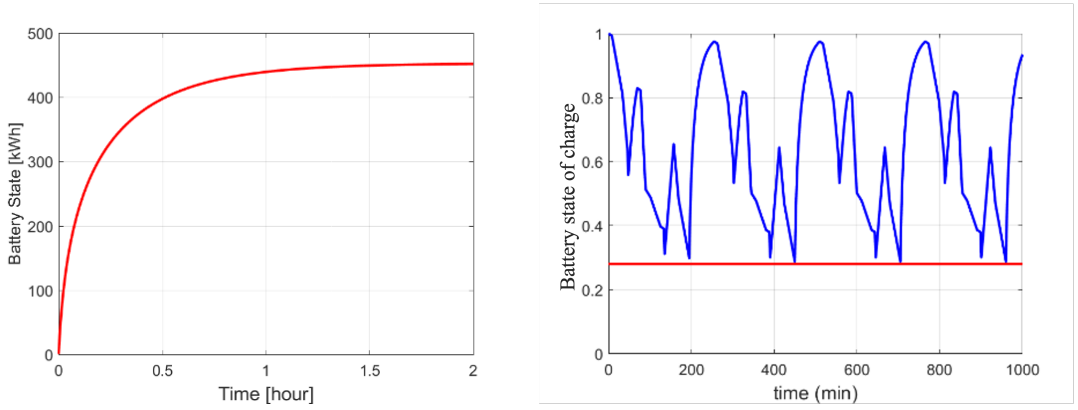

(a) (b)

Figure 6-9: (a) Battery state over time to max capacity of 452 kWh (b) Battery state of charge during baseline operating scenario

The ESS is designed to attain a full charge after two hours to allow a quick turnaround in its usage. The ability of the battery to meet this key performance criterion is imperative as the continuous usage of the battery will provide opportunities to maximize the earlier mentioned cost functions specifically to reduce hydrogen fuel consumption. It is observed that the ESS exhibits an asymptotic-like charging rate as it approaches full charge. This is to be expected as the charging rate approaches zero gradually from a peak of 700 kW.

As the tug completes one job and proceeds to the next, she will perform a total of four jobs in a 12-hour shift. The cyclic nature of this transition is well observed in

(a)

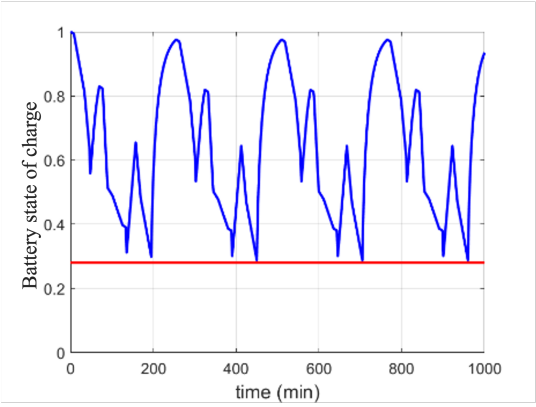

(b)

Figure 6-9. The baseline operating scenario incorporates a hard limit on the lowest state of charge for the battery at 30%. This is to ensure sufficient reserve power in the event of an emergency and/or loss of power from the hydrogen fuel cell/ICE.

6.3 Power Sharing Optimisation

Figure 6-10 illustrates the power-sharing model when the tugboat is travelling at 10 knots and 12 knots transit. The symbol, α, is the ratio of power $\frac{P_{Engine}}{P_{Total}}$ whereas the symbol, β is the ratio of time $\frac{T_{e-motor}}{T_{Total}}$. The power is shared using the hydrogen engine/fuel cell and (1-α) of the remaining power comes from the batteries whereas at 12 knots transit, time spent on the engine/fuel cell to deliver the required power is (1-β) in a power take-off mode and the remaining power is supplied by the batteries (β).

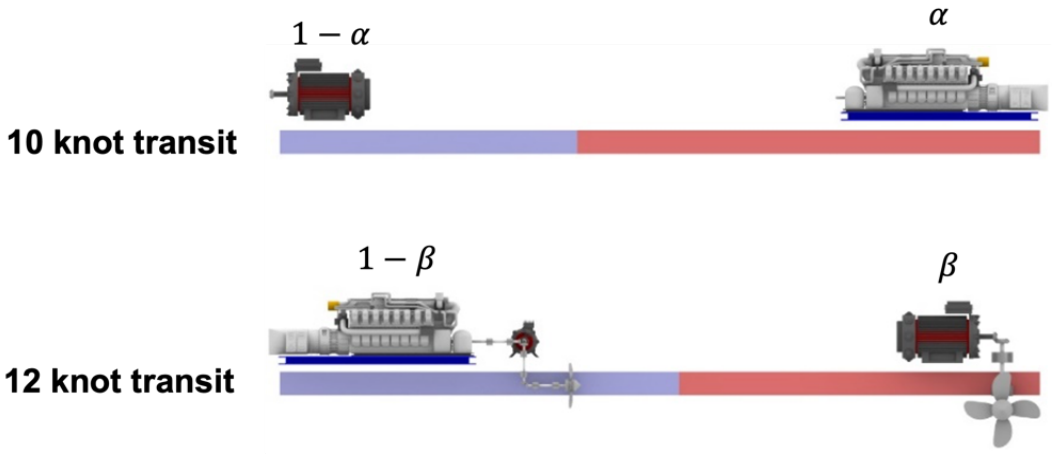

Figure 6-10: Power sharing between e-motor (batteries) and H_2 Fuel Cell/ICE

As the tugboat's daily operational requirement differs due to its deployment's dynamic nature, a parameter sweep is performed by running several iterations of this model. Besides the two operating profiles shown above in Figure 6-10, changes include varying the power source inputs in which the battery can operate in PTI or PTO modes as indicated in Table 6-1. This provides an in-depth analysis of the capabilities of the battery design capacity and its corresponding effect on the cost function, which remains unchanged. The desired measure is the number of towing jobs completed per full tank of LH_2. This measured variable would denote the operational performance of the tugboat with a higher value indicating more on-hire availability. The result of the parameter sweep is seen in Figure 6-11.

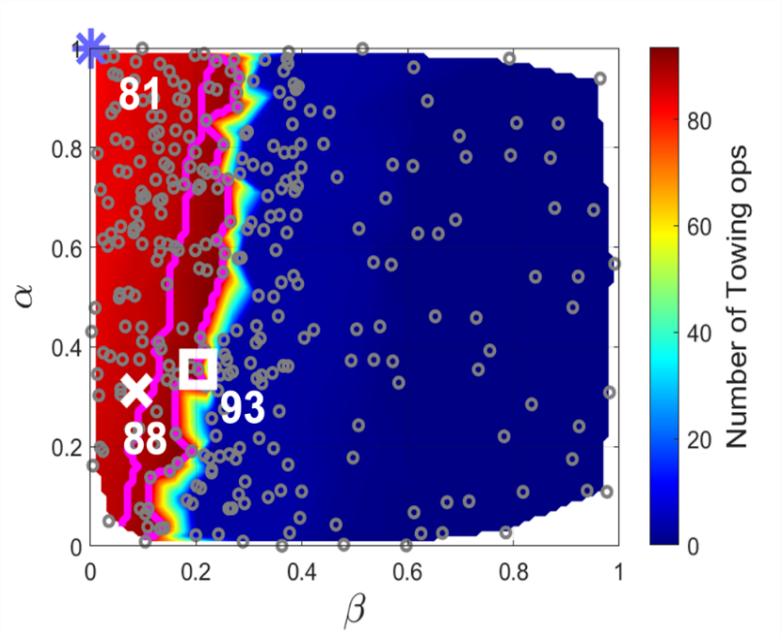

Figure 6-11: Power sharing optimisation results

To orientate Figure 6-11, the y-axis is α which is the ratio of power produced by the H2 ICE/fuel cell, and the x-axis is β which is the ratio of time in which the e-motor (batteries) delivers the power. The total for both will equate to 1, whereby the remaining power is either produced by e-motor (1-α) or H_2 ICE/fuel cell (1-β). The baseline scenario allows the tug to perform 81 towing operations. In this scenario, the H_2 ICE/fuel cell delivers 100% of the required power at 8 knots and 12 knots (i.e., the batteries were never used). Under this scenario, the hybrid mode is not activated, and the effect is the quick depletion of LH_2.

Under various hybrid conditions, results indicate an optimised number of towing jobs at 93. This represents a 15% increase, potentially enhancing the commercial viability of using hydrogen as a fuel source to fulfil IMO's decarbonisation agenda. However, this increase in the number of towing jobs completed was achieved by periodically infringing the batteries' 30% state of charge limit. This situation was observed during the 100% bollard pull operation, where the batteries operate in PTI mode (i.e., discharging). The state of charge recovers above this limit relatively quickly before initiating the next job. The implications of this infringement are

minimal unless an unlikely scenario arises where the tug loses power when the state of charge is below 30%. The severity of this situation depends on the tug's location when it occurs. Should the tug be relatively near shore, the remaining power available from the batteries would be sufficient to return the tug to shore for diagnostics safely. Lastly, should the SOC for the batteries' remain above the hard limit of 30%, a compromise on the total number of jobs completed will be required. The total number of jobs that will be able to be performed will be 88.

Furthermore, a power distribution strategy can be implemented as following:

- Primary source of power from H_2 cell, i.e. H_2 cell powers all operations, battery supplements power output if power from H_2 cell is insufficient
- Battery should retain battery state of charge between 0.4-0.8
- Charging is turned on when battery state of charge is less than 0.5
- Charging is turned off when battery state of charge is above 0.8
- Tug performs job starting with battery state of charge at 0.8

Simulations are then carried out using the above job profile. By simulating various combinations of stack sizes against battery capacity, the following contour plot is obtained as seen in Figure 6-12. It can be seen from the plot that the battery capacity and fuel cell stack size, as indicated by the maximum power afforded by the fuel cells are interchangeable.

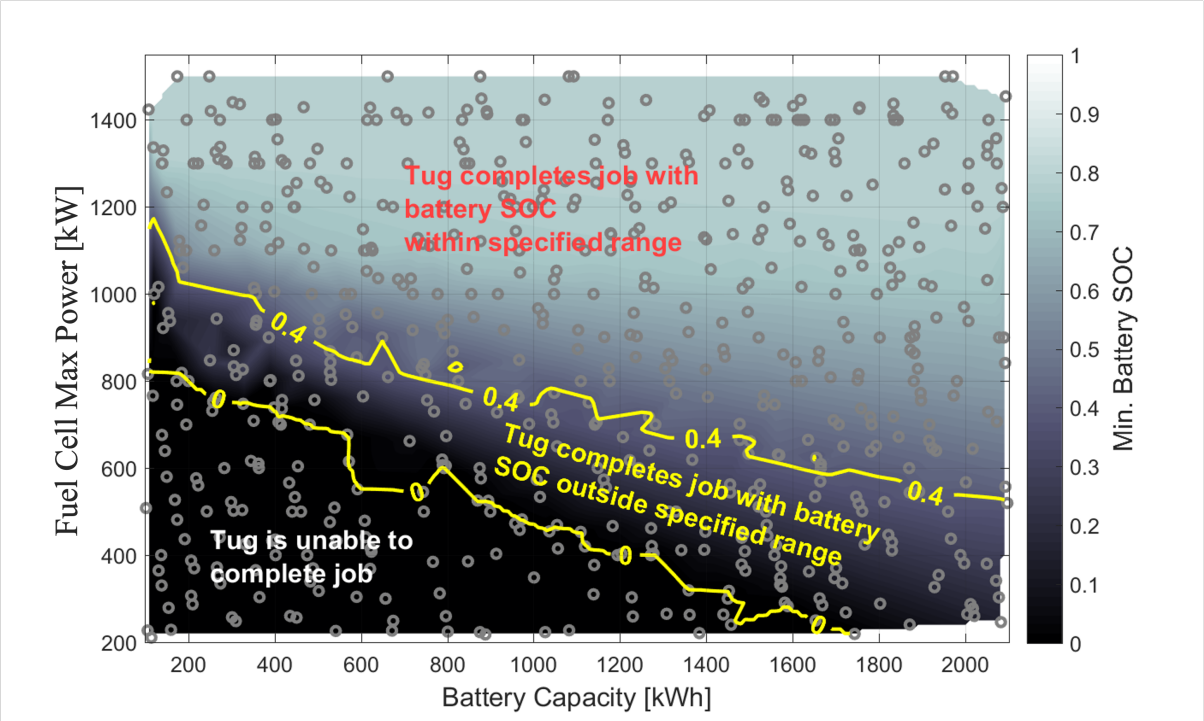

Figure 6-12: Fuel cell and battery sizing options for HyForce

From Figure 6-12 above, the spread of possible fuel cell stack size and battery capacity options which would enable the completion of towing jobs under the specified conditions. A significant number of jobs can be completed with the design power of the fuel cell and battery capacity, reiterating the viability of this powertrain. Furthermore, the battery's SOC hard limit of 30%, which ensures sufficient reserve power to bring the tug back to shore safely, does not have a controlling effect on the equipment sizing, as seen by the spread in-between the yellow lines in the figure above.

Optimised power-sharing provides the unique opportunity to enhance the value proposition of alternative fuels further. Due to liquefaction, hydrogen is inherently disadvantaged with a low energy density and high energy penalty. With the optimised use of hydrogen, increasing the number of towing jobs between each bunkering interval by 12, tugboat owners will be further incentivised to consider switching to alternative fuels to ensure compliance with any regulatory requirements. To this effect, an integrated framework can be incorporated that encapsulates the

environmental elements, optimised power-sharing, and a controller to ensure the desired goal is achieved. This is illustrated in Figure 6-13 below:

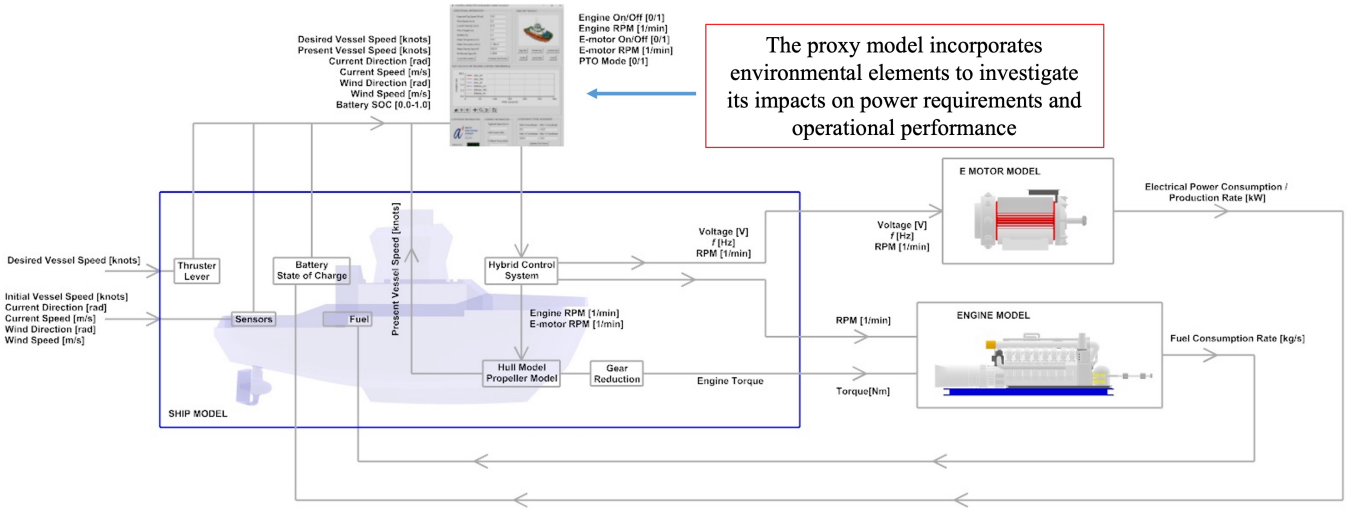

Figure 6-13: Integrated framework with proxy model

Chapter 7

Model Predictive Control Framework

This chapter first presents a sweeping review of the literature on the developments of optimization-based power management strategies from a multi-industry perspective. This review aims to leverage the merits, address the challenges, and evaluate the applicability to the marine environment. The novel model predictive control is selected and applied to HyForce. for applicability

7.1 Concept Development

Electrification of marine powertrains has taken centre stage in the marine industry's transformation to a less carbon-intensive era in recent years. Although efficient, the traditional 2-stroke heavy fuel oil Internal Combustion Engines (ICE) will not meet IMO's net-zero Greenhouse Gas (GHG) emission target by 2050. Consequently, this ambitious target has motivated incremental developments in technology to aid the shift to the use of green electrons or molecules as fuel. The introduction of these new technologies has been studied robustly and demonstrated in pilot and full-scale projects globally [161, 162]. These studies and demonstration projects underscore the various pathways to marine decarbonisation. They include using green molecules such as hydrogen and ammonia and green electrons such as electricity harnessed through renewable energy.

Unlike their ICE predecessors, electrified vessels typically incorporate more than one (1) power source, typically including power conversion equipment such as a fuel cell and an energy storage system. Depending on the vessel's size, range, and profile, the ESS would comprise either supercapacitors or batteries to meet the intended operational demand [46]. Hybrid vessels are

also gaining popularity as an interim solution to minimise emissions during operations by leveraging on the existing proven technology and efficient 2-stroke engines with Proton Exchange Membrane (PEM) fuel cells [163]. Typically, these hybrid vessels utilise a low-carbon fuel such as LNG or methanol, which is subsequently reformed onboard the vessel to comply with the selected powertrain configurations. The proposed concept of marine hybridisation aims to achieve high levels of efficiency through a well-designed system that captures and utilises waste heat and optimal load distributions to ensure that the engines operate at the most desirable setpoint [164]. Besides the apparent benefits of reducing shipping emissions, marine hybridisation and electrification also provide the opportunity for knowledge transfer from land-based automotive industries that have studied, tested, and validated control strategies for power management systems.

Currently, the marine industry predominantly relies on rule-based controls to address energy management in electrified and hybrid vessels [165, 166]. As the name suggests, this approach sets a predetermined "rule" under which the energy management system will be designed to operate. This rule is typically based on previous experiences and the operator's preferences. This rule simplifies and reduces any computational load on the management system while maintaining a desired operating point. A previous study utilised a rule-based control approach for an electrified tugboat [167]. A "rule" was applied for the three identified operating profiles, which included (i) standby (ii) transit (iii) bollard pull. The rule dictated that the power flow during the standby mode would exclusively be delivered by the batteries as the load demand is low, as illustrated in Figure 7-1. As the tugboat picks up speed during the transit, one generator will come online to complement the battery power, and both generators will come online during the bollard pull. The batteries are charged either during the transit or bollard pull operation. Based on its generic application, it is evident that a rule-based technique has its drawbacks, as

this static approach will inevitably have its blind spots in ensuring optimality in the power split configuration.

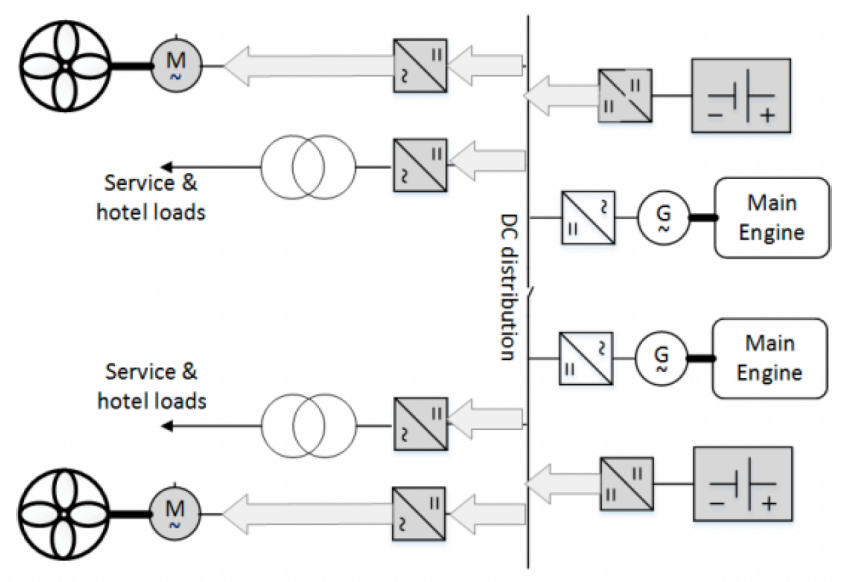

Figure 7-1: Direction of power distribution during standby operation mode

In this chapter, the drawbacks of rule-based techniques will be addressed by introducing novel strategies that capture the real-time determination of the power split between the various energy sources available in hybrid and electrified vessels. These strategies aim to reduce the identified cost function that addresses energy consumption and environmental concerns. This study also considers the implementation of a novel strategy, a Model Predictive Control (MPC), to an electrified hydrogen-powered tugboat. This first-of-its-kind application would provide key insights into the electric drivetrain powered by PEM fuel cells and batteries to deliver the optimal solution for power-split for minimized fuel consumption.

7.2 Overview of Optimisation – Based Power Management Strategies

A vessel's power management control can be optimised with the eventual goal of minimizing or maximizing a desired cost function. This involves the cost function being incorporated as a basis for the control objectives without compromising the reliability and rigor of the operational demand. Essentially, the optimised strategy would not be detrimental (i.e. should meet or exceed) to the design requirements of the vessel. Examples of cost functions usually requested by shipowners are (i) reduced fuel consumption (ii) maximized peak power (iii) reduced emissions (iv) maximized life expectancy (e.g. reduced running hours/charge cycles) of high-value equipment such as generators, fuel cells or batteries. In many instances, there is a likelihood that the cost function would comprise several different factors, and, in such instances, weighting functions are generally assigned to moderate the influence on the solution.

Much of the power management strategies for marine applications can be cascaded from the more mature and widely researched automotive industry. This knowledge transfer can form the fundamentals of an optimisation framework where marine-specific elements and considerations can be incorporated for further refinement. HEVs are one such example of how optimised power management strategies are being deployed [168-171]. Two distinct topics have been widely discussed: Global and Instantaneous Optimisations. As the name suggests, the latter employs the technique of addressing the cost function in the present state. As illustrated in Figure 7-2, This provides the opportunity to optimise the system in real-time. However, the drawback is the reactive approach as the optimised solution trails behind the movement across the different operational cycles. Examples of instantaneous optimisation methods include ECMS and MPC. Generally, both techniques are robust and provide reliable performance [172]. Global optimisation, however, takes into consideration the full operational cycle (i.e. present and future) to influence the optimal solution. The solution is made possible only if the future operational cycle is known and hence relies on expert knowledge or experience. This technique

thus provides the benefit of holistically addressing the identified cost function, albeit computationally intensive [173]. Consequently, this method is performed offline and is used to benchmark against instantaneous optimisation methods. Based on Bellman's principle of optimality, Dynamic Programming (DP) is one such method.

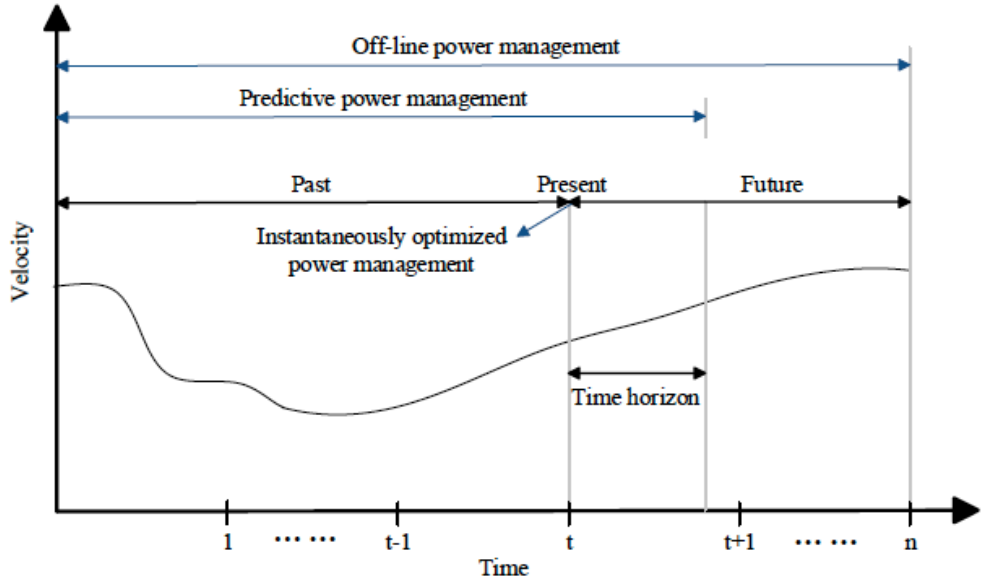

Figure 7-2: Comparison of optimisation methods

7.2.1 Dynamic Programming

The concept of DP attempts to solve and provide an optimum solution over the entire range of a vessel's operational profile. This is achieved by optimizing each node and sub-node over a predefined range of initial and final conditions (i.e. boundary conditions). The computation, when restricted by the boundary conditions, dictates the trajectory of the solution toward the final objective. The eventual performance of the optimality is governed by (i) the number of sub-nodes (ii) the stage size (iii) the step size. This is illustrated in Figure 7-3.

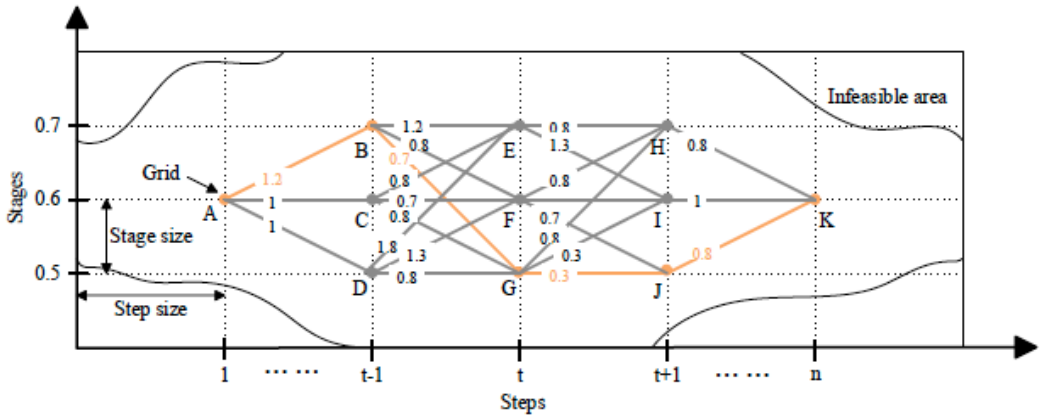

Figure 7-3: Dynamic programming computational path

The control objective can be expressed mathematically using a discrete-time linear state-space form:

$$x(k+1) = f(x(k), u\,(k)) \tag{7-1}$$

Where $x(k)$ is the initial or preceding condition, $u\,(k)$ is the input sequence resulting in the state trajectory and output sequence $x(k+1)$.

To put equation (7-1) into context, an electrified hybrid vessel with ESS and minimize fuel consumption, J, as a cost function to give:

$$J = \sum_{k=0}^{N-1} L\,(x(k), u\,(k)) \tag{7-2}$$

Where L is the instantaneous fuel consumption rate and N is the time length of the total vessel's operation. The above equation does not incorporate constraints on the battery's State of Charge (SOC) and hence:

$$SOC_{min} \leq SOC \leq SOC_{max} \tag{7-3}$$

However, the addition of the inequality constraint above does not contain an optimisation strategy regarding the battery management system, the battery would drain to meet the minimal fuel consumption. This is an undesirable consequence as batteries are preferred to operate within

a prescribed discharge range to maximize longevity. To counteract this, a final state constraint for the SOC is added:

$$\alpha(SOC(N) - SOC_f)^2 \tag{7-4}$$

Where equation (7-4) corresponds to the penalty attributed to the cost function. α is the weighting factor and SOC_f is the desired SOC's final state.

Combining equation (7-2) and (7-4), we get:

$$J = \sum_{k=0}^{N-1} L\left(x(k), u\,(k)\right) + \alpha(SOC(N) - SOC_f)^2 \tag{7-5}$$

As IMO also imposes restrictions on pollutants such as sulfur oxides (SO_x), Nitrous Oxides (NO_x), and particulate matter (PM), we can further refine equation (7-5) above to include weighting factors (α, β, γ) for the above emissions should the vessel's powertrain use a fossil-based fuel that could potentially emit such gases. This is shown by at time (k) :

$$J = \sum_{k=0}^{N-1} Fuel + \alpha(SOC(N) - SOC_f)^2 + \beta(SO_x) + \gamma NO_x + \delta PM \tag{7-6}$$

7.2.2 Equivalent Consumption Minimisation Strategy (ECMS)

The ECMS generally solves the optimum control problem with certain distinct features. This includes a battery management strategy where an external source does not charge the battery but instead by internal energy conversion devices (i.e. fuel cells, or engines). Taking fuel economy as the premise, the total equivalent consumption of fuel by the powertrain can be given by the power split ratio between fuel cell batteries can be given by the below cost function:

$$J(t) = \dot{m}_f + \dot{m}_{batt} \tag{7-7}$$

Where J (g/s) is the instantaneous total fuel consumption, $\dot{m}_f$ is fuel consumption from the fuel cells (g/s), and $\dot{m}_{batt}$ is the energy consumption from the batteries derived from transformed electricity (g/s). The energy for transformed electricity is given by the fuel consumption of the fuel cells to charge the batteries. ECMS attempts to solve for the optimised target that

instantaneously minimises the cost function, resulting in a lower total equivalent fuel consumption. It does this by:

$$\dot{m}_{batt}(t) = \frac{s(t)}{Q_{IHV}} P_{batt}(t) \quad (7\text{-}8)$$

where $s(t)$ is the equivalence factor at time (t), Q_{IHV} is the heating value of the fuel and P_{batt} is battery power. The equivalence factor (EF) above influences the results of ECMS drastically and generally has the following characteristics [174]:

- EF oscillations should be kept at a minimum as they adversely affect the performance of ECMS
- EF values affect battery discharge. Large EF values should result in charging of the battery and battery discharge is encouraged for small EF values
- EF reflects the efficiency of the powertrain in energy conversion

Considering the above, the EF can be shown as:

$$s = \frac{1}{\eta_{batt} \times \eta_e} = charging;\ s = \eta_{batt} \times \eta_e = discharging \quad (7\text{-}9)$$

Where η_{batt} and η_e are the efficiencies of the battery and motor, respectively. The efficiency of the motor determines the torque delivered to the drive shaft to the propellor for the vessel, whilst the battery's efficiency factors in losses in the energy transmission.

Previous studies have shown that the EF can be categorized into four (4) different approaches, and it is selected based on the intended purpose and system (i.e., hardware) architecture [175, 176]. Groups 1 to 4 are explained in increasing levels of complexity and computational load below. The first group utilises a blanket EF across the entire operating range of the available power on the vessel. It is determined by a static average of the efficiencies given in Equation 7-9 above. The second group determines the lowest instantaneous fuel consumption or the desired

cost function and calculates the corresponding EF. The third group calculated the EF in real-time, leveraging dynamic parameters to ensure that the battery SOC is within the desired operating range. The fourth group takes the computation further by using adaptive prediction techniques to calculate the EF in real-time.

7.2.3 Model Predictive Control

Model Predictive Control (MPC) is a closed-loop control strategy that can be proposed for power management on board the vessel. Based on the algorithm given by the plant model, MPC tracks the desired reference by predicting the required output given the input variables. The plant model can be mathematically expressed using a linear state-space system model:

$$x(k+1) = Ax(k) + Bu(k), \tag{7-10}$$

where $x(k)$ is the system state at the time step (k), $u(k)$ is the input variable and A and B are the state variables. The output will hence be given by:

$$y(k) = Cx(k) \tag{7-11}$$

Within the boundaries of the predictive horizon, MPC minimizes the desired cost function to achieve the optimum control input by:

$$J = \sum_{i=1}^{N_p}(y(k+i) - w(k+i))^2 + \lambda \sum_{i=1}^{N_c}(\Delta\, u(k+i-1))^2, \tag{7-12}$$

where N_p and N_c are the prediction and control windows, respectively. The tracked reference point is given as $w(k+i)$ and the change in input is given as $\Delta\, u$ accordingly. Similarly, a weighting factor is imposed and is given by λ. Feedback correction based on the measured output and the control input ensures a rolling optimisation through receding horizon control, forming a closed loop.

Studies have shown the demonstrated ability of MPC to minimise output error while accurately tracking the desired reference [177-179]. In [179], an all-electric propulsion system was

optimised using MPC to split the power delivered by a hybrid energy storage system comprising both batteries and ultracapacitors. This unique case study benchmarked the power tracking error of the MPC against individual control of either the batteries or ultracapacitors. Results from this study suggest that the power fluctuations from the electric drivetrains were accurately predicted by the MPC, consequently reducing losses. This strategy was further developed to incorporate uncertainties and disturbances associated with environmental conditions experienced by the vessel in a subsequent study [178]. This multi-level predictive control strategy investigated a two (2) step MPC approach to minimise the cost function of optimised energy management, as illustrated in Figure 7-4. The first step was to develop a nonlinear robust tube-based MPC that factored in the hydrodynamics affecting the vessel's forward motion (i.e. propellor shaft speed) under disturbances applied. While the hydrodynamics affecting the propellor speed, such as (i) thrust deduction coefficient, (ii) wetted area of the ship, and (iii) wave-making coefficient were clearly defined and quantified, the study was unclear on the governing principles and corresponding magnitude behind the disturbances applied. The second controller steers to meet the power split between the batteries and ultracapacitors based on the load demand given by the first controller. The results showed that the two controllers working concurrently tracked the load demand accurately.

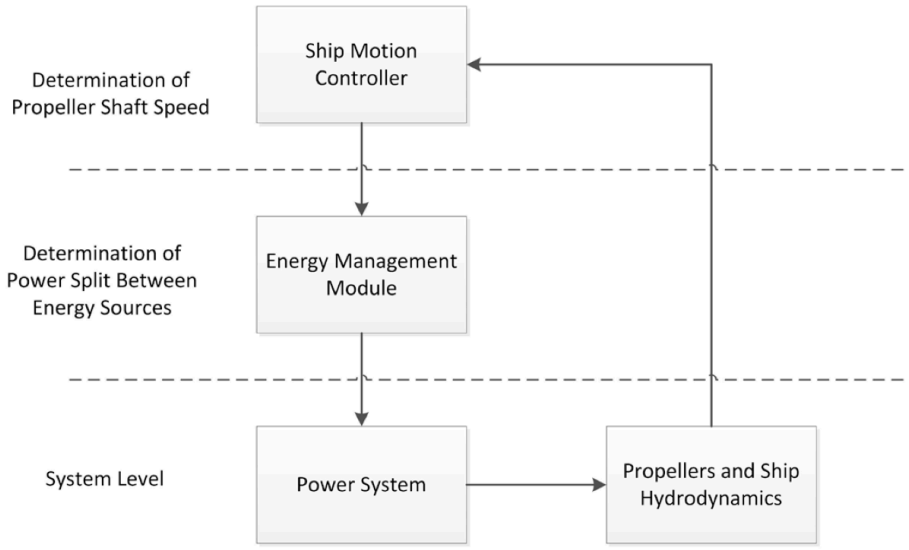

Figure 7-4: Multi-level predictive control strategy

7.3 Model-Based Controller Development

In this section, the development of a distributed model predictive control system for HyForce is outlined. The control system comprises a proxy model, process models, control policies, and distributed model predictive controllers. The proxy model translates operational and environmental conditions into reference set points for monitoring and control. The process models serve as data representations of the fuel cells and electric motors, linking control inputs (such as fuel consumption rate, voltage, and frequency) to motor speed and fuel cell power. Control policies are developed based on process optimisation recommendations to ensure effective fuel consumption and operation. Finally, the distributed model predictive controllers are designed to optimally manage the fuel cells and electric motors in accordance with the established control policies.

7.3.1 Overall Design of the Control System

In this study, the control system includes a user interface (UI), a sensor system, a proxy model, process models for fuel cells and electric motors/generators, two fuel cells, two electric

motor/generators, model predictive controllers, and actuators. The operator can adjust operational settings via the UI (e.g., selecting operational modes and setting vessel speed). The sensor system measures environmental conditions (such as wind speed, wind direction, current speed, current direction, water depth, water temperature, salinity, and wave height), as well as onboard information (including fuel cell power, electric motor power, electric motor speed, propeller speed, vessel speed, and vessel direction) for real-time feedback control. The proxy model assesses correction speed, total resistance, and reference set points for propeller speed, gas engine power, electric motor power, effective power, and delivered power. The schematic of the designed control system is illustrated in Figure 7-5. The process models which serve as inputs to the MPC controllers are shared in Chapter 6.

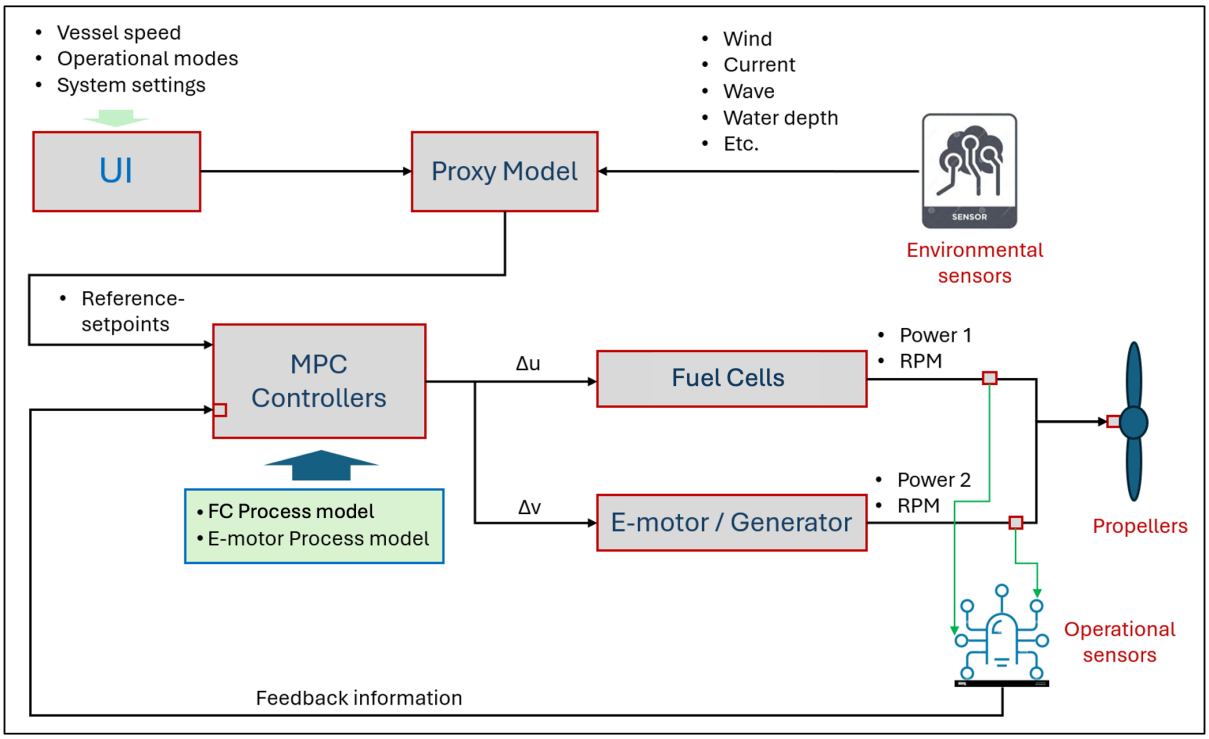

Figure 7-5: Schematics of the designed control system

7.3.2 Design of Control Policies

The vessel is designed to operate in various modes: idle, transit, towing, boost, FiFi, and take-me-home. To ensure optimal performance in each mode, the control system has been meticulously designed to manage the power mix efficiently. Below are the details of the control policies.

7.3.2.1 Idle / Harbour Mode

This operational mode is designed for various scenarios, including leaving or entering the harbour, idling, station keeping, and free sailing at speeds up to 6 knots. During this mode, the vessel is powered solely by electric motors, with the fuel cells powered down. The batteries are operating in the discharge mode. The vessel's speed can be adjusted via the designed Graphical User Interface (GUI) of the control panel.

7.3.2.2 Transit Mode

Transit mode is designed for the vessel to travel between locations during its operational profile. In this mode, the vessel is powered solely by fuel cells, which also supply power for hotel load and battery charging when Power Take-Off (PTO) mode is active. PTO mode engages when the battery's state of charge falls below 35%, and the generator stops charging the batteries once the SOC exceeds 80%.

As the vessel's speed increases, the hotel load often demands more power for systems like the cooling pump and other devices, and consequently, the charging rate may decrease. For this vessel, Figure 7-6 (a) illustrates the power required from the fuel cells to meet hotel load and battery charging needs, in addition to powering the vessel. Figure 7-6 (b) shows the battery charging rate at different propeller speeds (vessel speed). During free sailing, the vessel can adjust to a maximum speed of up to 12 knots via the GUI.

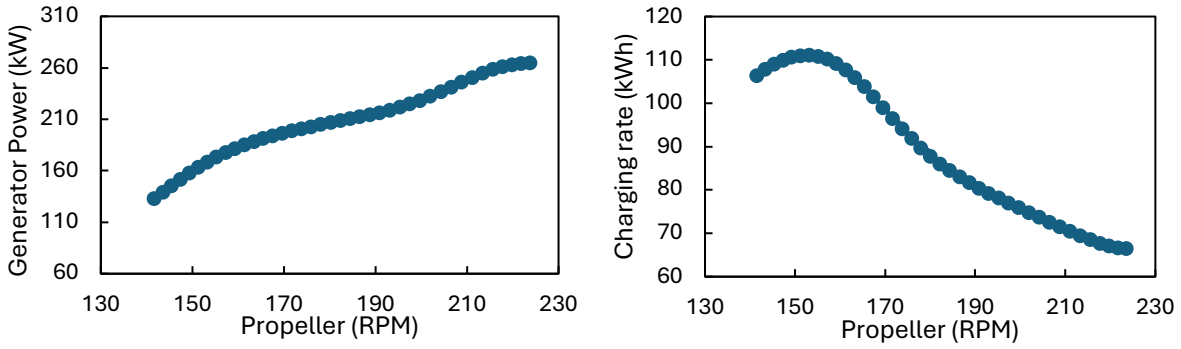

(a) (b)

Figure 7-6: (a) Total power requirement to meet battery charging and hotel loads (b) Battery charging rates

7.3.2.3 Towing Mode

Towing mode enables the vessel to operate in pushing, pulling, and free sailing during both 'transit-in towing' and 'boost-in towing' operations. In transit-in towing mode, the vessel is powered by the fuel cells, with the batteries charging depending on the remaining available power. In boost-in towing mode, both the e-motors and fuel cells are engaged, with the e-motors providing additional power and thrust. The vessel can operate at any speed up to a maximum of 12 knots.

7.3.2.4 Boosting Mode

Boost mode is designed to deliver maximum power for bollard pull, utilising both the fuel cells and e-motors. In this mode, the fuel cells operate at full capacity, while the batteries discharge as needed to meet the required power demand. The operator can activate boost mode by increasing the power request to the control system once the full capacity of the fuel cells has been utilised. The Power Take-In (PTI) mode can only be initiated if there is sufficient battery power available till the designed hard limit of 30% SOC.

7.3.2.5 FIFI Mode

The FIFI (Firefighting) mode is specifically designed for firefighting operations. In this mode, the vessel is powered by the starboard (SB) fuel cell and the port-side (PS) electric motor. The PS fuel cell drives the FIFI pumps, while the SB generator operates in PTO mode. Depending on available power, the batteries either charge or discharge. Both propellers run to keep the vessel stationary during operation. Any excess power from the SB generator is used to charge the batteries. If the SB generator cannot supply enough power for the PS e-motor to maintain position, the PS motor will draw power from the batteries. For a detailed overview of the control policy in FIFI mode, refer to Figure 7-7. It is also important to note that the PS fuel cells can adjust their speed to ensure adequate power for the FIFI pumps.

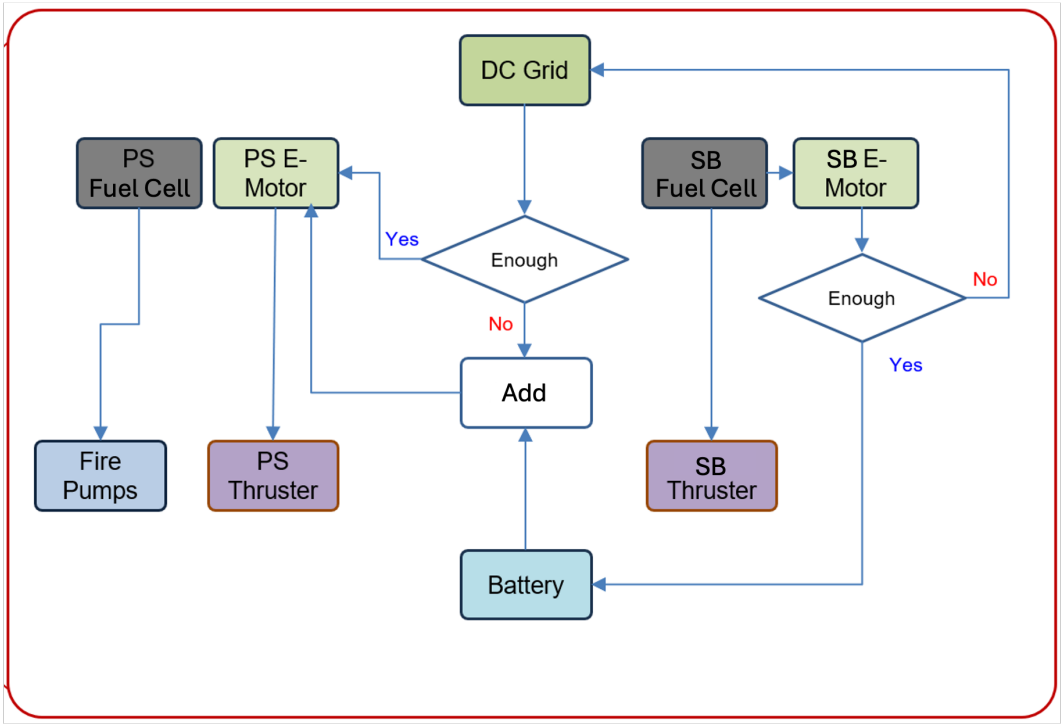

Figure 7-7: Control policies for FIFI mode

7.3.2.6 Take-me-Home Mode

The "Take-Me-Home" mode is designed to safely return the vessel to the harbour or port when the batteries reach their reserved capacity of 30%. In this mode, the vessel is powered solely

by the batteries (via e-motors), with the fuel cells turned off. The vessel can operate at speeds of up to 6 knots.

7.3.3 In-Silico Control Demonstrations

This section presents various in-silico control scenarios to demonstrate the capability and performance of the developed control system. Several operational modes, including harbour mode, transit mode, towing mode, boost mode, and take-me-home mode, are employed. For each mode, different vessel speeds are tested to exemplify the control system's robustness, accuracy, and stability. Additionally, various control gains are applied in these scenarios to assess their impact on control performance.

7.3.3.1 Idle / Harbour

In harbour/idle mode, simulations are conducted for in-silico control demonstrations, with the vessel operating at various speeds of 4, 6, 2, and 5 knots. The vessel is powered solely by the e-motor. Figure 7-8 illustrates the operational settings using the designed GUI and Figure 7-9 display the vessel's operational profile through the power of the e-motor the pre-determined environmental conditions, respectively.

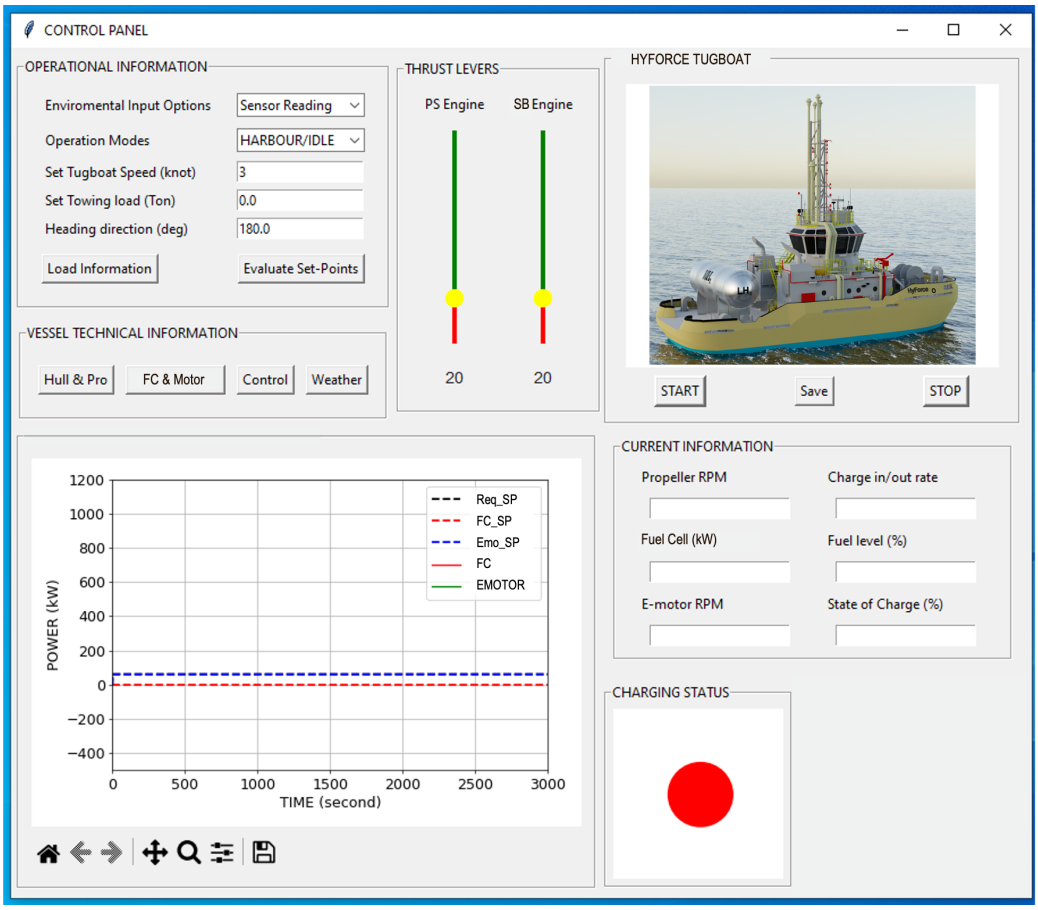

Figure 7-8: Operational setting for idle/harbour mode in designed GUI

No wind, waves, or currents are considered in the calm water scenario. In contrast, the environmental conditions considered in this simulation were: (i) wind speed at 4.0 knots, (ii) wind direction of 180 degrees (opposite the vessel moving direction), (iii) speed of current set to 1.0 knot in the same direction as the wind, and (iv) wave height is set at 0.25 meters. Table 7-1 compares the simulated results for power delivered by the e-motor and the propeller speed for both calm water and environmental conditions. The results show that the vessel requires a higher propeller speed, a higher power of e-motor, and a higher e-motor speed to move under environmental conditions compared to calm water conditions at the same speed. This also emphasises the importance of optimal vessel voyage planning to minimise or eliminate operating the vessel under adverse environmental conditions.

Table 7-1: Comparison of the required power, propeller speed, and e-motor speed between the operations in calm water and environmental conditions for different vessel speeds.

Vessel speed	Calm water			With Environmental Conditions		
	Power, kW	Propeller, RPM	E-motor, RPM	Power, kW	Propeller, RPM	E-motor, RPM
2	21.6316	73	442	26.2463	78	468
4	32.1178	81	489	58.5119	95	571
5	53.5533	93	558	93.2893	107	644
6	125.9853	105	633	145.4287	120	723

The response to the change by the controller on the desired e-motor power setpoint is given in Figure 7-9 below. The control results indicate that the control system effectively drives the e-motors to attain the reference power set points corresponding to the different vessel speeds. The control can accurately and stably manipulate the e-motor to the required power levels during acceleration and deceleration. However, a higher control gain may be needed in this operational mode to reach the set points more quickly.

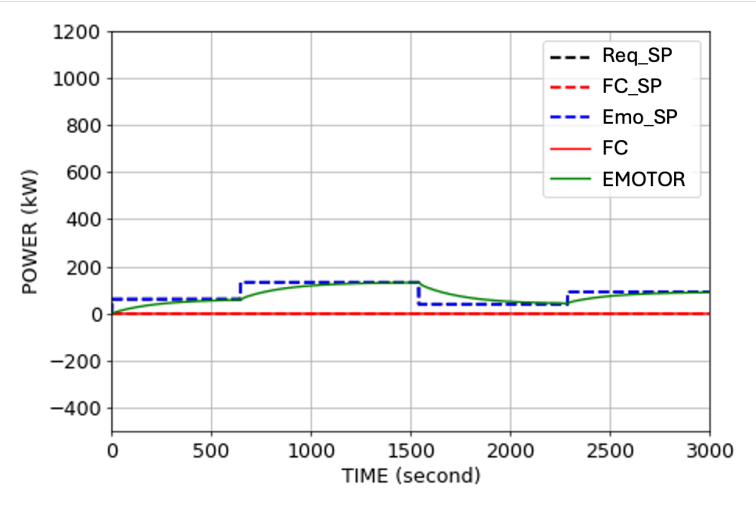

Figure 7-9: In-silico control in idle/harbour mode under environmental conditions

7.3.3.2 Transit

This subsection demonstrates the performance of the designed control system for the transit operational mode. Four control scenarios are examined:

- Calm water with no charging
- Calm water with charging (PTO)
- Environmental conditions with no charging
- Environmental conditions with charging.

Like the previous section, the demonstrations do not include wind, wave, and current effects in the calm water cases. For environmental conditions, (i) wind is set at a speed of 4.0 knots, (ii) wind direction of 180 degrees, (iii) speed of current is set at 1.0 knots with a direction at 180 degrees (iv) Wave height is approximately 0.25 meters, and (v) water temperature is at 25°C with salinity concentration at 30 g/kg. The roughness of the vessel hull surface is about 160 μm.

For the non-charging cases, calm water and environmental effect scenarios are tested at five different vessel speeds: 10, 12, 8, 11, and 9 knots. The results indicate that sea conditions significantly affect the power required to maintain the same vessel speed as when the water is calm. For example, approximately 1400 kW is required under environmental conditions, while only about 973 kW is needed in calm water, as shown in Figure 7-10 (a) and Figure 7-11(a) without charging the batteries, respectively.

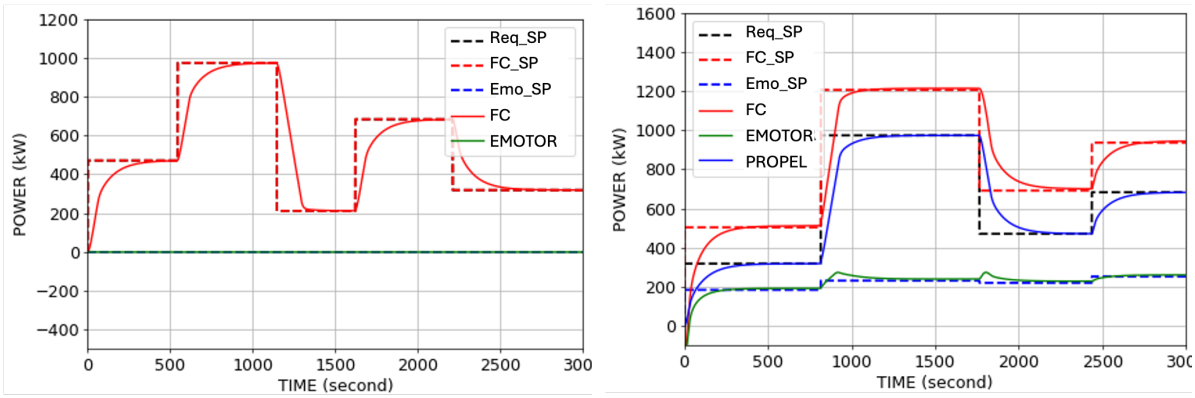

(a) (b)

Figure 7-10: In-silico control for transit mode under calm water conditions (a)without battery charging at vessel speeds of 10,12,8,11 and 9 knots (b)with battery charging at vessel speeds of 9,12,10, and 11 knots

Figure 7-10 (b) and Figure 7-11 (b) show the performance results of the control system for the transit operational mode with charging (PTO). In addition to the required power for the propulsion system (PROPEL, shown by the blue line), a certain amount of power is allocated for the driving generator (EMOTOR, shown by the green line), which is added to the power delivered by the fuel cell. The results also show that the power required for the generator varies with different vessel speeds.

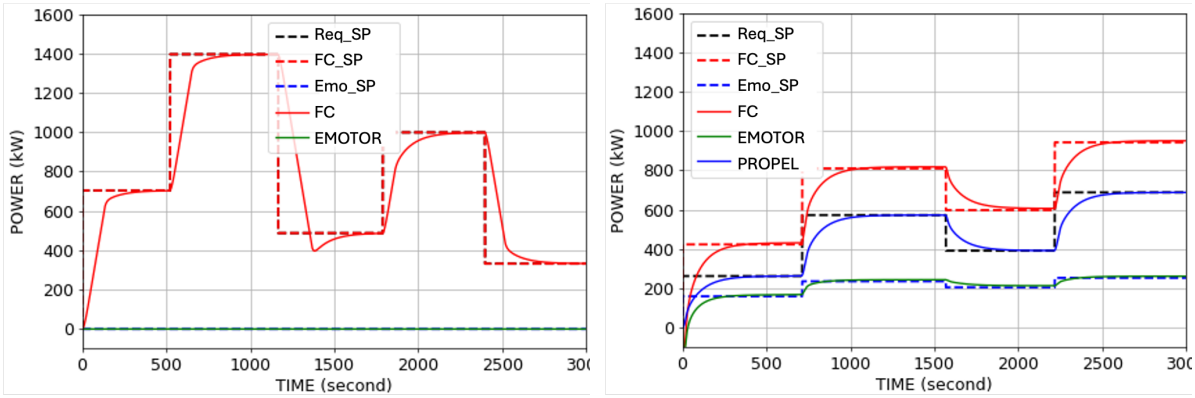

(a) (b)

Figure 7-11: In-silico control for transit mode under environmental conditions (a)without battery charging at vessel speeds of 10,12,8,11 and 9 knots (b)with battery charging at vessel speeds of 8,10,9, and 10.5 knots

In this control design, a small control gain was selected K=50. Whilst this might take a slightly longer time to reach the set points, the objective here was to first establish a smooth control performance with minimal to no undershoot or overshoot. This is an important performance criterion of the controller as it ensures that the fuel cell and e-motors do not have high variations (i.e. fuzzy) in their operating point. However, due to the high inertial force of the vessel during its operation in the water, ramping up or down could provide a faster response and this will be investigated.

7.3.3.3 Towing

This section demonstrates the control performance of the towing operational mode under two scenarios: “towing in transit” and “towing with boost”, both without PTO, for calm water and under environmental conditions. The environmental conditions set are consistent with the above test cases. In addition, HyForce will be towing/pulling a load of 40 tons. Figure 7-12 shows the towing mode settings using the designed GUI.

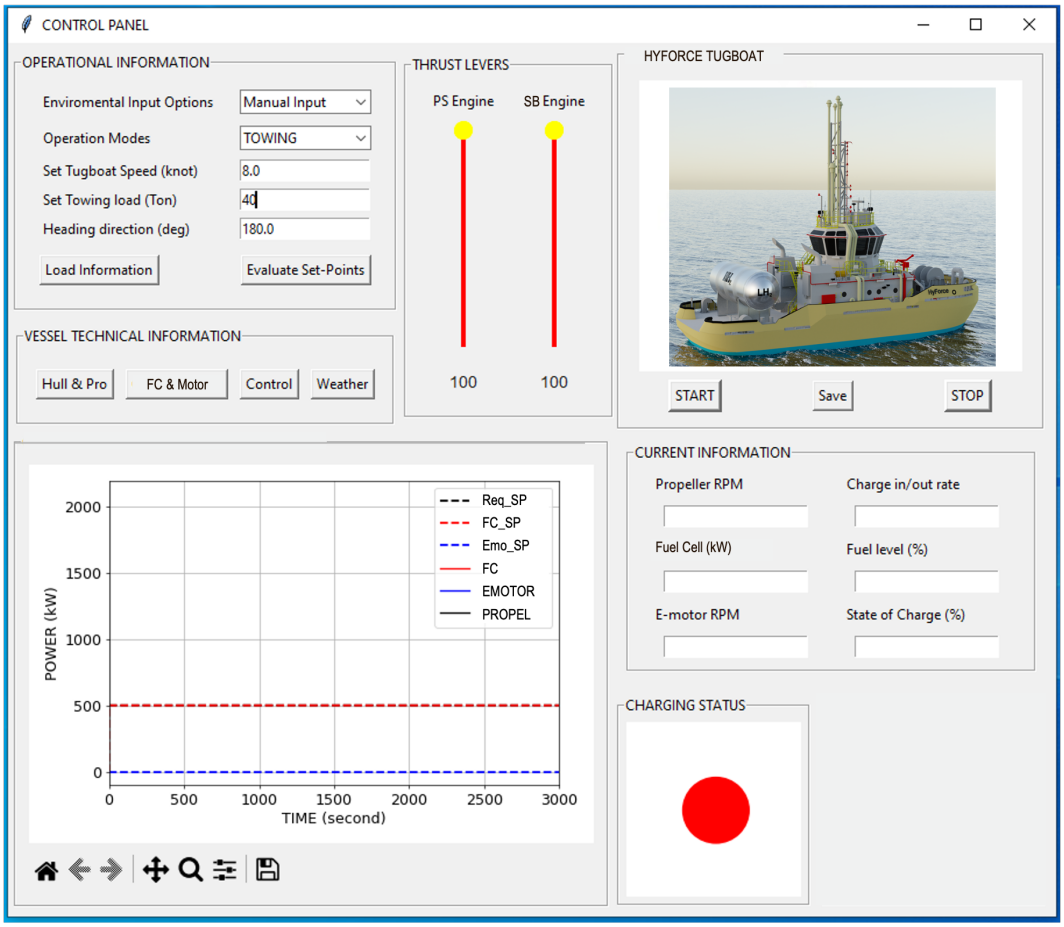

Figure 7-12: Operational setting for towing mode in designed GUI

Figure 7-13 and Figure 7-14 show the control performance of the vessel in towing mode under both calm water and environmental condition cases, respectively. For both scenarios, the "towing with boost" mode is required when the vessel speed is set to 12.0 knots, as the required propulsion power exceeds the maximum power of the fuel cell. Consequently, additional power from the E-motors is utilised to achieve the desired speed. In calm water, only a small amount of additional power is needed, whereas significantly more power is required under environmental conditions.

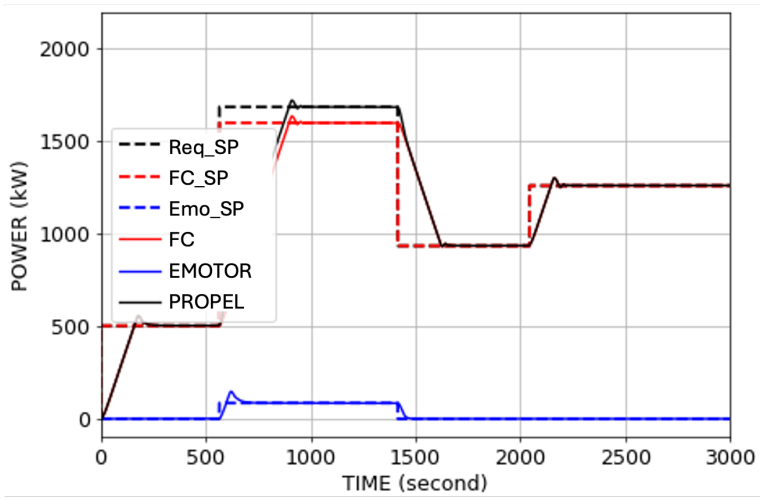

Figure 7-13: In-silico control demonstration for the towing mode in calm water: 8, 12, 10, and 11 knots

In these cases, the control gain is set at K=150K = 150K=150. Overshoots are observed in both the fuel cell and the E-motor. However, the control system brought both the fuel cell and E-motor to the set points in a shorter time validating that the control performance is accurate, robust, and stable.

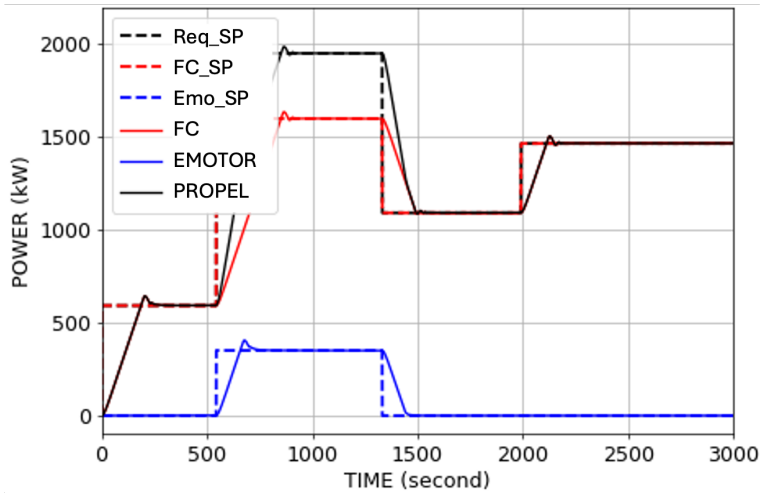

Figure 7-14: In-silico control demonstration for the towing mode under environmental conditions: 8, 12, 10, and 11 knots

7.3.3.4 Boosting

Figure 7-15 shows the settings and live operation of the boost mode during the towing/pulling operation of the vessel. The results indicate that the vessel operates in "transit-in towing" mode when the required propulsion power is less than the maximum power of the fuel cells. No additional power is required in this mode, as the fuel cells can deliver enough power for the propulsion system when the vessel travels at 8, 10, and 11 knots.

However, additional power from the e-motors is necessary when the required propulsion power exceeds 1600 kW, particularly when the vessel speed is set at 12 knots, requiring approximately 1950 kW. About 390 kW of power from an e-motor is needed in this case.

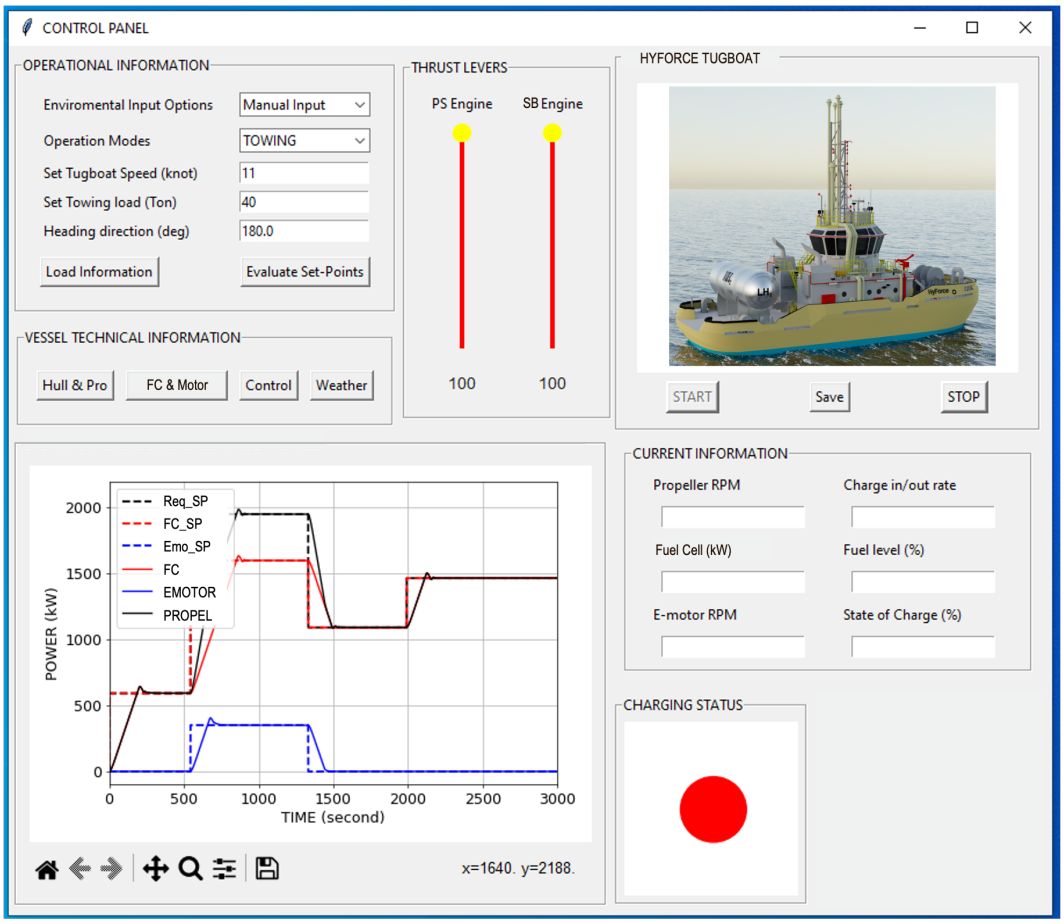

Figure 7-15: Operational setting for boosting mode in designed GUI

7.3.3.5 Take-me-Home

In this mode, "take me home" is activated when the batteries' SOC falls below 30%, and e-motors power the vessel. The vessel can travel at speeds up to 6 knots. Figure 7-16 shows the settings for the "take me home" operational mode. Figure 7-17 and Figure 7-18 displays the control performance in this mode for different vessel speeds (2.5, 6, 2, 5, and 4 knots).

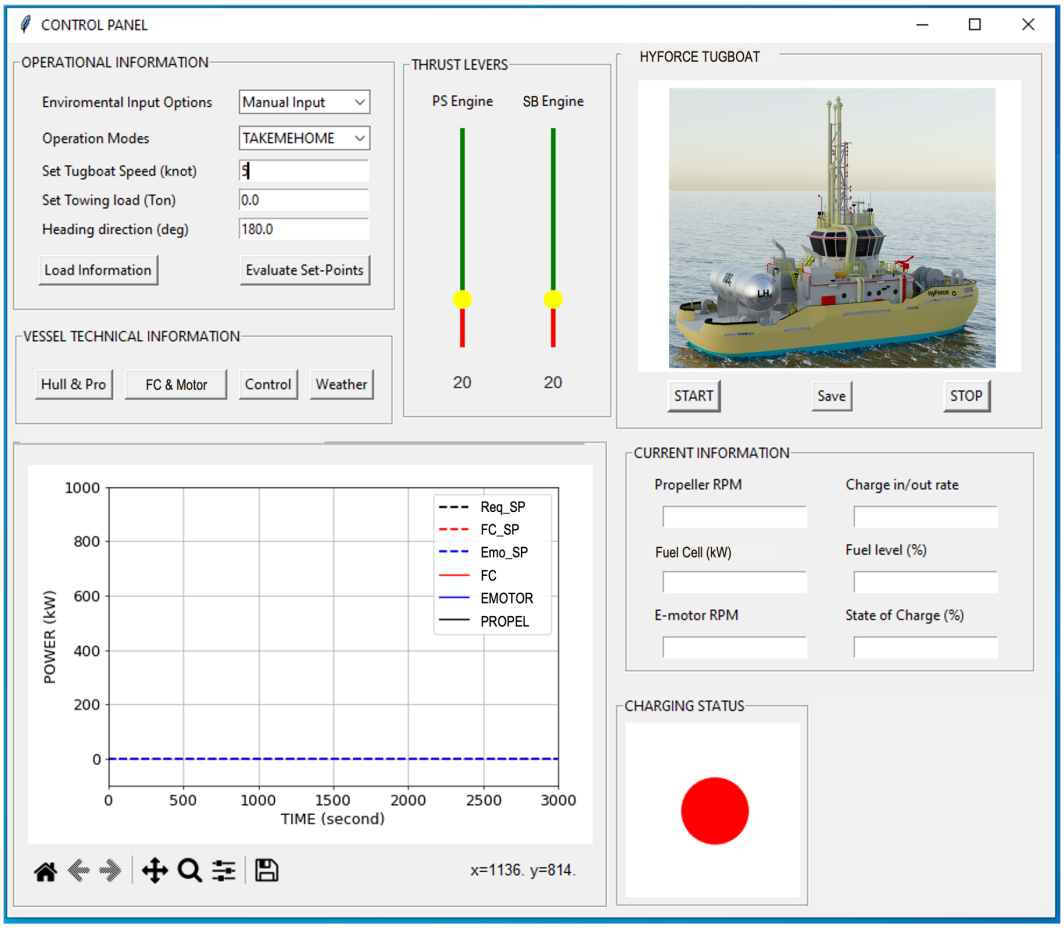

Figure 7-16: Operational setting for take me home mode in designed GUI

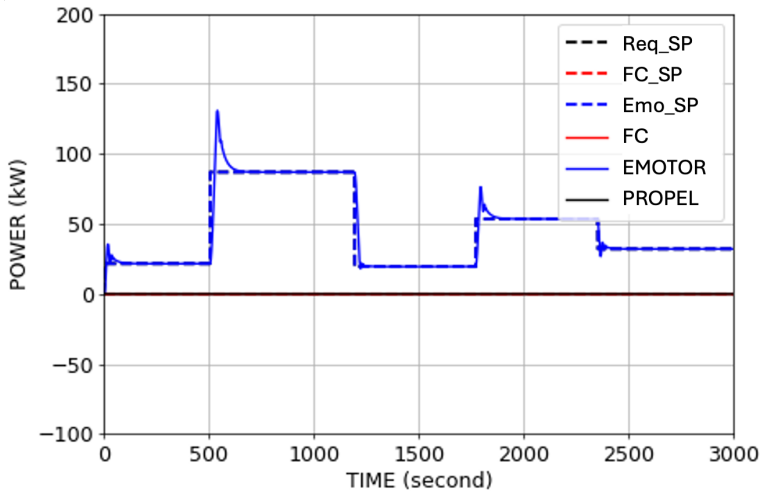

Figure 7-17: In-silico control demonstration for the take me home mode with calm water conditions for different speed of 2.5, 6, 2, 5, and 4 knots

In these cases, the control gain is set at K=250K. The results indicate significant overshoots in the e-motors as the power reaches the set points. However, the control system can quickly drive the e-motors to attain the power set points. While some small instabilities are observed, the control system remains robust and accurate. Therefore, selecting a suitable control gain is crucial for achieving good control performance.

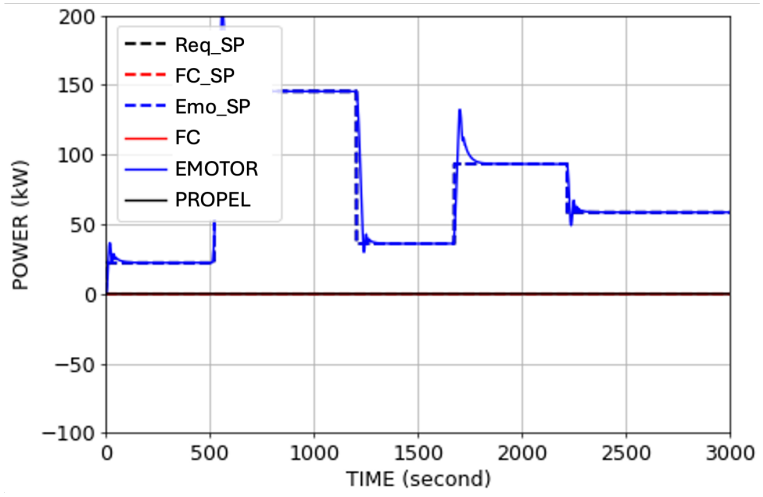

Figure 7-18: In-silico control demonstration for the take me home mode under environmental conditions for different speed of 2.5, 6, 2, 5, and 4 knots.

A proxy model is developed to evaluate the reference set points for the required power and propeller speed based on inputs such as vessel speed, operational mode, and environmental conditions. This model is validated with data provided by the respective equipment vendors.

Additionally, a process model for the fuel cell is developed to link the fuel consumption rate to the delivered power for control development. A process model for the e-motor is also developed to link the provided voltage to the power based on the rated frequency for model predictive control development.

A distributed model predictive control system is developed for the optimal operation of the vessel. This control system is benchmarked against data from the combined model. Different control modes are implemented to achieve optimal operation, and control performance is demonstrated in-silico for various scenarios.

Environmental conditions have a strong impact on vessel operation, making it necessary to account for these conditions in vessel planning and operation. Control parameters, such as control gain, play a crucial role in control performance, affecting accuracy, robustness, stability, and response time.

Chapter 8

Conclusion and Future Work

The concluding chapter details this study's key findings and primary contributions and makes recommendations for future research.

8.1 Conclusion

This thesis addresses the techno-economic and environmental assessments leading to the formulation of a power management problem in advanced maritime power systems, particularly optimising power allocation in an all-electric hybrid power and propulsion system. The primary goal is to enhance fuel efficiency and reduce emissions, which are critical concerns in modern maritime industries. The power management problem is tackled by first developing a comprehensive understanding of the power system’s dynamic response. This is achieved by formulating a detailed all-electric hybrid power system model. The central challenge of this thesis is determining the optimal power split between multiple power sources to achieve the desired improvements in fuel efficiency and emission reductions. Among the options considered, which include equivalent consumption minimisation strategy (ECMS), the Model Predictive Control (MPC) is proposed as an instantaneous optimisation-based approach to be considered. This strategy optimises power distribution between power sources in real-time by minimising the equivalent fuel consumption, thus improving the system's overall performance. The effectiveness of the proposed optimisation strategy is tested and validated on a digital twin model, ensuring that the results apply to real-world scenarios.

Compared with the conventional rule-based strategies typically used in the industry, the proposed strategy demonstrates substantial improvements in fuel savings, highlighting its potential for widespread adoption in the maritime sector.

Building on these promising results, the optimisation strategy is refined in two critical areas. Firstly, the approach is extended to include emission control. A novel method is introduced to manage the trade-off between emissions and fuel consumption, an essential consideration for regulatory compliance and environmental sustainability in maritime operations. This strategy extension allows for more comprehensive control over emissions and fuel use, enhancing the system's overall performance. Secondly, the strategy is enhanced to include extending the bunkering intervals of hydrogen and consequently increasing the number of towing jobs HyForce can complete. This vital metric was selected as it provides a critical signpost for the commercial viability of this concept design. The number of towing jobs illustrates the revenue-generating capability of HyForce, and this metric is referenced against the baseline of a traditional fossil-based tugboat. The developed methodology in this study aims to address a diverse range of marine applications which utilises a multi-source powertrain. This study can be replicated for improved control and load sharing for optimised energy management.

8.2 Main Contributions

Through this work, the three (3) main contributions are:

1. **Techno-economic-environmental assessment of HyForce**

HyForce, a 2000 kW hydrogen-powered 45-ton bollard pull virtual tugboat, has the potential to revolutionise the harbour craft industry with zero carbon emissions during operation. The two powertrains considered, a PEMFC and an ICE system, have been shown to be technologically feasible for performing the demanding mission-centric operational profiles expected by a tugboat. The PEMFC is designed with an energy storage system to provide the necessary dexterity to handle transient loads. In contrast, the ICE system is supported by dedicated generators that offer auxiliary power as required.

The results have shown that the powertrain choice, a PEMFC or ICE, differs in economic and environmental evaluations. The PEMFC system provides a better outlook when considering the operational costs, albeit a higher capital outlay. The ICE system emits NO_x because of the high-temperature combustion process but can be well mitigated by incorporating a lean burn Otto cycle with selective catalytic reduction.

Market-based measures, such as an emissions tax, significantly impact the breakeven price of liquified hydrogen. For example, a $50/tCO2 tax levied on a diesel tug increases the breakeven cost of hydrogen by $1 for a PEMFC powertrain. In Singapore, where the carbon tax is $3.66 (SGD 5), we need systemic change to expedite the adoption and incentivise the uptake of low-carbon solutions to bring forward the 2040 tipping point.

Hydrogen PEMFC is a promising technology that will lead the charge as the industry pivots into adopting alternative fuels to meet the GHG reduction targets set by IMO. PEMFC has a strong track record for land-based stationary power and automotive applications, which boosts their confidence in marinising this technology. Our results showed that under the current operating climate, a liquified hydrogen-based propulsion system is not viable even with a breakeven point at the threshold limit of 15 years. As the projected liquified hydrogen cost is expected to decrease with increasing uptake of hydrogen production across the world coupled with improvements in liquefaction efficiency, HyForce with a PEMFC powertrain has the potential to be cost competitive by 2040 without the introduction of an emission tax. A sensitivity analysis of the expected CAPEX reductions for PEMFC is a signpost for HyForce's overall improved economics.

2. Modelling Guided Energy Management System

This study quantified the propulsion, power prediction, and total resistance acting on the vessel to further investigate HyForce's overall performance characteristics. The meticulous calculations of propulsion and power consider the total resistance, incorporating insights from

CFD simulation and empirical methods, specifically focusing on dynamic environmental conditions. Notably, the study identifies vessel speed as a pivotal factor influencing total resistance, exhibiting a tenfold increase from 5 knots, registering at 7.2 kN, to 11.0 knots, reaching 73.1 kN. Moreover, examining appendages on the hull suggests their limited contribution to overall resistance.

Further exploration encompasses the impact of seawater depth, properties, wind, and waves on HyForce's resistance during deployment. CFD simulation studies reveal that the viscosity of seawater becomes a significant contributor when temperatures drop below 15°C. Wind resistance at a speed of 10.0 m/s, particularly from headwind (0.0 degrees or 360.0 degrees), contributes 3.0 kN, posing a potential constraint on HyForce's maximum speed of 12.0 knots. Shallow seawater depth below 10 m in coastal waters is identified as an inevitable limiting factor.

The propeller design is scrutinized to ensure it generates sufficient thrust to overcome inherent resistance, facilitating optimal performance across various operational profiles. Results indicate that two propellers with a 2.5 m diameter each are adequate, delivering 1892.0 kW. The onboard energy storage system, through peak shaving, contributes the remaining power to meet the 2.0 MW stipulation.

The digital twin and modelling and simulation framework established for HyForce in this study serves as a foundation and valuable tool for developing a model predictive controller for onboard power management. Incorporating a closed-loop controller aims to ensure that the desired power reference is dynamically and optimally tracked while executing embedded power management strategies. The development direction of this controller will be designed to track the targeted cost functions material to the end user. This includes (i) lengthening the refuelling intervals, (ii) minimising the charge cycles of batteries, and (iii) reducing the well-to-wake emissions or other desired parameters.

Once implemented, this controller ensures the optimization of hydrogen energy by accurately representing environmental conditions and inherent resistance forces acting on HyForce. By embedding these insights into the controller's design, the study ensures optimised outputs align with the envisaged operating scenarios for which HyForce is purposefully designed.

3. Model Predictive Controller

A systemic approach to develop an optimized power-sharing model for HyForce. A theoretical model framework for the powertrain was first developed to provide an overview of the potential power-sharing strategies. Statistical data were digitized to create a virtual digital environment as the platform to implement the power-sharing strategies. The results are promising, indicating a 15% increase in the total number of towing jobs in between bunkering intervals, which was the cost function used to govern the optimization potential.

The power-sharing model provides a solid foundation for future work. Moving forward, a proxy model of HyForce can be incorporated to include environmental considerations such as wind speed, wave height and current, hull resistance, seawater temperature, and salinity to fully encapsulate the factors that might influence the performance of HyForce. This will also indicate whether the current powertrain and design capacity of 2MW is sufficient even in the worst-case operating scenarios, as well as the ability to quantify the operational windows in which HyForce would be able to perform remarkably well. Furthermore, an analysis on the transient loads during load profile changes can be studied to verify that instantaneous power is available. A MPC framework is developed to ensure maximum potential is realised to optimise material cost functions. The control system framework is envisaged to optimise the battery’s SOC and fuel consumption, allowing HyForce to operate longer between bunkering intervals. This is achieved through power-sharing strategies that split the load demand optimally at the various operating profiles. The minimum battery SOC was imposed with a hard limit of 30% to ensure the safe return of HyForce if there were inadvertently any issues with the fuel cells during

operation. This paper provides the foundation to which the MPC can be tested in silico under a controlled environment for further refinement. To ensure a more realistic simulation and testing of the MPC, environmental factors such as wind, wave, and drag can be incorporated to ensure the robustness of the controller and solidify the value proposition of HyForce as the next-generation tugboat.

A systemic approach to develop an optimized power-sharing model for HyForce. A theoretical model framework for the powertrain was first developed to provide an overview of the potential power-sharing strategies. Statistical data were digitized to create a virtual digital environment as the platform to implement the power-sharing strategies. The results are promising, indicating a 15% increase in the total number of towing jobs in between bunkering intervals, which was the cost function used to govern the optimization potential.

The power-sharing model provides a solid foundation for future work. Moving forward, a proxy model of HyForce can be incorporated to include environmental considerations such as wind speed, wave height and current, hull resistance, seawater temperature, and salinity to fully encapsulate the factors that might influence the performance of HyForce. This will also indicate whether the current powertrain and design capacity of 2MW is sufficient even in the worst-case operating scenarios, as well as the ability to quantify the operational windows in which HyForce would be able to perform remarkably well.

8.3 Recommended Future Work

This work has made significant progress in using hydrogen as a fuel source for marine propulsion. While this work has achieved its intended objective, there is potential for advancements to be made in this area of research.

- **Reinforcement learning-based power management strategy**

Reinforcement Learning (RL) is an innovative artificial intelligence-based control method that has been recently gaining significant attention. It is one of the three main categories of machine

learning, which include (i) unsupervised learning and (ii) supervised learning. In contrast to unsupervised learning, which is used to identify patterns or hidden structures in unlabelled datasets, and supervised learning, which trains a system to assign labels to inputs, reinforcement learning works with data from a dynamic environment rather than a static dataset. Its goal is not to cluster or classify data but to identify the optimal sequence of actions to achieve the best possible outcome. This is accomplished by enabling a controller, called an agent, to explore, interact with, and learn from the environment.

The core concept maximises the numerical reward by allowing the agent to interact with the environment, ultimately developing the optimal control strategy. The strength of the RL approach lies in its ability to handle learning scenarios even when the system dynamics are unknown. Additionally, RL algorithms utilize powerful function approximation techniques to represent the environment's value functions in a compact form, enabling them to manage systems with high-dimensional state and action spaces effectively.

Most RL-based PMSs are currently deployed in land-based applications such as electric vehicles and utility-scale power plants. The difficulty of managing data collection onboard vessels curtails penetration into the maritime environment.

With the availability of more vessel operation data, RL-based PMS is expected to become a prominent research focus in the future. However, the RL agent functions as a "black box" comprised of neural networks that lack explainability, which could result in unpredictable behaviours that are difficult to interpret. Therefore, rather than serving as the primary controller, RL could be utilised as a tool to optimise weight factors within traditional control systems, such as the MPC developed in this study.

- **Load Profiles and Weightage of Cost Functions**

The load profile considered in this dissertation is based solely on average data from a single source, and the results are significantly influenced by the load profile data provided by the

industry. However, ship operating profiles vary by location, depending on geography. For instance, Singapore's natural deep-water harbours allow tugboats to tow ocean-going vessels to piers quickly. In contrast, tugboats must pull ships for longer durations through narrow inland channels to reach harbours in other regions. Load profile studies are invaluable for understanding tugboat operations and improving optimisation results. However, such data is highly confidential, as a tugboat's load profile can reflect a port's operational skills and efficiency, providing a competitive advantage. Therefore, data gathering requires collaboration between governments, industries, and academic institutions.

The weight values in the cost functions have been selected arbitrarily, largely based on the designer's judgment of their importance. This arbitrary selection may not achieve the ideal multi-objective optimum, occurring when each objective independently reaches its optimal value. An alternative approach involves using an ideal procedure to identify Pareto points and developing a Pareto surface through iterative adjustments of the weights. Further research could explore this Pareto-surface search method, potentially leading to more effective weight parameter selection.

References

1. Dinneen, J., *The world just had the hottest February ever recorded.* New Scientist, 2024. **261**(3482): p. 10.
2. Choudhary, B.K., A.K. Tripathi, and J. Rai, *Can 'poor' cities breathe: Responses to climate change in low-income countries.* Urban Climate, 2019. **27**: p. 403-411.
3. Yu, B., et al., *Countries' green total-factor productivity towards a low-carbon world: The role of energy trilemma.* Energy, 2023. **278**: p. 127894.
4. Charabi, Y., et al., *GHG emissions from the transport sector in Oman: Trends and potential decarbonization pathways.* Energy Strategy Reviews, 2020. **32**: p. 100548.
5. Umer, M., et al., *GHG emissions estimation and assessment of Pakistan's power sector: A roadmap towards low carbon future.* Results in Engineering, 2024. **22**: p. 102354.
6. IPCC, *Climate Change 2023: Synthesis Report. Contribution of Working Groups I, II and III to the Sixth Assessment Report of the Intergovernmental Panel on Climate Change*, J.R. H. Lee, Editor. 2023: Geneva, Switzerland. p. 184.
7. Islam Rony, Z., et al., *Alternative fuels to reduce greenhouse gas emissions from marine transport and promote UN sustainable development goals.* Fuel, 2023. **338**: p. 127220.
8. Fan, A., et al., *Characteristics of real-world ship energy consumption and emissions based on onboard testing.* Marine Pollution Bulletin, 2023. **194**: p. 115411.
9. Han, J., J.-F. Charpentier, and T. Tang *An Energy Management System of a Fuel Cell/Battery Hybrid Boat*. Energies, 2014. **7**, 2799-2820 DOI: 10.3390/en7052799.
10. McCoy, T.J., *Electric Ships Past, Present, and Future [Technology Leaders].* IEEE Electrification Magazine, 2015. **3**(2): p. 4-11.
11. Doerry, N., J. Amy, and C. Krolick, *History and the Status of Electric Ship Propulsion, Integrated Power Systems, and Future Trends in the U.S. Navy.* Proceedings of the IEEE, 2015. **103**(12): p. 2243-2251.
12. McCoy, T.J., *Integrated Power Systems—An Outline of Requirements and Functionalities for Ships.* Proceedings of the IEEE, 2015. **103**(12): p. 2276-2284.
13. Sáiz, V.M.M. and A.P. López, *Future trends in electric propulsion systems for commercial vessels.* Journal of Maritime Research, 2007. **4**(2): p. 81-100.
14. Geertsma, R.D., et al., *Design and control of hybrid power and propulsion systems for smart ships: A review of developments.* Applied Energy, 2017. **194**: p. 30-54.
15. Haxhiu, A., et al., *Electric Power Integration Schemes of the Hybrid Fuel Cells and Batteries-Fed Marine Vessels—An Overview.* IEEE Transactions on Transportation Electrification, 2022. **8**(2): p. 1885-1905.
16. Sürer, M.G. and H.T. Arat, *Advancements and current technologies on hydrogen fuel cell applications for marine vehicles.* International Journal of Hydrogen Energy, 2022. **47**(45): p. 19865-19875.
17. Hansen, J.F., et al., *Onboard DC grid.* 2012: p. 29-33.
18. Kennedy, L., J. Soong, and J.O. Lindtjorn, *All-electric hybrid propulsion for the next generation of tugboats.* Tugnology, Hamburg, 2013.
19. Kanellos, F.D., G.J. Tsekouras, and J. Prousalidis, *Onboard DC grid employing smart grid technology: challenges, state of the art and future prospects.* IET Electrical Systems in Transportation, 2015. **5**(1): p. 1-11.
20. Zincir, B.A. and Y. Arslanoglu, *Comparative Life Cycle Assessment of Alternative Marine Fuels.* Fuel, 2024. **358**: p. 129995.

21. Mukherjee, A., P. Bruijnincx, and M. Junginger, *Techno-economic competitiveness of renewable fuel alternatives in the marine sector.* Renewable and Sustainable Energy Reviews, 2023. **174**: p. 113127.
22. Gray, N., et al., *An assessment of decarbonisation pathways for intercontinental deep-sea shipping using power-to-X fuels.* Applied Energy, 2024. **376**: p. 124163.
23. van Leeuwen, J. and J. Monios, *Decarbonisation of the shipping sector – Time to ban fossil fuels?* Marine Policy, 2022. **146**: p. 105310.
24. Shi, Q., et al., *Finite-time adaptive anti-disturbance constrained control design for dynamic positioning of marine vessels with simulation and model-scale tests.* Ocean Engineering, 2023. **277**: p. 114117.
25. Shi, Q., et al., *Barrier Lyapunov function-based adaptive optimized control for full-state and input-constrained dynamic positioning of marine vessels with simulation and model-scale tests.* Ocean Engineering, 2024. **301**: p. 117534.
26. Nebb, O.C., et al. *Increased fuel efficiency in ship LVDC power distribution systems*. in *2012 IEEE Vehicle Power and Propulsion Conference*. 2012.
27. Hayton, M. *Marine Electrification is the Future: A Tugboat Case Study*. in *Proceedings of PIANC Smart Rivers 2022*. 2023. Singapore: Springer Nature Singapore.
28. Abdelrahman, M., H. Hussein, and O. Mohammed, *Rule-Based Power and Energy Management System For Shipboard Microgrid With HESS To Mitigate Propulsion and Pulsed Load Fluctuations*. 2023.
29. Jamal, S., J. Pasupuleti, and J. Ekanayake, *A rule-based energy management system for hybrid renewable energy sources with battery bank optimized by genetic algorithm optimization.* Scientific Reports, 2024. **14**(1): p. 4865.
30. Wang, Y., Z. Sun, and Z. Chen, *Rule-based energy management strategy of a lithium-ion battery,supercapacitor and PEM fuel cell system.* Energy Procedia, 2018. **158**: p. 2555-2560.
31. Acciaro, M., et al., *Environmental sustainability in seaports: a framework for successful innovation.* Maritime Policy & Management, 2014. **41**(5): p. 480-500.
32. Testik, M.C. and O. Sarikulak, *Change points of real GDP per capita time series corresponding to the periods of industrial revolutions.* Technological Forecasting and Social Change, 2021. **170**: p. 120911.
33. Yang, J., et al., *Evolution of energy and metal demand driven by industrial revolutions and its trend analysis.* Chinese Journal of Population, Resources and Environment, 2021. **19**(3): p. 256-264.
34. Shahbakhsh, M., G.R. Emad, and S. Cahoon, *Industrial revolutions and transition of the maritime industry: The case of Seafarer's role in autonomous shipping.* The Asian Journal of Shipping and Logistics, 2022. **38**(1): p. 10-18.
35. Watanabe, M.D.B., et al., *Drop-in and hydrogen-based biofuels for maritime transport: Country-based assessment of climate change impacts in Europe up to 2050.* Energy Conversion and Management, 2022. **273**: p. 116403.
36. Iris, Ç. and J.S.L. Lam, *A review of energy efficiency in ports: Operational strategies, technologies and energy management systems.* Renewable and Sustainable Energy Reviews, 2019. **112**: p. 170-182.
37. Panayides, P.M., F. Parola, and J.S.L. Lam, *The effect of institutional factors on public–private partnership success in ports.* Transportation Research Part A: Policy and Practice, 2015. **71**: p. 110-127.
38. Bach, H. and T. Hansen, *IMO off course for decarbonisation of shipping? Three challenges for stricter policy.* Marine Policy, 2023. **147**: p. 105379.

39. Oberthür, S., *Institutional interaction to address greenhouse gas emissions from international transport: ICAO, IMO and the Kyoto Protocol.* Climate Policy, 2003. **3**(3): p. 191-205.
40. Faber, J.H., Shinichi; Zhang, Shuang; Pereda, Paula; Comer, Bryan; Hauerhof, Elena; Loeff, Wendela; Smith, Tristan; Zhang, Yan; Kosaka, Hiroyuko, *Fourth IMO GHG study*. 2020.
41. P.R. Shukla, J.S., R. Slade, A. Al Khourdajie, R. van Diemen, D. McCollum, M. Pathak, S. Some, P. Vyas, R. Fradera, M. Belkacemi, A. Hasija, G. Lisboa, S. Luz, J. Malley, (eds.), *IPCC, 2022: Climate Change 2022: Mitigation of Climate Change. Contribution of Working Group III to the Sixth Assessment Report of the Intergovernmental Panel on Climate Change*. 2022: Cambridge University Press, Cambridge, UK and New York, NY, USA.
42. Cret, L., M. Baudry, and F. Lantz, *How to implement the 2023 IMO GHG strategy? Insights on the importance of combining policy instruments and on the role of uncertainty.* Marine Policy, 2024. **169**: p. 106332.
43. UNCTAD, *Review of maritime transport 2020*. 2020: New York.
44. Bouman, E.A., et al., *State-of-the-art technologies, measures, and potential for reducing GHG emissions from shipping – A review.* Transportation Research Part D: Transport and Environment, 2017. **52**: p. 408-421.
45. Horvath, S., M. Fasihi, and C. Breyer, *Techno-economic analysis of a decarbonized shipping sector: Technology suggestions for a fleet in 2030 and 2040.* Energy Conversion and Management, 2018. **164**: p. 230-241.
46. Menon, N.V. and S.H. Chan, *Technoeconomic and environmental assessment of HyForce, a hydrogen-fuelled harbour tug.* International Journal of Hydrogen Energy, 2022. **47**(10): p. 6924-6935.
47. Chen, Z. and J.S.L. Lam, *Life cycle assessment of diesel and hydrogen power systems in tugboats.* Transportation Research Part D Transport and Environment, 2022. **103**: p. 103192.
48. Bilgili, L., *Comparative assessment of alternative marine fuels in life cycle perspective.* Renewable and Sustainable Energy Reviews, 2021. **144**: p. 110985.
49. Tomos, B.A.D., et al., *Decarbonising international shipping – A life cycle perspective on alternative fuel options.* Energy Conversion and Management, 2024. **299**: p. 117848.
50. Singh Verma, A., et al., *A review on performance, combustion and emissions utilizing alternative fuels.* Materials Today: Proceedings, 2022.
51. Sangeeta, et al., *Alternative fuels: An overview of current trends and scope for future.* Renewable and Sustainable Energy Reviews, 2014. **32**: p. 697-712.
52. Ashrafi, M., J. Lister, and D. Gillen, *Toward a harmonization of sustainability criteria for alternative marine fuels.* Maritime Transport Research, 2022. **3**: p. 100052.
53. Carvalho, F., et al., *Prospects for carbon-neutral maritime fuels production in Brazil.* Journal of Cleaner Production, 2021. **326**: p. 129385.
54. Lane, B., B. Shaffer, and S. Samuelsen, *A comparison of alternative vehicle fueling infrastructure scenarios.* Applied Energy, 2020. **259**: p. 114128.
55. MacFarlane, D.R., et al., *A Roadmap to the Ammonia Economy.* Joule, 2020. **4**(6): p. 1186-1205.
56. Wang, J., P.A. Webley, and T.J. Hughes, *Thermodynamic modelling of pressurised storage and transportation of liquid hydrogen for maritime export.* International Journal of Hydrogen Energy, 2024. **62**: p. 1273-1285.
57. Machaj, K., et al., *Ammonia as a potential marine fuel: A review.* Energy Strategy Reviews, 2022. **44**: p. 100926.

58. Zhu, Y. and G. Seong, *Conversion of Oil and Heavy Residual Oil for Syngas Production*, in *Reference Module in Chemistry, Molecular Sciences and Chemical Engineering*. 2024, Elsevier.
59. Santos, G.R.S., et al., *Techno-economic assessment of Fischer-Tropsch synthesis and direct methane-to-methanol processes in modular GTL reactors.* Catalysis Today, 2021. **371**: p. 93-112.
60. Yang, N., et al., *A strategy for CO2 capture and utilization towards methanol production at industrial scale: An integrated highly efficient process based on multi-criteria assessment.* Energy Conversion and Management, 2023. **293**: p. 117516.
61. Güllü, D. and A. Demirbaş, *Biomass to methanol via pyrolysis process.* Energy Conversion and Management, 2001. **42**(11): p. 1349-1356.
62. Leonzio, G. and E. Zondervan, *Carbon Dioxide to Methanol: A Green Alternative to Fueling the Future*, in *Reference Module in Chemistry, Molecular Sciences and Chemical Engineering*. 2024, Elsevier.
63. Guo, S., et al., *All-electric ship operations and management: Overview and future research directions.* eTransportation, 2023. **17**: p. 100251.
64. Kersey, J., N.D. Popovich, and A.A. Phadke, *Rapid battery cost declines accelerate the prospects of all-electric interregional container shipping.* Nature Energy, 2022. **7**(7): p. 664-674.
65. Wang, J., et al., *Shore power for reduction of shipping emission in port: A bibliometric analysis.* Transportation Research Part E: Logistics and Transportation Review, 2024. **188**: p. 103639.
66. Campana, E., et al., *New global optimization methods for ship design problems.* Optimization and Engineering, 2009. **10**: p. 533-555.
67. Dimopoulos, G.G., A.V. Kougioufas, and C.A. Frangopoulos, *Synthesis, design and operation optimization of a marine energy system.* Energy, 2008. **33**(2): p. 180-188.
68. Cui, H., O. Turan, and P. Sayer, *Learning-based ship design optimization approach.* Computer-Aided Design, 2012. **44**(3): p. 186-195.
69. Sciberras, E. and R. Norman, *Multi-objective design of a hybrid propulsion system for marine vessels.* Electrical Systems in Transportation, IET, 2012. **2**: p. 148-157.
70. Papanikolaou, A., *Holistic ship design optimization.* Computer-Aided Design, 2010. **42**(11): p. 1028-1044.
71. D'Epagnier, K.P., *AUV Propellers: Optimal Design and Improving Existing Propellers for Greater Efficiency*. 2006. 1-7.
72. Liu, A. and S. Fan. *The Research on the Matching Design of the Ship-Engine-Propeller Based on Multi-Objective Particle Swarm Optimization*. in *2010 2nd International Workshop on Intelligent Systems and Applications*. 2010.
73. Torrez, J.B., *Light-weight materials selection for high-speed naval craft*. 2007, Massachusetts Institute of Technology.
74. Cha, M., et al., *Towards a future electric ferry using optimisation-based power management strategy in fuel cell and battery vehicle application — A review.* Renewable and Sustainable Energy Reviews, 2023. **183**: p. 113470.
75. Oh, D., D.-S. Cho, and T.-W. Kim, *Design and evaluation of hybrid propulsion ship powered by fuel cell and bottoming cycle.* International Journal of Hydrogen Energy, 2023. **48**(22): p. 8273-8285.
76. Jung, W., et al., *Design and analysis of liquid hydrogen-fueled hybrid ship propulsion system with dynamic simulation.* International Journal of Hydrogen Energy, 2024. **50**: p. 951-967.
77. Zamboni, G., et al., *Comparative analysis among different alternative fuels for ship propulsion in a well-to-wake perspective.* Heliyon, 2024. **10**(4): p. e26016.

78. Chowdhury, J.I., A. Faieq, and O.M. Amin, *Seakeeping analysis of a tanker with hard sail-based wind propulsion system in various seaways.* Ocean Engineering, 2023. **278**: p. 114481.
79. Li, C., et al., *Energy and configuration management strategy for solid oxide fuel cell/engine/battery hybrid power system with methanol on marine: A case study.* Energy Conversion and Management, 2024. **307**: p. 118355.
80. Sang, Y., et al., *Ship voyage optimization based on fuel consumption under various operational conditions.* Fuel, 2023. **352**: p. 129086.
81. Gao, J., et al., *A coordinated generation and voyage planning optimization scheme for all-electric ships under emission policy.* International Journal of Electrical Power & Energy Systems, 2024. **156**: p. 109698.
82. Zaccone, R., et al., *Ship voyage optimization for safe and energy-efficient navigation: A dynamic programming approach.* Ocean Engineering, 2018. **153**: p. 215-224.
83. Jia, S., C.-L. Li, and Z. Xu, *A simulation optimization method for deep-sea vessel berth planning and feeder arrival scheduling at a container port.* Transportation Research Part B: Methodological, 2020. **142**: p. 174-196.
84. Xu, C., et al., *A multi-objective optimization energy management strategy for marine hybrid propulsion with waste heat recovery system.* Applied Thermal Engineering, 2024. **236**: p. 121548.
85. Chen, W., et al., *Optimal Power and Energy Management Control for Hybrid Fuel Cell-Fed Shipboard DC Microgrid.* IEEE Transactions on Intelligent Transportation Systems, 2023. **PP**: p. 1-18.
86. Shakeri, N., et al., *Modeling and Stability Analysis of Fuel Cell-Based Marine Hybrid Power Systems.* IEEE Transactions on Transportation Electrification, 2023: p. 1-1.
87. Paganelli, G., et al., *General supervisory control policy for the energy optimization of charge-sustaining hybrid electric vehicles.* JSAE Review, 2001. **22**(4): p. 511-518.
88. Zoelch, U. and D. Schroeder, *Dynamic optimization method for design and rating of the components of a hybrid vehicle.* International Journal of Vehicle Design, 1998. **19**(1): p. 1-13.
89. Chan-Chiao, L., et al. *Energy management strategy for a parallel hybrid electric truck*. in *Proceedings of the 2001 American Control Conference. (Cat. No.01CH37148)*. 2001.
90. Koot, M., et al., *Energy management strategies for vehicular electric power systems.* IEEE Transactions on Vehicular Technology, 2005. **54**(3): p. 771-782.
91. Jeong, B., et al., *Multi-criteria decision-making for marine propulsion: Hybrid, diesel electric and diesel mechanical systems from cost-environment-risk perspectives.* Applied Energy, 2018. **230**: p. 1065-1081.
92. Ådnanes, A.K., *Maritime Electrical Installations and Diesel Electric Propulsion*. 2003: ABB.
93. Kistner, L., A. Bensmann, and R. Hanke-Rauschenbach, *Potentials and limitations of battery-electric container ship propulsion systems.* Energy Conversion and Management: X, 2024. **21**: p. 100507.
94. Bayraktar, M. and G. Cerit, *An assessment on the efficient use of hybrid propulsion system in marine vessels.* World Journal of Environmental Research, 2020. **10**: p. 61-74.
95. Jaurola, M., et al., *Optimising design and power management in energy-efficient marine vessel power systems: a literature review.* Journal of Marine Engineering & Technology, 2018. **18**: p. 1-10.

96. Kanellos, F.D., *Optimal Power Management With GHG Emissions Limitation in All-Electric Ship Power Systems Comprising Energy Storage Systems.* IEEE Transactions on Power Systems, 2014. **29**(1): p. 330-339.
97. Kanellos, F.D., G.J. Tsekouras, and N.D. Hatziargyriou, *Optimal Demand-Side Management and Power Generation Scheduling in an All-Electric Ship.* IEEE Transactions on Sustainable Energy, 2014. **5**(4): p. 1166-1175.
98. Javadli, R. and A. de Klerk, *Desulfurization of heavy oil.* Applied Petrochemical Research, 2012. **1**(1): p. 3-19.
99. IEA, *Global hydrogen review 2021*. 2021: Paris.
100. Su, B., et al., *Energy consumption and energy efficiency trends in Singapore: The case of a meticulously planned city.* Energy Policy, 2022. **161**: p. 112732.
101. Hermesmann, M. and T.E. Müller, *Green, Turquoise, Blue, or Grey? Environmentally friendly Hydrogen Production in Transforming Energy Systems.* Progress in Energy and Combustion Science, 2022. **90**: p. 100996.
102. Ho, A., et al., *Dynamic simulation of a novel nuclear hybrid energy system with large-scale hydrogen storage in an underground salt cavern.* International Journal of Hydrogen Energy, 2021. **46**(61): p. 31143-31157.
103. Faheem, H.H., et al., *Comparative study of conventional steam-methane-reforming (SMR) and auto-thermal-reforming (ATR) with their hybrid sorption enhanced (SE-SMR & SE-ATR) and environmentally benign process models for the hydrogen production.* Fuel, 2021. **297**: p. 120769.
104. Ebrahimian, S. and D. Iranshahi, *An investigative study on replacing the conventional furnaces of naphtha reforming with chemical looping combustion for clean hydrogen production.* International Journal of Hydrogen Energy, 2020. **45**(38): p. 19405-19419.
105. Mamlouk, M., *4.19 - Alkaline Anion Exchange Membrane (AEM) Water Electrolysers—Current/Future Perspectives in Electrolysers for Hydrogen*, in *Comprehensive Renewable Energy (Second Edition)*, T.M. Letcher, Editor. 2022, Elsevier: Oxford. p. 473-504.
106. Ginsberg, M.J., et al., *Minimizing the cost of hydrogen production through dynamic polymer electrolyte membrane electrolyzer operation.* Cell Reports Physical Science, 2022. **3**(6): p. 100935.
107. Meduri, S. and J. Nandanavanam, *Materials for hydrogen storage at room temperature – An overview.* Materials Today: Proceedings, 2022.
108. Srinivasan, S.S. and E.K. Stefanakos, *Clean Energy and Fuel Storage.* Applied Sciences, 2019. **9**(16).
109. de Miguel, N., et al., *Compressed hydrogen tanks for on-board application: Thermal behaviour during cycling.* International Journal of Hydrogen Energy, 2015. **40**(19): p. 6449-6458.
110. Zhao, L., et al., *Thermodynamic analysis of the emptying process of compressed hydrogen tanks.* International Journal of Hydrogen Energy, 2019. **44**(7): p. 3993-4005.
111. Van Hoecke, L., et al., *Challenges in the use of hydrogen for maritime applications.* Energy & Environmental Science, 2021. **14**(2): p. 815-843.
112. Li, H., et al., *Safety of hydrogen storage and transportation: An overview on mechanisms, techniques, and challenges.* Energy Reports, 2022. **8**: p. 6258-6269.
113. Yin, L. and Y. Ju, *Review on the design and optimization of hydrogen liquefaction processes.* Frontiers in Energy, 2020. **14**(3): p. 530-544.
114. Krasae-in, S., J.H. Stang, and P. Neksa, *Development of large-scale hydrogen liquefaction processes from 1898 to 2009.* International Journal of Hydrogen Energy, 2010. **35**(10): p. 4524-4533.

115. Berstad, D., G. Skaugen, and Ø. Wilhelmsen, *Dissecting the exergy balance of a hydrogen liquefier: Analysis of a scaled-up claude hydrogen liquefier with mixed refrigerant pre-cooling.* International Journal of Hydrogen Energy, 2021. **46**(11): p. 8014-8029.
116. Faye, O., J. Szpunar, and U. Eduok, *A critical review on the current technologies for the generation, storage, and transportation of hydrogen.* International Journal of Hydrogen Energy, 2022. **47**(29): p. 13771-13802.
117. E4tech, *The fuel cell industry review 2020*. 2020.
118. Yan, H., et al., *Techno-economic evaluation and technology roadmap of the MWe-scale SOFC-PEMFC hybrid fuel cell system for clean power generation.* Journal of Cleaner Production, 2020. **255**: p. 120225.
119. *UK starts work on public-private roadmap for hydrogen, fuel cells.* Fuel Cells Bulletin, 2016. **2016**(3): p. 10-11.
120. Abeleda Jr, J.M.A. and R. Espiritu, *The status and prospects of hydrogen and fuel cell technology in the Philippines.* Energy Policy, 2022. **162**: p. 112781.
121. Hong, X., et al., *Hydrogen Economy Assessment & Resource Tool (HEART): A python-based tool for ASEAN H2 roadmap study.* International Journal of Hydrogen Energy, 2022.
122. Kim, C., et al., *Review of hydrogen infrastructure: The current status and roll-out strategy.* International Journal of Hydrogen Energy, 2023. **48**(5): p. 1701-1716.
123. Gurau, V., A. Ogunleke, and F. Strickland, *Design of a methanol reformer for on-board production of hydrogen as fuel for a 3 kW High-Temperature Proton Exchange Membrane Fuel Cell power system.* International Journal of Hydrogen Energy, 2020. **45**(56): p. 31745-31759.
124. Authayanun, S., et al., *Comparison of high-temperature and low-temperature polymer electrolyte membrane fuel cell systems with glycerol reforming process for stationary applications.* Applied Energy, 2013. **109**: p. 192-201.
125. Zheng, L., et al., *Experimental investigation on alternative fuel combustion performance using a gas turbine combustor.* Applied Energy, 2019. **238**: p. 1530-1542.
126. Zareei, J., A. Rohani, and W.M.F. Wan Mahmood, *Simulation of a hydrogen/natural gas engine and modelling of engine operating parameters.* International Journal of Hydrogen Energy, 2018. **43**(25): p. 11639-11651.
127. Gómez Montoya, J.P., et al., *Strategies to improve the performance of a spark ignition engine using fuel blends of biogas with natural gas, propane and hydrogen.* International Journal of Hydrogen Energy, 2018. **43**(46): p. 21592-21602.
128. Li, G., et al., *Performance and emissions characteristics of a lean-burn marine natural gas engine with the addition of hydrogen-rich reformate.* International Journal of Hydrogen Energy, 2019. **44**(59): p. 31544-31556.
129. Hao, D., et al., *Experimental study of hydrogen enriched compressed natural gas (HCNG) engine and application of support vector machine (SVM) on prediction of engine performance at specific condition.* International Journal of Hydrogen Energy, 2020. **45**(8): p. 5309-5325.
130. Niu, R., et al., *Effect of hydrogen proportion on lean burn performance of a dual fuel SI engine using hydrogen direct-injection.* Fuel, 2016. **186**: p. 792-799.
131. Sapra, H., et al., *Hydrogen-natural gas combustion in a marine lean-burn SI engine: A comparitive analysis of Seiliger and double Wiebe function-based zero–dimensional modelling.* Energy Conversion and Management, 2020. **207**: p. 112494.

132. He, F., et al., *Comparison study and synthetic evaluation of combined injection in a spark ignition engine with hydrogen-blended at lean burn condition.* Energy, 2018. **157**: p. 1053-1062.
133. Taljegard, M., et al., *Cost-Effective Choices of Marine Fuels in a Carbon-Constrained World: Results from a Global Energy Model.* Environmental Science & Technology, 2014. **48**(21): p. 12986-12993.
134. Piaggio, B., D. Villa, and M. Viviani, *Numerical analysis of escort tug manoeuvrability characteristics.* Applied Ocean Research, 2020. **97**: p. 102075.
135. Klebanoff, L.E., et al., *Comparative study of a hybrid research vessel utilizing batteries or hydrogen fuel cells.* International Journal of Hydrogen Energy, 2021. **46**(76): p. 38051-38072.
136. Madsen, R.T., et al., *Feasibility of the Zero-V: A zero-emissions hydrogen fuel-cell coastal research vessel.* International Journal of Hydrogen Energy, 2020. **45**(46): p. 25328-25343.
137. Melideo, D. and U. Desideri, *The use of hydrogen as alternative fuel for ship propulsion: A case study of full and partial retrofitting of roll-on/roll-off vessels for short distance routes.* International Journal of Hydrogen Energy, 2024. **50**: p. 1045-1055.
138. Lovibond, O., et al., *Numerical analysis of propellers for electric boats using computational fluid dynamics modelling.* Energy Conversion and Management: X, 2023. **17**: p. 100349.
139. Chen, C., G. Delefortrie, and E. Lataire, *Effects of water depth and speed on ship motion control from medium deep to very shallow water.* Ocean Engineering, 2021. **231**: p. 109102.
140. Lackenby, H., *THE EFFECT OF SHALLOW WATER ON SHIP SPEED.* Naval Engineers Journal, 1964. **76**(1): p. 21-26.
141. Sharqawy, M. and S. Zubair, *Thermophysical properties of seawater: A review of existing correlations and data.* Desalination and Water Treatment - DESALIN WATER TREAT, 2010. **16**: p. 354-380.
142. Menter, F.R., *Two-equation eddy-viscosity turbulence models for engineering applications.* AIAA Journal, 1994. **32**(8): p. 1598-1605.
143. Koop, A., B. Rossin, and G. Vaz. *Predicting Wind Loads on Typical Offshore Vessels Using CFD*. in *ASME 2012 31st International Conference on Ocean, Offshore and Arctic Engineering*. 2012.
144. Larsen, S., *The atmospheric Boundary Layer over land and sea: Focus on the offshore Southern Baltic and Southern North Sea region*. 2013. 1-36.
145. Yuck, R.H., H.S. Choi, and S.Y. Hong. *Estimation of Current Loads On Offshore Vessels*. in *The Fifteenth International Offshore and Polar Engineering Conference*. 2005.
146. Liu, S. and A. Papanikolaou, *On the prediction of the added resistance of large ships in representative seaways.* Ships and Offshore Structures, 2017. **12**(5): p. 690-696.
147. Fang, L., et al., *Research on Scale Effect of Ship Appendage Resistance Based on CFD*, in *The 29th International Ocean and Polar Engineering Conference*. 2019. p. ISOPE-I-19-471.
148. Zou, Y., et al., *Impacts of different characteristics of marine biofouling on ship resistance.* Ocean Engineering, 2023. **278**: p. 114415.
149. Strasser, G., et al., *A verification of the ITTC/ISO speed/power trials analysis.* Journal of Marine Science and Technology, 2015. **20**(1): p. 2-13.

150. Liu, X., W. Zhao, and D. Wan, *Hull form optimization based on calm-water wave drag with or without generating bulbous bow.* Applied Ocean Research, 2021. **116**: p. 102861.
151. Díaz-Ojeda, H.R., F. Pérez-Arribas, and S.R. Turnock, *The influence of dihedral bulbous bows on the resistance of small fishing vessels: A numerical study.* Ocean Engineering, 2023. **281**: p. 114661.
152. Tran, T.G., C. Van Huynh, and H.C. Kim, *Optimal design method of bulbous bow for fishing vessels.* International Journal of Naval Architecture and Ocean Engineering, 2021. **13**: p. 858-876.
153. Hakim, M.L., I.K. Suastika, and I.K.A.P. Utama, *A practical empirical formula for the calculation of ship added friction-resistance due to (bio)fouling.* Ocean Engineering, 2023. **271**: p. 113744.
154. García, S., et al., *Predicting ship frictional resistance due to biofouling using Reynolds-averaged Navier-Stokes simulations.* Applied Ocean Research, 2020. **101**: p. 102203.
155. Song, S., et al., *Investigating roughness effects on ship resistance in shallow waters.* Ocean Engineering, 2023. **270**: p. 113643.
156. Piaggio, B., et al., *Z-Drive Escort Tug manoeuvrability model and simulation.* Ocean Engineering, 2019. **191**: p. 106461.
157. Piaggio, B., et al., *Z-Drive Escort Tug manoeuvrability model and simulation, Part II: A full-scale validation.* Ocean Engineering, 2022. **259**: p. 111881.
158. Chen, Z.S. and J.S.L. Lam, *Life cycle assessment of diesel and hydrogen power systems in tugboats.* Transportation Research Part D: Transport and Environment, 2022. **103**: p. 103192.
159. Chen, W., et al., *DC-Distributed Power System Modeling and Hardware-in-the-Loop (HIL) Evaluation of Fuel Cell-Powered Marine Vessel.* IEEE Journal of Emerging and Selected Topics in Industrial Electronics, 2022. **3**(3): p. 797-808.
160. Motori, M. *Technical Features*. B_J/B_JH [cited 2024 1/1/2024]; Available from: https://www.marellimotori.com/product/b4j-b5j-lv-b4jh-b5jh-mv/.
161. Koričan, M., L. Frković, and N. Vladimir, *Electrification of fishing vessels and their integration into isolated energy systems with a high share of renewables.* Journal of Cleaner Production, 2023. **425**: p. 138997.
162. Sarantakos, I., et al., *A Robust Logistics-Electric Framework for Optimal Power Management of Electrified Ports Under Uncertain Vessel Arrival Time.* Cleaner Logistics and Supply Chain, 2024: p. 100144.
163. Qu, J., et al., *Assessment of a methanol-fueled integrated hybrid power system of solid oxide fuel cell and low-speed two-stroke engine for maritime application.* Applied Thermal Engineering, 2023. **230**: p. 120735.
164. Wu, X., et al., *Numerical investigations on charge motion and combustion of natural gas-enhanced ammonia in marine pre-chamber lean-burn engine with dual-fuel combustion system.* International Journal of Hydrogen Energy, 2023. **48**(30): p. 11476-11492.
165. Roslan, S.B., et al. *Rule-Based Control Studies of LNG–Battery Hybrid Tugboat*. Journal of Marine Science and Engineering, 2023. **11**, DOI: 10.3390/jmse11071307.
166. Balsamo, F., et al., *Hybrid Storage System Control Strategy for All-Electric Powered Ships.* Energy Procedia, 2017. **126**: p. 1083-1090.
167. Chan, R., L. Chua, and T. Tjahjowidodo, *Enabling technologies for sustainable all — Electric hybrid vessels (Invited paper)*. 2016. 401-406.

168. Ahmadian, S., M. Tahmasbi, and R. Abedi, *Q-learning based control for energy management of series-parallel hybrid vehicles with balanced fuel consumption and battery life.* Energy and AI, 2023. **11**: p. 100217.
169. Luo, D., W. Ji, and X. Hu *Parameter Optimization and Control Strategy of Hybrid Electric Vehicle Transmission System based on Improved GA Algorithm*. Processes, 2023. **11**, DOI: 10.3390/pr11051554.
170. Schlüter, F. and P. Wältermann, *Hierarchical Control Structures for Hybrid Vehicles - Modelling, Simulation, and Optimization1.* IFAC Proceedings Volumes, 1995. **28**(1): p. 115-120.
171. Vora, A.P., et al., *Simulation Framework for the Optimization of HEV Design Parameters: Incorporating Battery Degradation in a Lifecycle Economic Analysis.* IFAC-PapersOnLine, 2015. **48**(15): p. 195-202.
172. Marano, V., et al., *Comparative study of different control strategies for Plug-In Hybrid Electric Vehicles*. 2009, Consiglio Nazionale delle Ricerche.
173. Zhang, Y., et al., *Energy management strategy for plug-in hybrid electric vehicle integrated with vehicle-environment cooperation control.* Energy, 2020. **197**: p. 117192.
174. Williamson, S.S., *Hybrid Electric and Fuel Cell Hybrid Electric Vehicles*, in *Energy Management Strategies for Electric and Plug-in Hybrid Electric Vehicles*, S.S. Williamson, Editor. 2013, Springer New York: New York, NY. p. 31-63.
175. Couch, J., L. Fiorentini, and M. Canova, *An ECMS-Based Approach for the Energy Management of a Vehicle Electrical System.* IFAC Proceedings Volumes, 2013. **46**(21): p. 115-120.
176. Chen, Z., et al., *A neural network-based ECMS for optimized energy management of plug-in hybrid electric vehicles.* Energy, 2022. **243**: p. 122727.
177. Haseltalab, A. and R.R. Negenborn. *Predictive on-board power management for all-electric ships with DC distribution architecture*. in *OCEANS 2017 - Aberdeen*. 2017.
178. Haseltalab, A., R.R. Negenborn, and G. Lodewijks, *Multi-Level Predictive Control for Energy Management of Hybrid Ships in the Presence of Uncertainty and Environmental Disturbances**This research is supported by the project ShipDrive: A Novel Methodology for Integrated Modelling, Control, and Optimization of Hybrid Ship Systems (project 13276) of the Dutch Technology Foundation STW.* IFAC-PapersOnLine, 2016. **49**(3): p. 90-95.
179. Hou, J., J. Sun, and H.F. Hofmann, *Mitigating Power Fluctuations in Electric Ship Propulsion With Hybrid Energy Storage System: Design and Analysis.* IEEE Journal of Oceanic Engineering, 2018. **43**(1): p. 93-107.